

**β 1 integrin-dependent mechanotransduction
induces angiocrine signaling required to
promote liver growth and survival**

Inaugural-Dissertation

zur Erlangung des Doktorgrades
der Mathematisch-Naturwissenschaftlichen Fakultät
der Heinrich-Heine-Universität Düsseldorf

vorgelegt von

Jennifer Axnick
aus Oberhausen

Düsseldorf, September 2016

aus dem Institut für Stoffwechselfysiologie
der Heinrich-Heine-Universität Düsseldorf

Gedruckt mit der Genehmigung der
Mathematisch-Naturwissenschaftlichen Fakultät der
Heinrich-Heine-Universität Düsseldorf

Referent: Prof. Dr. Eckhard Lammert

Korreferent: Prof. Dr. Ulrich Rüther

Tag der mündlichen Prüfung: 01. Dezember 2016

Zusammenfassung

Endothelzellen sind nicht länger nur als Bausteine von Blutgefäßen bekannt, die passiv Blut transportieren. Sogenannte angiocrine Faktoren sind parakrine Signale, die von Endothelzellen produziert werden und maßgeblich zum Organwachstum, sowie zur Regeneration, aber auch zur Aufrechterhaltung der Organfunktion beitragen oder an der Entstehung von Krankheiten beteiligt sind. Als Modellsystem wurde die Leber für diese Arbeit ausgewählt, da die Leber ein Organ mit vielen lebenswichtigen Funktionen ist und die sinusoidalen Leberendothelzellen (LSECs) ein sehr besonderes vaskuläres System darstellen.

In dieser Dissertation wurde eine breite Auswahl an anspruchsvollen *in vivo*, *ex vivo* und *in vitro* Methoden benutzt, um zu zeigen, dass angiocrine Signale durch Mechanotransduktion induziert werden. Mit Hilfe der sich entwickelnden Leber im Mausembryo konnten wir zeigen, dass das Organwachstum mit der Organperfusion korreliert, sowie dass durch die Perfusion der Leber endotheliales $\beta 1$ Integrin und vascular endothelial growth factor receptor 3 (VEGFR3) aktiviert werden. Dies konnte durch die Manipulierung des Herzschlags von *ex vivo* kultivierten Mausembryonen gezeigt werden. Genetische knockout Embryonen wurden genutzt, um zu zeigen, dass endotheliales $\beta 1$ Integrin in der Signaltransduktion oberhalb von VEGFR3 aktiv ist und dass sowohl $\beta 1$ Integrin als auch VEGFR3 für die angiocrine Produktion des Hepatozyten Wachstumsfaktors (HGF), sowie für das Leberwachstum und -überleben benötigt werden.

Die *ex vivo* Perfusion adulter Lebern wurde genutzt, um Flussraten durch die Leber unter Ausschluss von Blutkomponenten zu manipulieren. Es konnte gezeigt werden, dass die Perfusionsraten mit der Stärke der Aktivierung von endotheliale $\beta 1$ Integrin und der Tyrosin Phosphorylierung von VEGFR3 korrelieren, sowie mit dem angiocrinen Signalweg über HGF. Desweiteren wurde ein erster Beweis für einen mechanoinduzierten angiocrinen Signalweg geliefert. Durch mechanische Streckung humaner LSECs konnten wir zeigen, dass die Proliferation humaner Hepatozyten *in vitro* gesteigert werden kann.

Kardiale Erkrankungen werden häufig mit daraus resultierenden Leberfehlfunktionen assoziiert. Induzierte linksventrikuläre Myokardinfarkte in Mäusen wurden als Model genutzt, um den Blutfluss *in vivo* zu manipulieren, sowie die Leberschädigung nach Myokardinfarkt zu untersuchen. Es ist davon auszugehen, dass die beobachteten Leberschädigungen im Zusammenhang mit dem hier erforschten Signalweg stehen und von einem schlecht perfundiertem Lebergewebe resultieren.

In dieser Arbeit wurden neue Methoden erarbeitet und ein neuer Mechanismus aufgedeckt. Dieser zeigt, dass endotheliales $\beta 1$ Integrin und VEGFR3 den Blutfluss durch

die Leber in angiocrine Signale übersetzen, wie es hier für HGF gezeigt wurde, um das Organwachstum und die Aufrechterhaltung der Organfunktion zu gewährleisten. Diese Erkenntnisse ermöglichen einen Einblick in physiologische und pathophysiologische Prozesse, in denen Blutflussveränderungen festgestellt wurden. Somit ergibt sich eine hohe Relevanz der hier gezeigten Ergebnisse dieser Arbeit zur Erforschung des Leberwachstums, der Leberregeneration und Leber-assoziiierter Erkrankungen.

Summary

Endothelial cells are no longer seen as merely compartments of blood vessels that passively transport blood. Endothelial cell-derived angiocrine signals were found to play a key role in organ growth, regeneration and maintenance, but also in diseases. The liver was chosen as model system for these purposes, as the liver is an organ with many important vital functions and liver sinusoidal endothelial cells (LSECs) form a specialized vascular bed.

A range of sophisticated experimental setups *in vivo*, *ex vivo* and *in vitro* was used in this thesis to conclude that angiocrine signals are induced by mechanotransduction. Using the developing liver, it was shown that organ growth correlates with blood perfusion and that perfusion activates endothelial $\beta 1$ integrin as well as vascular endothelial growth factor receptor 3 (VEGFR3). This was demonstrated by manipulating the embryonic heartbeat in *ex vivo* cultivation of mouse embryos. Genetic knockout embryos were also analyzed to show that endothelial $\beta 1$ integrin is upstream of VEGFR3 signaling and that both, $\beta 1$ integrin as well as VEGFR3, are required for angiocrine production of hepatocyte growth factor (HGF), as well as for liver growth and survival. *Ex vivo* perfusion of adult livers was used to manipulate flow rates through the liver in the absence of blood components. Using this approach, it was demonstrated that the perfusion rate correlates with endothelial $\beta 1$ integrin activation and VEGFR3 tyrosine phosphorylation, as well as with angiocrine signaling via HGF. Furthermore, it was shown that proliferation of primary human hepatocytes *in vitro* is enhanced by culture in conditioned medium from human LSECs after mechanical stretching, providing evidence for mechanoinduced angiocrine signaling in a human *in vitro* system.

Cardiogenic diseases are often reported to be associated with liver dysfunction. In this thesis, a left ventricular myocardial infarction (MI) model was used to manipulate the blood flow through the liver *in vivo* and to create a model system for cardiogenic-induced hepatic dysfunctions. It was observed that liver damage after MI and impaired activation of endothelial $\beta 1$ integrin and VEGFR3 occurred possibly due to decreased cardiac output.

For this thesis, new methods were developed and a novel mechanism was provided demonstrating that endothelial $\beta 1$ integrin and VEGFR3 translate organ blood perfusion by mechanotransduction into angiocrine signaling to promote organ growth and maintenance. The findings of this thesis provide a new view on physiological and pathophysiological processes, which are associated with blood flow alterations. Thus, these findings are highly relevant to the study of liver development, regeneration, and disease.

Table of Contents

Zusammenfassung	I
Summary.....	III
1. Introduction	1
1.1 The liver	1
1.1.1 Liver anatomy.....	2
1.1.2 Cell types in the liver.....	3
1.1.3 Fluid flow in the liver and microarchitecture.....	3
1.1.4 Liver sinusoids	5
1.1.5 Liver development.....	6
1.2 Mechanotransduction and angiocrine signaling.....	7
1.2.1 Blood flow as physiological mechano-signal.....	8
1.2.2 β 1 Integrin	8
1.2.3 VEGFR3.....	10
1.2.4 Angiocrine signals.....	11
1.3 Medical Application.....	12
1.4 AIM.....	14
2. Experimental Procedures.....	15
2.1 Mouse Strains	15
2.2 Genotyping.....	15
2.3 Mouse embryo Experiments.....	17
2.3.1 Embryo isolation, injections and whole embryos culture (WEC).....	17
2.3.2 Vascular painting.....	18
2.3.3 EDU incorporation.....	18
2.3.4 Loss- and gain-of-perfusion	18
2.4 Ex vivo perfusion.....	19
2.5 Myocardial infarctions.....	20
2.5.1 Liver function test.....	20
2.5.2 Infarction size determination	20
2.6 In vitro studies	21
2.6.1 LSEC cell length determination.....	21
2.6.2 Coculture.....	21

2.7 Immunostaining and imaging	22
2.7.1 Cryosectioning	22
2.7.2 Morphometric analysis	22
2.7.3 Immunostaining.....	22
2.7.4 EDU Click-IT® reaction	24
2.7.5 Proximity ligation assays (PLA).....	24
2.7.6 Imaging and image analysis.....	24
2.8 ELISA	25
2.9 Statistical analysis	26
2.10 Personal Contribution	27
3. Results	28
3.1 Embryonic liver growth	29
3.1.1 Perfusion of the liver periphery and peripheral liver growth zones	30
3.1.2 Liver vessels have specialized ECs and peripheral activation of β1 integrin and tyrosine phosphorylation of VEGFR3	32
3.2 Correlation of heart beat, VEGFR3 tyrosine phosphorylation and HGF expression in the growing liver	33
3.2.1 Loss-of-perfusion experiments	33
3.2.2 Gain-of-perfusion experiments	34
3.3 Deletion of endothelial β1 integrin	36
3.3.1 Endothelial β1 integrin deletion on LSECs.....	36
3.3.2 Endothelial β1 integrin is required for growth of the developing liver.....	37
3.3.3 Endothelial β1 integrin is required for organ survival and proliferation in the developing liver	38
3.3.4 Endothelial β1 integrin regulates VEGFR3 signaling and HGF levels	41
3.3.5 Endothelial β1 integrin is required for perfusion-dependent VEGFR3 tyrosine phosphorylation	42
3.4 Deletion of VEGFR3 – Requirement of VEGFR3 for HGF production, liver growth and survival	43
3.5 Ex vivo liver perfusion	46
3.6 In vitro studies – Human hepatocytes	48
3.7 In vivo loss-of-perfusion experiments by myocardial infarction	50
3.7.1 MI success	50
3.7.2 Analysis of the liver damage after myocardial infarction	51
3.7.3 Liver function tests	53
3.7.4 Mechanotransduction of the liver after MI	54

4. Discussion	56
4.1 Mechanism	56
4.2 Critical Discussion	57
4.2.1 Mechanotransduction via β 1 integrin and VEGFR3	57
4.2.2 Perfusion induced angiocrine signaling.....	59
4.3 Outlook	60
References	62
List of Publications	IV
Abbreviations	V
List of Figures	VII
Acknowledgements	IX
Declaration	X

1. Introduction

Endothelial cells are more than just passive linings of blood vessels. Endothelial cell-derived angiocrine signals are important for organ growth, regeneration and maintenance, but also in diseases (Rafii et al., 2016). Taking the liver as model organism, as it is an organ of high relevance in the body with a specialized vasculature, the mechanotransduction of angiocrine signals was investigated in this thesis. Furthermore, the role of $\beta 1$ integrin and vascular endothelial growth factor receptor 3 (VEGFR3) for the mechanotransduction of angiocrine hepatocyte growth factor (HGF) was analyzed.

1.1 The liver

The liver is a vital organ of high importance for every vertebrate. As the largest visceral organ, it is a very specialized tissue and has a wide range of metabolic functions, including the regulation of blood glucose homeostasis, the synthesis of plasma proteins important for osmoregulation and blood coagulation, and detoxification (Häussinger, 2014; Tortora and Derrickson, 2006). It is the largest endocrine gland in the body and it also degrades red blood cells and breaks down hemoglobin to bilirubin (Tortora and Derrickson, 2006). One of its main functions is to metabolize absorbed food ingredients from the gut, such as lipids, peptides, carbohydrates and other nutrients (Häussinger, 2014). It is also a storage for vitamins and carbohydrates, the latter are stored as glycogen (Tortora and Derrickson, 2006). The urea cycle to metabolize toxic ammonia to harmless urea takes also place in the liver, as well as the detoxification of other metabolic waste products and drugs (Häussinger, 2014). Furthermore, the liver produces bile fluids and coordinates its storage in the gall bladder and its release into the duodenum upon food intake, necessary for the emulsion and digestion of lipids (Häussinger, 2014; Ishibashi et al., 2009). Most important, the liver is the only organ that has the ability to completely regenerate, defined as compensatory growth, following partial hepatectomy, *i.e.* the removal of up to 75% liver tissue (Michalopoulos, 2007; Palmes and Spiegel, 2004).

Since the liver holds a central role for a healthy organism, liver dysfunction is the origin of diseases. In the United States, liver diseases are under the top 5 leading causes of death for middle-aged adults and therefore research in this field is of major interest (National Vital Statistics System. 2010; Si-Tayeb et al., 2010). The most common diseases of the liver include those that are characterized by excessive accumulation of fat in the liver (steatosis) accompanied by obesity (non-alcoholic steatohepatitis, NASH) or excessive alcohol consumption (alcoholic steatohepatitis, ASH), and viral infections

(Hepatitis-B or -C Virus) (Ishibashi et al., 2009). Over time, an acute inflammation of the liver (hepatitis) can become a chronic disorder with accumulation of connective tissue (fibrosis), followed by a nodular tissue transformation (cirrhosis) and even tumor formation (hepatocellular carcinoma) (Anthony et al., 1978; Bataller and Brenner, 2005; Hata et al., 2007).

1.1.1 Liver anatomy

The liver is located in the upper right area of abdomen, right under the diaphragm. It is a lobular organ that is separated into several liver lobes. Those lobes are different in mice and humans, as the livers have different anatomy. However, due to a very similar microscopic anatomy (Rogers and Dintzis, 2012) mice are commonly used as a model organism, especially when functional analyses, using gene knockouts (KOs), are performed. In humans, the liver is divided into two major lobes, the left and the right lobe. In mice, it is divided into four lobes – the median, left, right and caudate lobe. In both cases, the liver is connected to several membranes in the body cavity (Rogers and Dintzis, 2012).

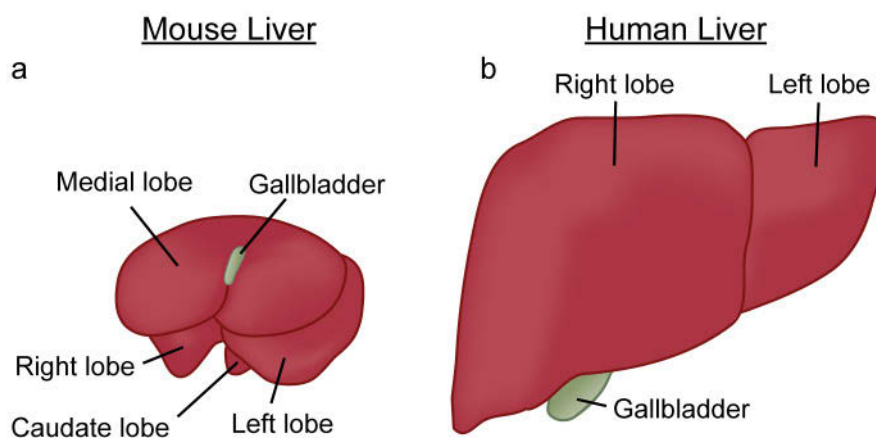


Figure 1.1: Mouse and human livers. Schematic drawings of liver lobes from (a) a mouse and (b) a human liver. Scales between mouse and human liver are not proportional. Illustrations by J. Axnick, based on reviews (Abdel-Misih and Bloomston, 2010; Ishibashi et al., 2009).

The liver segmentation is done in functional segments. Every segment is supplied by a major blood vessel. This is important for clinical reasons, like liver transplantations in humans (Schünke et al., 2015) or partial hepatectomy in mice, where it is safe to cut out one functional segment, without destroying the function of other segments (Michalopoulos, 2007; Schünke et al., 2015).

1.1.2 Cell types in the liver

The liver consists of several cell types, containing parenchymal as well as non-parenchymal cells. Parenchymal cells are the largest fraction with approximately 80% of the whole liver mass, and are mainly hepatocytes (Buschmann et al., 2012; Ishibashi et al., 2009). Their functions are numerous, including metabolism of nutrients, detoxification, bile production, hormone production, production of plasma proteins and energy storage. Other parenchymal cells are cholangiocytes (<2%), as they develop from the same progenitor cells as the hepatocytes. They collect and also produce bile fluids and take care for water resorption. Kupffer cells are resident macrophages (8%) that play important roles during infections, e.g. phagocytosis and degradation of macromolecules (Ishibashi et al., 2009). Liver sinusoidal endothelial cells (LSECs) are specialized endothelial cells that contribute to 3-5% of the liver mass (Si-Tayeb et al., 2010). They were commonly known to function as a delivery system for nutrient supply and immune functions (Enzan et al., 1997). Hepatic stellate cells (5%) are liver-specific pericytes, which are also discussed to be stem cells in liver regeneration (Ishibashi et al., 2009; Kordes and Häussinger, 2013).

1.1.3 Fluid flow in the liver and microarchitecture

The blood supply of the liver is ensured by two major blood vessels - the portal vein and the hepatic artery (Abdel-Misih and Bloomston, 2010; Fernandez et al., 2009). While the portal vein delivers nutrient-rich blood from the gastrointestinal tract, the hepatic artery provides the liver with oxygen-rich blood from the heart. These two vessels cover 25% of the total cardiac output. The portal vein transports 75% of the total liver blood supply through the liver, which means the liver is a venous and low-pressure blood flow organ (Abdel-Misih and Bloomston, 2010; Fernandez et al., 2009). Deoxygenated blood leaves the liver via hepatic veins that drain into the inferior vena cava. Lymphatic vessels drain the interstitial fluid out of the liver. Bile fluids provide another flow that is directed outside of the liver (Abdel-Misih and Bloomston, 2010; Häussinger, 2014).

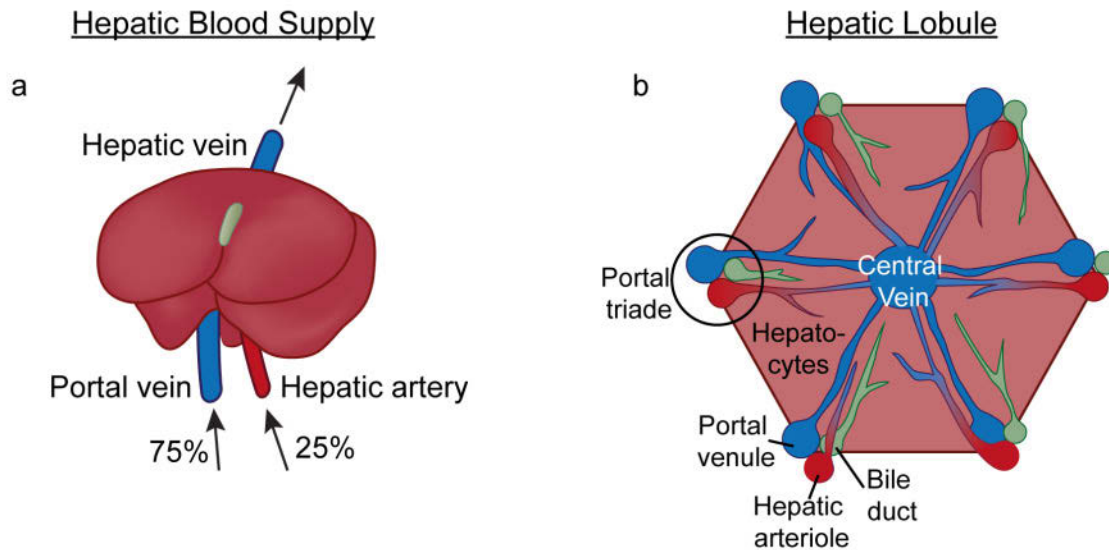


Figure 1.2: Blood flow through the liver. Schematic drawings of the blood flow in the liver. (a) Two supplying blood vessels of the liver; the portal vein covers 75% and the hepatic artery covers 25% of the total blood flow through the liver. The outflowing blood is drained into the hepatic vein. (b) Hexagonal shaped liver lobule, with portal triads on each edge. Blood flows from the portal venules and the hepatic arterioles through liver sinusoids and is drained from the central vein. Bile, produced by hepatocytes, flows in reverse direction to the blood stream. Illustrations by J. Axnick, based on reviews (Abdel-Misih and Bloomston, 2010; Buschmann et al., 2012).

On the cellular level, there is a very specialized architecture. The functional units are the liver lobules, arranged in a hexagonal shape. The blood flows from portal triads through liver sinusoids towards the central vein, which lies in the middle of the liver lobule and coalesces into the hepatic vein (Buschmann et al., 2012). The portal triads are branches of the delivering vessels, *i.e.* the hepatic artery and the portal vein, which lay in a bunch together with the collecting bile duct located periportally (Ishibashi et al., 2009; Tortora and Derrickson, 2006). One double layer of hepatocytes is separated by one sinusoid. The liver sinusoids are specialized liver capillaries, which harbor fenestrations and a discontinuous basement membrane in the adult situation (Sorensen et al., 2015). Thus, liver sinusoids function as selective sieves and allow a close connection between blood stream and hepatocytes to ensure a good exchange of blood components, such as oxygen and nutrients, but also toxins, which are metabolized by the hepatocytes, as well as drainage of metabolites, hormones and plasma proteins (Elvevold et al., 2008). Through hepatocytes the bile is produced and transported in reverse direction to the blood stream within hepato-apical intervening canaliculi towards the collecting bile ducts (Häussinger, 2014). Hepatocytes have different functions from periportal to pericentral. This so-called metabolic zonation is for example important for ureogenesis (Häussinger, 1983).

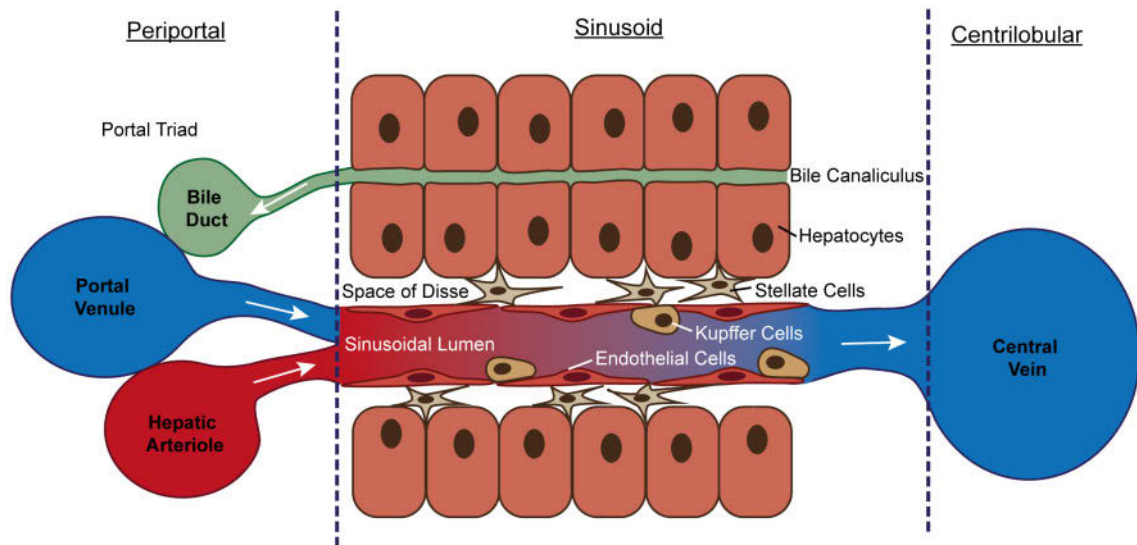


Figure 1.3: Portal liver lobule. Schematic drawing of the blood flow through a liver lobule. Blood flows from the portal triade through liver sinusoids towards the central vein. Liver sinusoids are lined by liver sinusoidal endothelial cells (LSECs). Stellate cells, pericytes of LSECs, are located in the space of Disse. Kupffer cells, resident macrophages are within the sinusoids. Hepatocytes produce baso-apical bile, which is drained into bile canaliculi in reverse direction to the blood stream. Proportions may not be accurately, due to better illustration of the blood flow. Illustration by J. Axnick, based on reviews (Buschmann et al., 2012; Ishibashi et al., 2009).

1.1.4 Liver sinusoids

Liver sinusoids are composed of liver sinusoidal endothelial cells (LSECs), which are very specialized endothelial cells (ECs). They are known to express lymphatic markers such as LYVE-1 and VEGFR3, but less strongly PECAM-1, a common endothelial cell marker (Si-Tayeb et al., 2010). LSECs are fenestrated, contact each other loosely as they were just connected by a few tight junctions, and have a discontinuous basement membrane (Elvevold et al., 2008). Thus, a good exchange of blood components with hepatocytes is ensured, as the liver is a highly metabolic organ. Instead of a continuous basement membrane, the so-called space of Disse can be found in adult liver sinusoids. This is a space between LSECs layer and hepatocytes, where stellate cells are located (Wisse et al., 1983). Studies support the hypothesis that this space has stem cell niche properties (Kordes and Häussinger, 2013).

1.1.5 Liver development

The understanding of developmental processes is important for the understanding and treatment of diseases (Hata et al., 2007; Zeeb et al., 2012). Organ development is also known to be similar to regeneration processes (Hata et al., 2007). Mice (*Mus musculus*) have a high genetic homology to humans, and multiple types of genetic knockout mice are available. Mouse embryos in particular are a good way to study the immediate consequences of genetic mutations, as some KOs are embryonic lethal which is why the direct cause of effects can be analyzed. Therefore, the mouse embryo model was chosen as a model system for this thesis.

Depending on the mouse strain, murine development takes 18 to 20 days of pregnancy. Embryos are staged in embryonic days post fertilization. As mice are nocturnal, conception happens around midnight and this is termed as embryonic day (E0). At E7, the endoderm starts to form. One day later at E8.0, the first intra-embryonic blood vessel is formed *de-novo* via vasculogenesis, before additional blood vessels are formed from existing blood vessels via angiogenesis (Drake and Fleming, 2000). In parallel, the cardiogenic plate forms out a primitive heart, which starts to pump the first blood cells through the embryonic vessels (Brand, 2003). The hepatic specification also starts to take place from E8.0, at E9.0 the liver diverticulum forms and at E9.5 a liver bud is formed (Zaret, 2000). For early liver development the communication between endoderm and mesoderm is of major importance. Liver progenitor cells, called hepatoblasts, arise from the endoderm at the foregut (Zaret and Grompe, 2008). Mesodermal signals such as fibroblast growth factors (FGFs) from the developing heart, or signals from the septum transversum mesenchyme (STM) trigger the liver bud formation (Calmont et al., 2006; Zorn, 2008). Upon liver bud formation ECs are attracted, as early endothelial signals are essential for liver bud outgrowth at E9.5 (Matsumoto et al., 2001). Recently, liver ECs were identified as having a cardiogenic origin (Zhang et al., 2016). During hepatogenesis, blood vessels sprout into STM (Collardeau-Frachon and Scoazec, 2008). Both vasculo- and angiogenesis are thought to form the complex hepatic vascular network (Sugiyama et al., 2010) (Gouysse et al., 2002). From E10-15 the liver forms as an organ (Zorn, 2008), and at E12.5 the liver has already a complex vascular network (Shin and Monga, 2013). At later developmental stages the delamination of the vessels takes place, as well as their maturation to fenestrated vessels (Enzan et al., 1997). Hepatoblast proliferation and survival are associated with hepatocyte growth factor (HGF), as HGF KOs are lethal and have smaller livers (Schmidt et al., 1995; Uehara et al., 1995). Hepatic growth zones located in the liver periphery were described for chick embryos (Suksaweang et al., 2004).

The maturation of hepatocytes into functional cells, the metabolic zonation (Häussinger, 1983) and the differentiation into bile duct epithelium take place at later embryonic stages (Lemaigre and Zaret, 2004; Zaret and Grompe, 2008).

During embryonic development, the liver is the place of hematopoiesis (Hata et al., 2007). Conditional inducible vascular endothelial growth factor-C (VEGF-C) KOs with later stage deletion of *vegfc*, show smaller livers due to hematopoietic defects at E14.5 (Fang et al., 2016). Postnatally, mature hepatocytes no longer support hematopoiesis (Kinoshita et al., 1999).

1.2 Mechanotransduction and angiocrine signaling

The mechanical properties, behavior and movements of our bodies are known to be important (Ingber, 2008), but only recently the research field started to pay attention to physiological mechanotransduction functions, such as mechanoinduced cell-shape, cell-behavior changes or cell signaling (Ingber, 2008; Mammoto et al., 2009; Ross et al., 2013). Up to now, only a few studies are available on this topic and even fewer *in vivo* studies.

ECs hold a special role in mechanotransduction as they are constantly exposed to the blood flow, a physiological mechanical stimulus, which is altered during developmental or pathological processes and constant during organ maintenance. Mechanosensory-complexes on ECs are required to translate the blood flow into a physiological signal. Furthermore, ECs are known to promote tissue growth, survival and homeostasis, particularly via the formation of new blood vessels (angiogenesis), but also via the release of so-called angiocrine signals (Ding et al., 2010; Hu et al., 2014).

This thesis indicates that angiocrine signals are regulated by a mechanotransduction of endothelial $\beta 1$ integrin and VEGFR3 on LSECs, via liver blood perfusion.

1.2.1 Blood flow as physiological mechano-signal

Blood flow is no longer seen as just a process to supply tissues with oxygen and nutrients. In addition, mechanical forces of blood flow, e.g. as surface tension, traction or fluid shear stress, are described to be crucial for organ growth and maintenance, but also in disease states (Baeyens et al., 2016; Mammoto and Ingber, 2010). From developmental to pathological processes, mechanotransduction is often supposed to play a crucial role. For the cardiovascular system the predominant mechano-stimulus is the blood flow itself, leading to fluid shear stress or stretching of ECs. Organ malformations associated with abnormal blood flow during development have been described for different tissues (Mammoto and Ingber, 2010). Blood flow alterations and vasodilatation, which includes EC stretching, were shown to be important for normal adult tissue function. For example, in pancreatic islets, vessels dilate upon insulin resistance, rather than conduct increased angiogenesis (Dai et al., 2013). ECs are also described to sense blood flow direction in atherosclerosis (Wang et al., 2013). Following partial hepatectomy, the same amount of blood passes a proportionally smaller liver (Michalopoulos, 2010), which possibly results in increased fluid shear stress (Buschmann et al., in prep.). In the liver, abnormal hepatic blood flow, particularly in peripheral hepatic vessels, is associated with liver diseases such as liver cirrhosis (Murray et al., 1958). New method approaches, e.g. organ-on-chips technology, an enhancement of 3D cell culture systems, therefore replicate blood flow to better mimic a physiologic environment (Huh et al., 2011).

However, an *in vivo* system to study blood flow alterations and related signaling processes is still missing.

1.2.2 β 1 Integrin

Integrins are heterodimeric transmembrane receptors, composed of an α and a β subunit that are non-covalently associated (Avraamides et al., 2008; Hynes, 2007). Variable compositions of integrin subunits can form different receptors, e.g. α 5 β 1 integrin is a fibronectin receptor (Serini et al., 2008), which was reported to be force-mediated activated (Friedland et al., 2009). Integrins have no intrinsic enzymatic or kinase activity. Signal transduction therefore involves the clustering with intracellular adaptor proteins or kinases (Avraamides et al., 2008). Integrins are involved in cell migration, survival, adhesion, cell cycle control and formation of the basement membrane (BM) (Avraamides et al., 2008; Hynes, 2007). Integrin-mediated cell death was also reported (Stupack, 2005). Furthermore, integrins, especially β 1 integrin, that represents the largest subgroup of

integrins, appear to play a key role in angiogenesis (Ingber, 1991; Planas-Paz et al., 2012; Ross et al., 2013), and it was shown that $\beta 1$ integrin is required for embryonic vascular patterning and postnatal vascular remodeling (Lei et al., 2008).

The importance of integrins is moreover visible in the lethality of single subunit deletions, as $\alpha 5$ integrin KO is embryonic lethal at E10.5 due to vessel defects (Yang et al., 1993). $\beta 1$ integrin global KOs are lethal at E5.5 due to implantation defects (Fassler and Meyer, 1995). Using Cre-LoxP recombination, endothelial-specific $\beta 1$ integrin KO mice (Potocnik et al., 2000) further show the importance of $\beta 1$ integrin on blood vessels, since embryos die at E11.5, when Tie2 Cre is used for conditional KOs, which is effective after implantation from E7.5 and integrin is deleted from E8.5 onwards (Carlson et al., 2008). Later endothelial KOs are also lethal, as found out by using VE-Cadherin Cre, which leads to embryos lethality from E13.5 onwards (Zovein et al., 2010) due to lack in lumen formation of mid-sized vessels and loss of the cell polarity. Further, Flk-1 Cre conditional $\beta 1$ integrin KO embryos die from E14.5 onwards. These KOs were used to show mechanotransduction of lymphatic vessels (Planas-Paz et al., 2012), whereby $\beta 1$ integrin was found to regulate VEGFR3 signaling upon mechanotransduction of interstitial fluid pressure.

Despite these interesting findings, a mechanotransduction for angiocrine signaling has not been investigated yet.

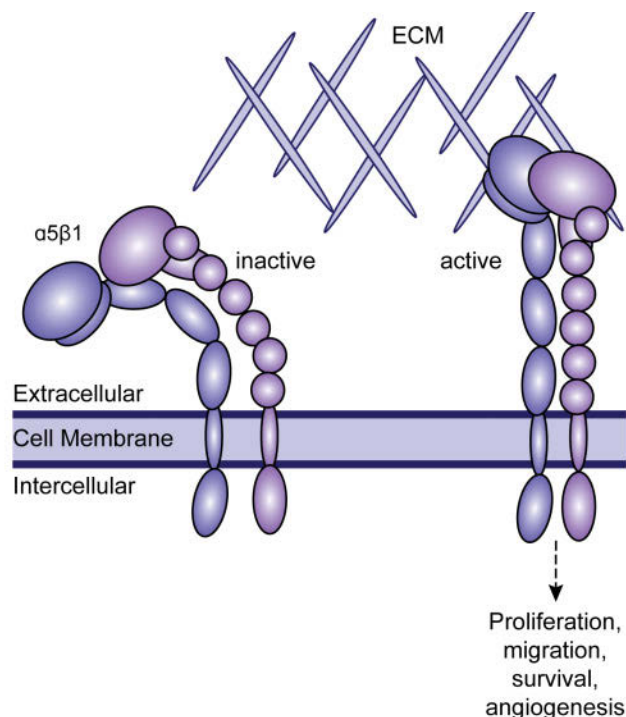


Figure 1.4: Integrins. Schematic drawing of $\alpha 5 \beta 1$ integrin in inactive and active state. Activation of integrins can lead to cell proliferation, migration, survival and angiogenesis. Integrins are receptors of the extracellular matrix (ECM), $\alpha 5 \beta 1$ integrin shown here is a fibronectin receptor. Illustrations from J. Axnick, based on reviews (Avraamides et al., 2008; Serini et al., 2008).

1.2.3 VEGFR3

Vascular endothelial growth factor receptors (VEGFRs) are dimeric tyrosine kinase receptors, composed of an extracellular ligand-binding domain and an intracellular kinase domain (Ferrara et al., 2003; Tallquist et al., 1999). Five different vascular endothelial growth factors (VEGFs) and their three VEGFRs have been described (Ferrara et al., 2003). VEGFR3 can be activated upon binding of its ligands VEGF-C or VEGF-D (Lohela et al., 2009) or via mechanotransduction (Planas-Paz et al., 2012). It is commonly known as a lymphatic marker in adults and was originally supposed to be restricted to embryonic blood vessels (Kaipainen et al., 1995). However, VEGFR3 has turned out to play also a role on blood vessels, e.g. for sprouting angiogenesis, in particular, for tip and stalk cell communication (Tammela et al., 2008). Moreover, it is now known that VEGFR3 is expressed on fenestrated blood vessels (Partanen et al., 2000) and as mentioned before to be localized on LSECs (Si-Tayeb et al., 2010).

VEGFR3 global KO embryos die very early at E9.5 due to cardiovascular defects (Dumont et al., 1998). VEGF-C global KO embryos die later from E12.5 onwards (Haiko et al., 2008; Karkkainen et al., 2004), due to lymphatic defects. VEGF-D KO embryos don't show vascular defects, but rather lymphatic abnormalities (Haiko et al., 2008). These results point to ligand-independent activation of VEGFR3 during embryonic development. Thus, mechanostimulation of VEGFR3 appears as important for VEGFR3 signaling as its activation by ligand-binding. In this regard, an interplay of integrins and VEGFRs has been reported. VEGFR3 is selectively associated with $\alpha 5 \beta 1$ integrins and integrin ligation is required for proper activation of VEGFR3, followed by Pi3 kinase and AKT pathway activation, known to be critical for cell growth and survival (Galvagni et al., 2010; Zhang et al., 2005). Furthermore, fibronectin increases VEGF-C induced VEGFR3 tyrosine phosphorylation and cell survival signaling (Zhang et al., 2005). Moreover, mechanoinduced $\beta 1$ integrin is known to interact with VEGFR3 on lymphatic vessels to promote lymphatic development (Planas-Paz et al., 2012). In addition, VEGFR3 and vascular endothelial (VE)-cadherin were described to form mechanosensory complexes (Baeyens et al., 2015; Coon et al., 2015).

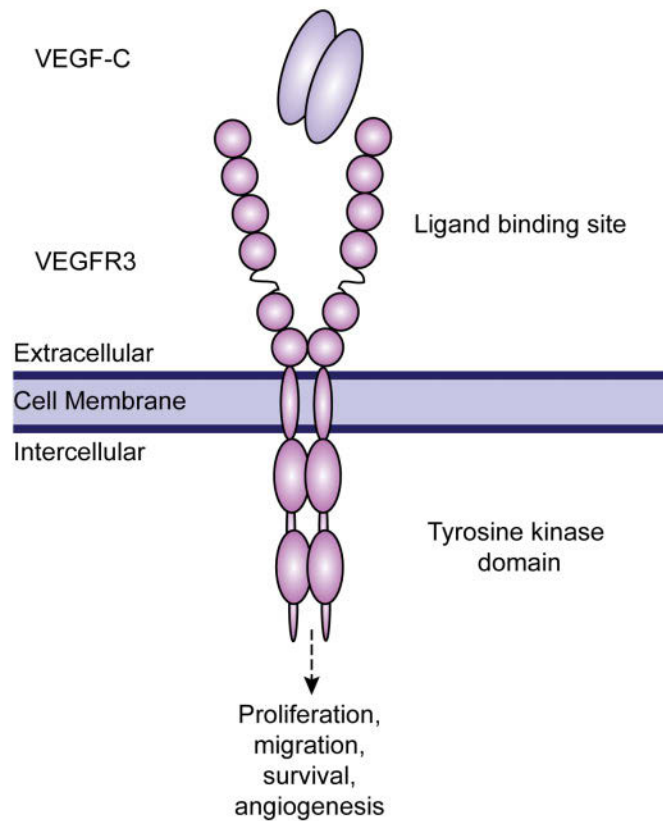


Figure 1.5: VEGFR3. Schematic drawing of VEGFR3. Activation of VEGFR3 by VEGF-C binding or mechanically can lead to cell proliferation, migration, survival and angiogenesis, via tyrosine phosphorylation of the receptor. VEGFR3 can also bind VEGF-D. Illustration by J. Axnick, based on reviews (Ferrara et al., 2003; Lohela et al., 2009).

1.2.4 Angiocrine signals

All tissues have a specialized vascular bed, or so-called vascular niches. It is well known that ECs do not only passively transport blood, as compartments of blood vessels. The presence of ECs alone is already necessary for organ growth as shown for pancreas (Lammert et al., 2001) or liver development (Matsumoto et al., 2001). Angiocrine signals were described for various tissues including the liver, lung alveoli and at the blood brain barrier (Rafii et al., 2016).

Angiocrine signals are defined as growth factors released from the endothelium to contribute to organ-specific growth and repair (Rafii et al., 2016). They are paracrine factors produced by ECs to regulate tissue homeostasis, regeneration or pathophysiological mechanisms. They actively participate in tissue induction, specification, patterning and regeneration (Rafii et al., 2016). Angiocrine signals are known to be important for liver regeneration, as they were found to control the so-called proangiogenic or inductive angiogenesis-independent phase of liver regeneration (day 1-4 after partial hepatectomy). Selective VEGFR1 stimulation was identified to have a protective effect on

the liver, as reduced hepatocyte damage was observed and HGF was found as angiocrine signal in coculture with LSECs (LeCouter et al., 2003). Inducible VEGFR2 deletion leads to decreased hepatocyte proliferation in the proangiogenic phase of liver regeneration after partial hepatectomy (Ding et al., 2010), through impaired inhibitor of DNA binding 1 (Id-1) production. Furthermore, Id-1 KO mice also have impaired regenerative capacities as angiocrine signals, such as HGF and Wnt family member 2 (Wnt2) protein levels, were decreased (Ding et al., 2010). Angiopoietin-2 was shown to be upregulated during liver regeneration and its deletion delays liver regeneration, through decreased transforming growth factor- β 1 (TGF- β 1) levels, identified as an angiocrine signal (Hu et al., 2014). A boost of liver regeneration induced by bone marrow derived ECs that have the capacity to produce HGF, was also observed (Wang et al., 2012). Stromal-derived factor-1 receptors – CXCR7 and CXCR4 – were identified as maintaining a balance between liver regeneration and liver fibrosis. Following acute liver injury, CXCR7 activation leads to liver repair without fibrosis (through apelin and follistatin-like-1), whereas CXCR4 activation after chronic liver injury leads to liver repair with fibrosis, via pro-fibrotic TGF- β 1 and bone morphogenic protein-2 (BMP2) (Ding et al., 2014).

HGF was identified in various studies as an important angiocrine signal, and it was shown to have a major impact on liver development, therefore it was chosen as the target angiocrine signal for the work in this thesis (Borowiak et al., 2004; Nakamura et al., 2011; Schmidt et al., 1995).

1.3 Medical Application

As the liver is a highly metabolic organ of great importance for a healthy organism, it is also involved in many life-threatening diseases. In addition to the common liver diseases, the liver is also involved in cardiogenic diseases. Cardiohepatic interactions are often described, but have not been fully investigated yet.

The left ventricle of the heart pumps blood to the tissues all over the body and supplies the organs with nutrients and oxygen. It furthermore ensures a constant blood flow through the organs. Left-sided heart failure can result in liver dysfunction and centrilobular necrosis, whereby the extent of liver failure correlates with the severity of hypotension (Iboleon-Dy, 2009). Acute cardiogenic liver injury (ACLI), or cardiogenic ischemic hepatitis, after critical cardiogenic shock or myocardial infarction (MI), followed by decreased cardiogenic output, decreased liver perfusion or hypotension, are commonly reported (Biasi et al., 1994; Bynum et al., 1979; Samsky et al., 2013; Seeto et al., 2000). Therefore, cardiogenic ischemic hepatitis has to be distinguished from hypoxic hepatitis (Seth and Nath, 2009). The ACLI is linked to the combination of hepatic congestion from

elevated hepatic venous pressure and impaired organ perfusion (Samsky et al., 2013). Depending on the duration of cardiac ischemia, a variable degree of architectural collapse around the central veins can occur, resulting in necrosis surrounding the central veins (Samsky et al., 2013). Centrilobular hepatic necrosis is reported in 15% of cases after MI (9 out of 61) (Clarke, 1950).

Liver function test abnormalities were often found after heart failures (Killip and Payne, 1960; Samsky et al., 2013). A 10- to 20-fold increase in lactate dehydrogenase (LDH) and aspartate transaminase (AST) levels 1-3 days after MI, as well as sharp increases in alanine transaminase (ALT) levels may point to cardiogenic ischemic hepatitis (Naschitz et al., 2000). Elevated serum bilirubin and a prolongation of prothrombin time can also be observed in such patients. Abnormal transaminase levels are associated with clinical signs of liver hypoperfusion and increased 31- and 180-day mortality following MI (Allen et al., 2009; Samsky et al., 2013). For example, when AST levels from more than 1,000 U/L are detected in ischemic hepatitis after left-ventricular failure the overall mortality after MI increases to 58% (17/29) (Hickman and Potter, 1990). Patients with chronic congestive heart failures also show higher ALT and AST levels (and other liver injury markers) in 27-80% of all cases (Kubo et al., 1987). Liver function abnormalities in patients with cardiac index less than 1.5 l/min per m² can be observed in up to 80% of all cases (Kubo et al., 1987; Naschitz et al., 2000). Shock liver induced by hypoxia, also called nutmeg liver, is often associated with right-sided heart failures (Naschitz et al., 2000; Sherlock, 1950).

Children with congenital heart defects also often suffer from liver diseases (Asrani et al., 2012; Cohen et al., 2013). Furthermore, children with early cardiac surgeries may later suffer from liver dysfunctions. Likewise, hepatic dysfunction was described after left-ventricular mechanical assist in heart failure patients (Masai et al., 2002) and in children with hypoplastic left heart syndrome with Fontan circulation (Wu et al., 2011). Centrilobular necrosis was found in children with hypoplastic left heart syndrome. Hepatic necrosis is present in about 42% of hypoplastic left heart syndrome patients (18/42 children) and in 22% of all young patients with congenital heart diseases (31/137 children)(Weinberg and Bolande, 1970). Taken together, these findings show that children exhibit liver dysfunction and liver necrosis when left cardiac output is decreased or impaired. In contrast, children with paroxysmal supraventricular tachycardia (faster beating hearts) show hepatomegaly (Griscom et al., 1977).

1.4 AIM

The aim of this thesis was the investigation of the role of mechanotransduction for angiocrine signaling. Hepatocyte growth factor (HGF) was chosen as an example for angiocrine signals. The liver was chosen as example tissue as it is an important vital organ in the body and has a specialized vascular bed. Furthermore, the role of endothelial β 1 integrin and VEGFR3 signaling in this scenario was analyzed. The blood flow was identified as mechano-stimulus for the activation of endothelial β 1 integrin and following VEGFR3 tyrosine phosphorylation. In addition, the angiocrine signal production via this mechanotransduction was shown for liver growth and survival. Taken together, the role of vascular liver perfusion for endothelial β 1 integrin and VEGFR3 activation followed by angiocrine signaling, shown for HGF, was investigated. Last, a medical application was found in a mouse model for left-ventricular cardiac diseases, which ended up in hepatic dysfunctions.

To achieve these goals, a wide range of sophisticated methods was applied. In the beginning of the thesis a protocols paper was published about pharmacological manipulation of mouse embryos in whole embryo culture (Zeeb et al., 2012). This method was further improved during this thesis for the needs of the new challenges. Liver perfusion and mechanotransduction in mouse embryos were analyzed. Loss- and gain-of-perfusion experiments were performed using whole embryo culture to show perfusion-dependent activation of endothelial β 1 integrin and VEGFR3 tyrosine phosphorylation, as well as angiocrine signaling. Furthermore, endothelial β 1 integrin KO and VEGFR3 KO embryos were analyzed for mechanistic analyses. *Ex vivo* perfusion of adult mouse livers was used to transfer the achieved knowledge to an adult system. And finally, a loss-of-perfusion *in vivo* experiment and the establishment of a human disease model was performed, using myocardial infarction model to induce low-perfusion of the liver and establish a model for cardiogenic hepatic diseases.

2. Experimental Procedures

2.1 Mouse Strains

C57BL/6J (Janvier) mice were used for wild-type studies and whole embryo culture (WEC). For genetic deletion of $\beta 1$ integrin, *Flk1-Cre* mice and $\beta 1$ integrin-*loxP* mice were used (Licht et al., 2004; Planas-Paz et al., 2012; Potocnik et al., 2000). Embryos from Rosa26-CreERT2 and VEGFR3-*loxP* breedings to generate VEGFR3 KOs were provided by K. Alitalo (Ventura et al., 2007; Haiko et al., 2008). For induction of Cre-mediated recombination in embryos, the pregnant mother received two consecutive intragastric doses of 4-OHTamoxifen (Sigma-Aldrich, MO, 25 mg/ml dissolved in 75 μ l ethanol/olive oil) by gavage at E10.5 and E11.5. Heterozygous littermates for $\beta 1$ integrin KOs or wild type littermates for VEGFR3 KOs were used as controls for comparison with homozygous embryos.

All experiments were performed according to the German and the Finnish animal protection laws.

2.2 Genotyping

The genotyping of $\beta 1$ integrin KOs was performed by lysis of a tissue biopsy of the respective mouse. Tail tips from stock mice were snipped off by staff from the animal house or yolk sacs were isolated directly or after WEC from embryos. Afterwards biopsies were incubated in 100 μ l lysis buffer at 56°C and 300 rpm for at least 4h or ON.

Lysis buffer	μ L
H ₂ O	78
white Flexi buffer (Promega)	20
Proteinase K (20mg/ml, Quiagen)	2

Supernatants were chilled on ice and further used for genotyping polymerase chain reaction (PCR).

PCR Master Mix	Flk-1 Cre [μl]	β1 integrin [μl]
H ₂ O	13.44	13.3
Green Flexi Buffer (Promega)	4	4
MgCl ₂ (Promega)	1.2	1.2
dNTPs (Promega)	0.4	0.4
Primer fwd (100 pmol/μl)	0.13	0.2
Primer rev (100 pmol/μl)	0.13	0.2
Taq (Promega)	0.2	0.2
Lysate	0.5	0.5

The primers (Eurogentec) were designed according to original publications of the mouse strains.

Mouse strain	Primer sequence (5'→3')		Resulting bands [base pairs]
β1 integrin -LoxP	fwd	GGGTTGCCCTTCCCTCTAG	Wild type: 350 bp Heterozygous: 350 bp + 450 bp Homozygous: 450 bp
	rev	GTGAAGTAGGTGAAAGGTAAC	
Flk1 Cre	fwd	CCGGCACAGTTCCGGGGTAGT	Hemi (Cre ⁺): 1 band 1500 bp
	rev	GTGGCAGATGGCGCGGCAACACCATT	

The mastermixes with lysates of the samples were ran with the following protocols in a Professional Trio PCR machine (Biometra).

Flk-1 Cre	β1 integrin
35 PCR cycles	10 PCR cycles
94°C 5min.	94°C 30sec.
94°C 1min.	63°C 30sec.
67°C 1min.	72°C 30sec.
72°C 1min.	

After PCR the samples were loaded on a 1% agarose gel and gelelectrophoresis with 120 V for 25 min was performed. The gels were imaged with a Chemidoc System (Biorad). Genotyping of VEGFR3 KO was performed by K. Alitalos Lab.

2.3 Mouse embryo Experiments

All embryo experiments were performed as previously described in Nature Protocols (Zeeb et al., 2012).

2.3.1 Embryo isolation, injections and whole embryos culture (WEC)

Embryos were staged by the date of the presence of a vaginal plug (embryonic day (E) 0.5) and isolated at different embryonic stages in pre-heated (for WEC) or ice-cold (for protein analysis) phosphate buffered saline (PBS).

2x PBS	2x Mg ²⁺ Ca ²⁺
KCl (5.4 mM)	MgCl ₂ x 6H ₂ O (5 mM)
NaCl (0.27 M)	CaCl ₂ x 2H ₂ O (9 mM)
KH ₂ PO ₄ (3 mM)	
Na ₂ HPO ₄ (1.3 mM)	

For injection into the heart or the liver an InjectMan® NI 2 microinjector connected to a FemtoJet® pump (Eppendorf, Germany) was used. Also, borosilicate glass capillaries with filament (Harvard Apparatus) were used for injections. Those were pulled with a needle puller (Narishige, Japan). 1% Fast Green (AppliChem, Germany) was added to all injected substances to visualize the injection side.

Directly after isolation or following the injection, embryos were cultured in a WEC system (RKI Ikemoto Scientific Technology, Narishige, Japan) in 1,600 µl DMEM (Gibco) and 400 µl fetal bovine serum (FBS, Gibco) per WEC bottle at 37°C, oxygenated with a flow rate of 75cc of 5% CO₂ in 95% O₂, and rotated at 25 rotations per minute (rpm). Following embryo isolation or after WEC, embryos were fixed with 4% paraformaldehyde (PFA) over night or livers were isolated on ice and immediately deep-frozen for protein analysis. For genotyping of KO embryos the yolk sacs were isolated direct after isolation or WEC. Since they were isolated randomized, KO embryos were analyzed randomized and blinded without knowing the genotype and listed with a continuous numbering.

2.3.2 Vascular painting

For vascular painting fluorescently labeled (FITC) *ricinus communis agglutinin* (RCA, 10% diluted in PBS, Sigma) was injected into the beating heart of E11.5 embryos. Afterwards, the embryos were cultured in WEC for 3 hours to allow the RCA to bind (paint) all perfused blood vessels. After WEC, the embryos were fixed and processed for liver isolation and immunofluorescent analyses.

2.3.3 EDU incorporation

For detection of all proliferating cells during WEC incubation time, 5-ethynyl-2'-deoxyuridine (EdU, thymidine base analog, Life Technologies, Germany) was diluted to 1 mg/ml and injected into the embryonic liver, the beating heart or added to the culture medium. EdU was allowed to incorporate into all proliferating cells for 3 hours. After fixation and cryosectioning of the embryos, the EdU Click-IT assay was performed according to the protocol provided by the company (Click-iT® copper-catalyzed covalent reaction between an azide (fluorophore) and an alkyne (EdU)).

2.3.4 Loss- and gain-of-perfusion

For loss- and gain-of-perfusion experiments, E11.5 wild type mouse embryos were isolated and cultured in WEC for 1 hour. For loss-of-perfusion experiments, 50 mM 2,3-Butanedione monoxime (BDM, Sigma, B0753) diluted in PBS was added to the culture medium to arrest the beating heart. For gain-of-perfusion experiments, (-)-epinephrine-(+)-bitartrate salt (short: Epinephrine, Sigma, E4375) diluted in PBS was added to the culture medium at a concentration of 2.5 µg/ml, and embryos were cultured in WEC for 1 hour. The success of the blockage or increasing the heart rate was controlled in the first minutes of WEC and after cultivation. For respective embryos, video documentation was performed to count the heart beats. Embryos were fixed and prepared for immunohistochemistry, or their livers were isolated on ice for protein analysis.

2.4 *Ex vivo* perfusion

Male 10-12 weeks old wild type mice were used for studies of adult livers. This method is based on previous studies conducted in rats (Sies, 1978). For open, non-recirculating perfusion, mice (male, 10-12 weeks) were sacrificed by cervical dislocation and the abdomen was opened with surgical instruments. The portal vein was used for influx by cannulating the vessel with a plastic tip and a rubber tube connected to the perfusion system. For the efflux, the vena cava or the right heart chamber were also cannulated with a plastic tip connected to a rubber tube, which drained directly into a measuring cylinder to monitor flow rate. KRH buffer containing pyruvate and lactate was pumped by a peristaltic pump (at different flow rates) through a thermostat (so that the buffer is heated to 37°C), an oxygenator (oxygenation with carbogen gas, 95% O₂ and 5% CO₂), a bubble trap (to prevent liver emboli), and finally through the cannulated liver. For this set up 4 ml/min was set as the normal perfusion rate and 2 ml/min as low perfusion, as well as 6 and 8 ml/min to be high perfusion rates. 4 ml/min/g was described as the perfusion rate for rats (Sies, 1978). After 1 hour of perfusion, the liver was either subsequently perfused with 4% PFA for fixation followed by immunohistochemical analyses or deep-frozen in liquid nitrogen for protein analyses. Livers from *ex vivo* perfusion were listed under a continuous numbering and were deblinded after analyses.

Krebs-Henseleit-Buffer	Additives
NaCl (115 mM)	Pyruvate (0.3 mM)
NaHCO ₃ (25 mM)	Lactate (2.1 mM)
KCl (5.5 mM)	
KH ₂ PO ₄ (3 mM)	
Na ₂ HPO ₄ (1.3 mM)	
MgCl ₂ (1.18 mM)	
CaCl ₂ (1.25 mM)	
NaH ₂ PO ₄ (1,23 mM)	
NaH ₂ SO ₄ (1,23 mM)	

2.5 Myocardial infarctions

After anesthetization according to the permitted animal proposal the mice chest was opened via a thoracotomy. For permanent myocardial infarctions (MI) a permanent suture with a 4/0 silk (Ethicon) ligation was stitched around the left anterior descending artery (LAD). Sham operated animals (Sham) underwent the same procedure but without ligation. The success of the infarction was monitored by an electro cardiogram (ECG) and a pale coloring heart. Mice underwent permanent MI for 1h, 1 day or 2 days. The recovery of the mice was monitored according to the animal license.

2.5.1 Liver function test

After the appropriate infarction time, after cervical dislocation livers and hearts were isolated and blood was taken from the right heart chamber for liver function tests. The blood was collected in Ethylenediaminetetraacetic acid covered tubes (EDTA-tubes) and centrifuged for 5 min at 2000 rpm at 4°C. The supernatant (Plasma) was diluted 1:10 and measured for ALT, AST and LDH with Liver-1 test stripes (Arkray) in a Spotchem EZ-SP 4430 (Arkray). Livers were deep frozen on liquid nitrogen for protein analysis or fixed in 4% PFA for immunohistochemical analyses.

2.5.2 Infarction size determination

The hearts were isolated for infarction size per area at risk analyses. Therefore, hearts were cannulated over the aorta and perfused with 1% evensblue in NaCl solution. After 1 hour of freezing the hearts were cut into 1 mm sections. Sections were incubated in 500 µl 1% Triphenyltetrazoliumchlorid (TTC) solution for 10 min at 38°C. Afterwards sections were placed on slides and captured with a Nikon SMZ stereomicroscope. The infarction area and the area at risk was determined with the help marker tool DISCUS software, differentiating white (dead cells) and red (living cells) areas per left ventricle area. The TTC is a redox stain and labels all viable cells by its Formazan state (red) when its reduced by dehydrogenases from living cells. In dead cells TTC will stay in its oxidized form and will be clear (white).

TTC-Solution	
14,2 g Na ₂ HPO ₄ in 1 l H ₂ O	80 ml
6 g NaH ₂ PO ₄ in 0,5 l H ₂ O	20 ml

Bring buffer to pH 7.4 add 100 mg TTC to 10 ml buffer.

2.6 *In vitro* studies

For *in vitro* studies, primary cells from human organ donors were used. Human liver sinusoidal microvascular endothelial cells (LSECs, PB-CH-153-5511, PELOBiotech) were cultured in microvascular endothelial cell growth medium kit enhanced (PB-MH-100-4099, PELOBiotech) and used up to passage (P) 7. Cryopreserved human hepatocytes (Invitrogen and KalyCell) were directly plated and used without expansion. CHRM® (CM7000), Williams E medium (CM6000) plus thawing supplement pack (CM300) and cell maintenance supplement pack (CM4000 (Invitrogen), as well as thawing (PB-KLC-TM), seeding (PB-KLC-SM) and maintenance medium plus additive 1 and additive 2 (PB-KLC-MM-Kit-50) (KalyCell) and rat collagen type I (1:1000) for coating (A10483-01, ThermoFisherScientific) were used as recommended by the companies to culture human hepatocytes.

2.6.1 LSEC cell length determination

Bright field images of LSECs were taken with and without mechanical stretching in STREX chambers with a Nikon Eclipse microscope. The length of the LSECs was determined by using length-measuring tool in FIJI (ImageJ). For visualization of LSEC length the stretch chambers were cut out and placed on SuperFrost-slides (ThermoFischerScientific). Afterwards, slides were stained with Phalloidin (A12379, Invitrogen) diluted 1:200 and DAPI (Sigma) diluted 1:1000 in PBS⁺ for 1 h at room temperature. LSM z-stacks images were taken, 100 cells per image and 3 images per $n = 1$ was quantified.

2.6.2 Coculture

For coculture, LSECs were plated on stretch chambers (STREX, ST-CH-04-BR, BioCat), pre-coated with speed coat solution (PB-LU-000-0002-00, PELOBiotech), and mechanically stretched for 1.5 hours in medium without supplements after 1 hour starvation. After mechanical stretching of LSECs, the conditioned medium was transferred to human hepatocytes in 6-well plates and incubated for 6 hours prior to collection for protein analyses. Alternatively, human hepatocytes were plated on Nunc® Lab-Tek® Chamber Slides™ (Lab-Tek, 177445) and incubated for 6 hours with addition of EdU (C10337, ThermoFisherScientific) to allow immunohistochemical analyses. One well (1 cm²) with hepatocytes was quantified for cell proliferation analyses and counted as $n = 1$.

2.7 Immunostaining and imaging

2.7.1 Cryosectioning

After WEC or directly following their isolation, embryos or livers were fixed with 4% PFA overnight at 4°C and subsequently equilibrated in 15% and 30% sucrose for cryopreservation. Afterwards, embryos were put transversally and left or right lobe of adult livers with the visceral side down into Peel-A-Way® embedding molds (Polyscience Inc., Germany), filled with OCT compound embedding medium (Tissue-Trak®, Sakura Finetek GmbH, Germany), frozen down, and stored at -80°C. A cryostat microtome HM 560 (ThermoFischer Scientific) and MX35 premier microtome blades (ThermoFischer Scientific) were used to obtain consecutive 12 µm cryosections that were placed onto SuperFrost-slides (J1800AMNZ, ThermoFischer Scientific).

2.7.2 Morphometric analysis

For morphometric analysis of embryonic livers, embryos were isolated and cryosectioned as described above. All consecutive sections of the embryonic liver were kept to be counted. For E11.5 embryos every 8th, for E12.5 embryos every 10th and for E13.5 embryos every 12th liver section was collected. For morphometric analysis, the DAPI stained liver area was determined by circulation with the marker tool in FIJI (ImageJ). For calculation of the liver volume the liver areas of all sections were extrapolated by multiplying the area average with the tissue section and slide number and section thickness.

2.7.3 Immunostaining

Immunostainings were performed according to the protocols in Nature Protocols (Zeeb et al., 2012). Slides were washed 5 min in PBS⁺ and 5 min in 0.02% Triton-X-100 in PBS⁺, before blocked with 150 µl blocking solution per slide in a humid chamber for 1 hour. Primary human cells were stained with the same protocol, but with 0.1% Saponin (Sigma) instead of Triton-X-100. For immunostaining of cryosections and human primary cells the following primary antibodies were used:

Primary Antibodies	Dilution
Goat anti-mouse Lyve-1 (AF2125, R&D)	1:200
Rabbit anti-mouse Lyve-1 (abcam, AB14917)	1:200
Goat anti-VEGFR3 (AF743, R&D)	1:50
Rat anti- β 1 Integrin (MAB1997, Millipore)	1:200
Rat anti-activated β 1 integrin (553715, BD)	1:200
Rabbit anti-phospho histone H3 (06-570, Millipore)	1:200
Rabbit anti-Caspase3, active (C8487, Sigma)	1:200
Goat anti-ICAM-1 (AF796, R&D)	1:50
Rabbit anti-ICAM-1 (10020-1-AP, Proteintech)	1:200
Rabbit anti-human HNF4- α (C11F12, Cell Signaling)	1:50

Primary antibodies were diluted in blocking solution as listed above and slides were incubated with 150 μ l per slide for 1 hour at room temperature (RT) or overnight at 4°C. After incubation the slides were washed twice 15 min in PBS⁺ and once for 15 min in 0.02% Triton-X-100 in PBS⁺. The following secondary antibodies were used:

Secondary Antibodies	Species	Dilution
Alexa Fluor 555 (Molecular Probes)	donkey anti-rabbit/goat	1:500
Alexa Fluor 488 (Molecular Probes)	donkey anti-rabbit/goat/rat	1:500
Cy5 (Jackson Immuno Research)	donkey anti-rat/goat/rabbit	1:500
Dapi (Sigma)	all nuclei	1:1000

Secondary antibodies were diluted in blocking solution and slides were incubated for 45 min at RT. Afterwards slides were washed 3x 15 min in PBS⁺ and mounted with fluoroshield (FG182, Sigma) and a coverslip. Mounted slides were directly imaged or stored at 4°C.

2.7.4 EDU Click-IT® reaction

According to the protocol provided by the company (Life Technologies), staining of proliferating cells which were allowed to incorporate with EDU during incubation time, was performed. EdU Click-IT reaction (Life Technologies) was performed on cryosections of WEC embryos or on chamber slides with primary human hepatocytes after treatment with different media. EDU Click-IT reaction buffer was incubated for 30 min on the slides previous to standard staining protocol.

Click-IT reaction buffer	Content [μl]
2x Click-iT reaction buffer	392
CuSO ₄	10
Oregon Green 488 azide	2.5
Click-iT EdU buffer additive	100

2.7.5 Proximity ligation assays (PLA)

The proximity ligation assay (PLA) was used to detect tyrosine phosphorylations on or next to VEGFR3. The PLA was performed on cryosections and stretch chambers according to the protocol recommended by the company (Olink Bioscience). For detection of tyrosine phosphorylation, a mouse anti-phospho-tyrosine antibody (05-1050, Millipore) was used in combination with goat anti-VEGFR3 (R&D, AF743). For counterstaining, rabbit anti-mouse LYVE-1 (AB14917, Abcam) or AF488 phalloidin for human LSECs were used. For PLA labeling anti goat-Plus-Probe (Duolink DUO92003, Sigma), anti mouse-Minus-Probe (Duolink DUO92004, Sigma), and Duolink in situ detection reagent orange (Duolink DUO92007, Sigma) were used.

2.7.6 Imaging and image analysis

Brightfield images were taken with a Nikon SMZ1500 stereomicroscope. For the capturing of all immunofluorescent sections, an Axio Vert LSM710 confocal laserscanning microscope (Zeiss) was used. For area quantification, a certain threshold was set in FIJI (ImageJ). For the analysis of endothelial cell staining, a mask was used to only measure the staining in the endothelial cell area (the latter stained for LYVE-1 or ICAM-1). Images with proliferating cells and PLA dots were taken as z-stacks and cells or dots were counted manually in FIJI (ImageJ). Averages of 3 to 5 images were quantified as n = 1. If images were edited, images that were compared with each other were always handled in the same way. For presentation γ -value was set to 0.9 and a Gaussian blur was applied.

2.8 ELISA

Embryonic livers were isolated in ice-cold PBS and washed in 1% PhosStop (04906837001, Roche). Afterwards, they were lysed in 100 µl ice-cold lysis buffer and sheared with a 1 ml syringe (Terumo). For E11.5 embryos five livers and for E12.5 livers two livers were pooled into one lysate to get a sufficient amount of protein. E13.5 livers were lysed separately. Parts of deep-frozen adult livers (approx. 0.02 g) were placed with 1 ml lysis buffer into a gentleMACS™ M Tube (Miltenyi Biotec) for tissue homogenization on gentleMACS Dissociator (Miltenyi Biotec) using the protein dissociation program.

Liver lysis buffer	Content
Hepes pH 7.0 (Carl Roth)	50 mM
NaCl (VWR)	150 mM
Glycerol (Sigma)	10%
Triton X-100 (Applichem)	1%
PhosStop phosphatase inhibitor (Roche)	1%
Complete cocktail protease inhibitors (Roche)	1%

Primary human cells were lysed with a protein lysis buffer described above plus 1mM Na_3VO_4 (Sigma). After homogenization, all lysates were centrifuged to remove cell trash. Supernatants were immediately measured for protein content using BCA assay (Pierce™ BCA Protein Assay Kit, 23225, ThermoFisherScientific) and stored at -80°C . All ELISAs were performed according to the protocols from the company (R&D, Germany) and all samples were measured in duplicates. DuoSet IC phospho-tyrosine-VEGFR3 normalized to total-VEGFR3 (DYC2724-2 and DYC3491-5, R&D) and DuoSet phospho-c-Met normalized to total-cMet (DYC2724-2 and DYC3491-5, R&D) were used for mouse liver lysates. DuoSet IC phospho-tyrosine-VEGFR3 and phospho-tyrosine-c-Met ELISAs were used for human primary cell lysates. Furthermore, mouse HGF DuoSet ELISA (DY2207, R&D) was used for liver lysates; human HGF DuoSet ELISA (DY294, R&D) was used for cell culture supernatants. GAPDH ELISA was used as control protein during ELISA experiment (DYC5718-5, R&D).

2.9 Statistical analysis

All data are means \pm standard deviation (SD). Unpaired two-tailed Student's t-tests or one-way ANOVAs with Tukey's post-hoc test were performed for statistical analysis using Excel (Microsoft) or PRISM (Graph-Pad) software ($P < 0.05$ was considered statistically significant). All data are considered to underlay the Gaussian normal distribution. For data $n > 4$ QQ-Plots and for data $n > 5$ a Shapiro Wilk Test were performed using "R" software.

2.10 Personal Contribution

J. Axnick performed most of the experiments and was supervised for her thesis by E. Lammert.

L. Planas-Paz has previously worked on Flk1 Cre- β 1 integrin floxed embryos and handed over the line to J. Axnick.

As partner project in the SBF 974 T. Buschmann was involved in the preliminary orientation of the project and involved in first experiments for liver size and cell death analyses. T. Buschmann worked in parallel on liver regeneration.

C. Klüppel was supervised by J. Axnick and E. Lammert for her Bachelor Thesis in 2014 and performed in this regard previous WEC experiments, to find a proper incubation time and dose concentration for embryo manipulation.

L. Lorenz was supervised by J. Axnick and E. Lammert for her Master Thesis in 2015-2016 and performed in this regard the *in vitro* experiments with primary human cells. Planning of the experimental setup, analyses and interpretation were performed according to the supervision of the Master Thesis together with J. Axnick.

N. Eichhorst and T. Buschmann planned and designed *ex vivo* liver perfusions for mice. N. Eichhorst did *ex vivo* liver perfusions and J. Axnick did all further experimental steps, including analyses and interpretation.

S. Becher and C. Klüppel performed myocardial infarction surgeries. C. Klüppel did infarction size analyses. Bright-field imaging of hearts and livers, lysis and protein analysis or cryosectioning, staining and imaging and analysis and interpretation of the results were done by J. Axnick.

Within the collaboration S. Fang, H. Nurmi and K. Alitalo provided litters from breeding of Rosa Cre and VEGFR3 floxed mice as pre-fixed embryos or deep-frozen livers, according genotyping and KO efficiencies. J. Axnick did cryosectioning, staining and analyses or lysis of deep-frozen livers and protein analyses and interpretation.

3. Results

The hypothesis that blood perfusion acts as mechano-stimulus for the production of angiocrine signals that are important for liver growth and survival was investigated in this thesis. The involvement of endothelial $\beta 1$ integrin and VEGFR3 was also proven. Both molecules have mechanotransductive properties and are of high relevance for embryonic development (Planas-Paz et al., 2012). The hepatocyte growth factor was used as angiocrine signal of choice, as it was often shown to be a critical angiocrine signal and even has dramatic effects on embryonic development (Rafii et al., 2016; Schmidt et al., 1995). Mouse embryos were chosen to investigate liver growth and the contribution of mechanostimulated angiocrine signals in this manner. Mouse embryos are easy to access, provide high similarities to the human genetic background and developmental setups are often used for the discovery of regeneration processes or diseases (Hata et al., 2007; Zeeb et al., 2012). Additionally, adult mouse livers were analyzed to confirm findings made in embryo model system and human primary cells were used to transfer the findings also to the human system. Finally, a model system for human cardiogenic hepatic dysfunctions was established.

3.1 Embryonic liver growth

First, liver growth was analyzed in wild-type (wt) embryos. E11.5, E12.5 and E13.5 mouse embryos (fig. 3.1 a-c) and their livers (fig. 3.1 a'-c') were visually analyzed. During this period, the liver growth visibly increases in size (fig. 3.1 d). For further growth analyses, the embryos were cut transversally and a morphometric analysis of the liver size was performed, whereby it was found that the liver volume dramatically increases from E12.5 to E13.5 (fig. 3.1 e).

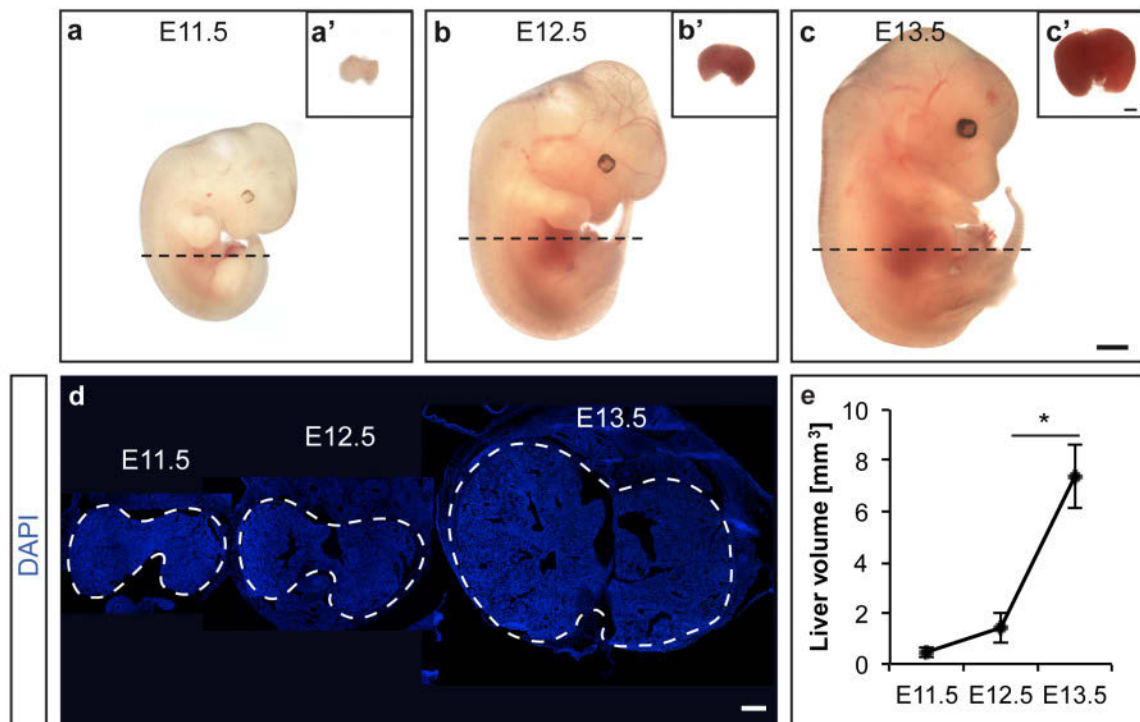


Figure 3.1: Liver growth during murine embryonic development. (a-c) Representative bright field images of (a) E11.5, (b) E12.5, and (c) E13.5 mouse embryos, and (a'-c') their isolated livers. The dotted lines indicate the areas of cross-sections used for image analyses. (d) Representative images of transversal cross-sections through E11.5, E12.5, and E13.5 livers (surrounded by dashed lines) stained with DAPI (cell nuclei, blue). (e) Embryonic liver volume assessed via morphometric analyses (n = 3). Scale bars in (a-c), 1 mm; (a'-c') 500 μ m; (d) 300 μ m. Reported values are the mean \pm standard deviation. Statistical significance was determined using Student's t-tests (* $P < 0.05$).

3.1.1 Perfusion of the liver periphery and peripheral liver growth zones

As the liver is growing dramatically after E12.5, the perfusion of liver vessels was visualized using vascular painting. Ricinus communis agglutinin (RCA) was injected into the beating heart of E11.5 and E12.5 wt embryos, which were afterwards cultured for 3 hours in WEC, allowing the RCA to bind to all perfused vessels. With the help of vascular painting, it was shown that in E11.5 wt embryos perfusion starts in the liver periphery (fig. 3.2 a-c), which expands to full liver perfusion in E12.5 wt embryos (fig. 3.2 d-f).

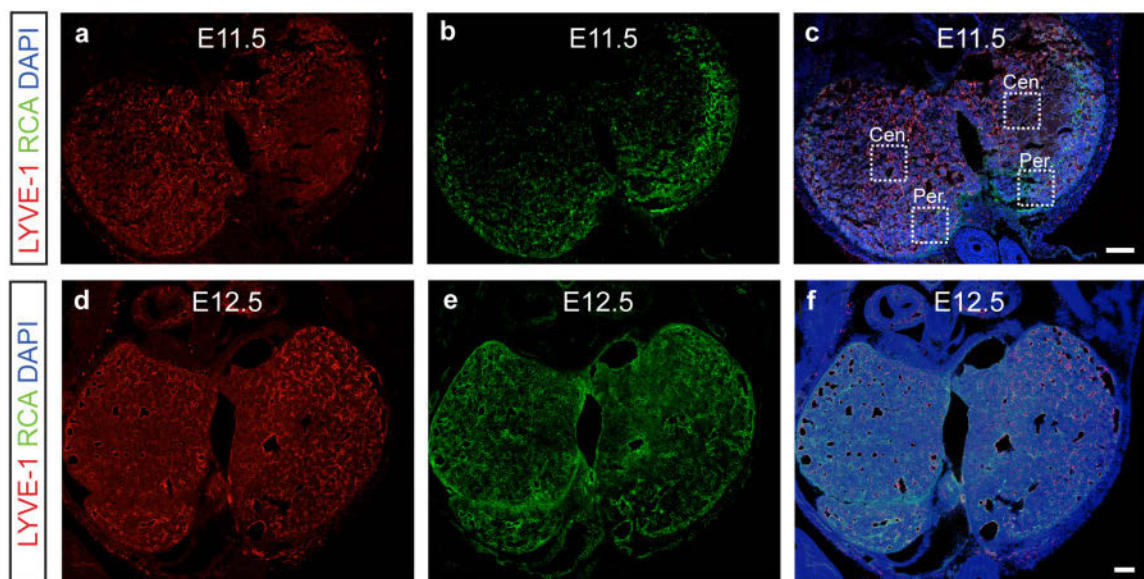


Figure 3.2: Hepatic vascular perfusion. (a-f) Representative images of transversal cross-sections through (a-c) E11.5 and (d-f) E12.5 livers stained for (a,d) hepatic blood vessels using LYVE-1 (red) and (b,e) perfused vessels using vascular painting with *ricinus communis agglutinin* (RCA, green). (c,f) Merge with DAPI (blue). ('Cen.' for center and 'Per.' for periphery). Scale bars indicate 200 μm .

After injection of EdU into the developing liver followed by 3 hours of WEC, a growth zone of proliferating cells in the liver periphery was observed in E11.5 wt embryos (fig. 3.3), compared to less-proliferating cells in the liver centers.

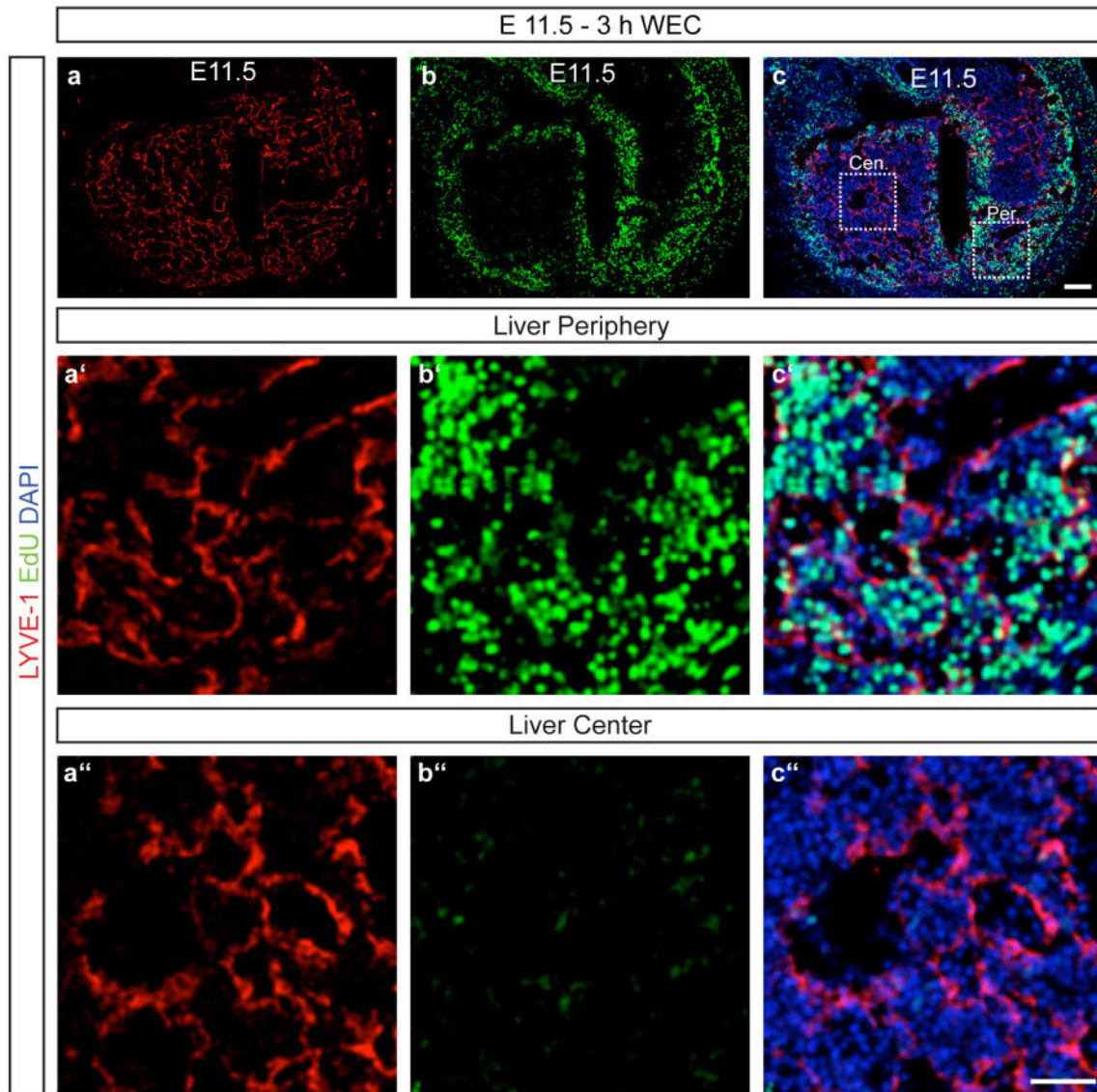


Figure 3.3: Hepatic cell proliferation in perfused liver periphery versus non-perfused liver center at E11.5. (a-c) Representative images of transversal cross-sections through E11.5 livers after whole embryo culture (WEC) for 3 h in the presence of 5-Ethynyl-2'-deoxyuridine (EdU) to detect proliferating cells. Sections were stained for (a) LYVE-1 (red), (b) EdU (green), and (c) merge with cell nuclei (DAPI, blue). Magnified fields of view in (a'-c') the liver periphery, and (a''-c'') the liver center. Areas of magnification are indicated in panel c by white boxes labeled with 'Cen.' and 'Per.' for liver center and periphery, respectively. Scale bars indicate in (a-c) 100 μ m and in (a'-c'') 50 μ m.

We conclude that blood perfusion starts in liver periphery at E11.5, where growth zones are located. The organ grows dramatically from E12.5 onwards, after the whole liver was perfused.

3.1.2 Liver vessels have specialized ECs and peripheral activation of $\beta 1$ integrin and tyrosine phosphorylation of VEGFR3

LSECs are known to be very specialized ECs as they express lymphatic markers, e.g. Lyve-1 (here used as blood vessel marker for embryonic liver vessels) and VEGFR3 (Si-Tayeb et al., 2010). $\beta 1$ integrin is expressed in all cell types of the liver, but it also colocalizes with VEGFR3 on LSECs (fig. 3.4 a). Mechanoactivation of $\beta 1$ integrin followed by VEGFR3 signaling was shown to be involved in lymphatic vessel development (Planas-Paz et al., 2012). Therefore, activation of $\beta 1$ integrin as well as tyrosine phosphorylation of VEGFR3 in perfused peripheral liver growth zones of E11.5 embryos compared to non-perfused center regions of the same livers were analyzed (see boxes indicated in fig. 3.2 c). In the perfused peripheral growth zones, $\beta 1$ integrin was significantly more activated compared to non-perfused center regions (fig. 3.4 b). In addition, the peripheral zones showed significantly increased tyrosine phosphorylation of VEGFR3 (fig. 3.4 c).

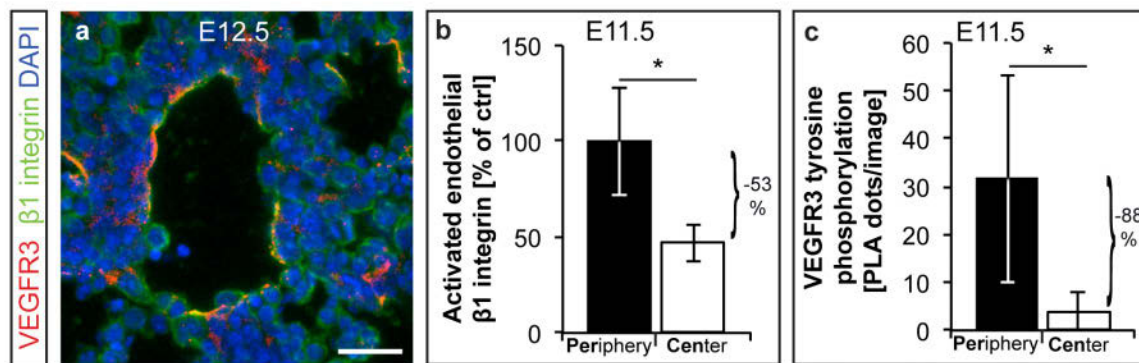


Figure 3.4: Specialized liver vessels and peripheral $\beta 1$ integrin activation and VEGFR3 tyrosine phosphorylation on LSECs. (a) Representative image of blood vessels in an E12.5 liver stained for $\beta 1$ integrin (green), VEGFR3 (red) and cell nuclei (DAPI, blue). (b) Activation of endothelial $\beta 1$ integrin ($n = 6$) and (c) tyrosine phosphorylation of VEGFR3 based on proximity ligation assay (PLA, $n \geq 5$) in E11.5 liver periphery versus liver center; example regions are indicated by boxes in figure 3.3 c. Scale bar (a) 25 μm . Reported values are the mean \pm standard deviation. Statistical significance was determined using Student's t-tests ($*P < 0.05$).

3.2 Correlation of heart beat, VEGFR3 tyrosine phosphorylation and HGF expression in the growing liver

The blood perfusion of organs is ensured by a regular pumping heart. Since perfusion at the liver periphery in embryos correlates with activation of β 1 integrin and VEGFR3 tyrosine phosphorylation, we ask whether the perfusion of the liver vessels acts as a mechano-stimulus for angiocrine signaling in the developing liver. Hepatocyte growth factor is known to be a major angiocrine signal and to be important for liver development (Ding et al., 2010; Schmidt et al., 1995). Therefore, HGF was chosen to investigate perfusion-induced angiocrine signaling in the developing liver.

To further investigate if the activation of β 1 integrin and the tyrosine phosphorylation of VEGFR3 (presented in 3.1.2) were induced by the perfusion of the liver vessels, loss- and gain-of-perfusion experiments were performed. Therefore, E11.5 embryos were cultured in WEC with either heart block or increased heartbeat for 1 hour.

3.2.1 Loss-of-perfusion experiments

In E11.5 wt embryos a heart block was induced by adding of 2,3-Butanedione monoxime (BDM) to WEC medium to eliminate blood perfusion. The experiment was repeated with KCl as an alternative heart blocker to confirm the results (data not shown). For the short incubation time the survival of the embryos was ensured by the culture conditions, as previous experiments showed that 1 hour of WEC incubation did not have an effect on the survival of the embryonic tissue even with blockade of heart beat (supervision of the bachelor thesis from C. Klüppel – data not shown here). The complete heart block was observed within the first minutes of incubation (video documentation of time until heart block - data not shown).

After *ex vivo* cultivation, the heartbeats of control and heart blocked embryos were checked. In all BDM treated embryos, a complete cardiac arrest was observed (-100% to control, fig. 3.5 a). A time-lapse video analysis of the embryonic heartbeat after WEC was performed to visualize heartbeats of control and treated embryos. Representative images of empty, half full or filled embryonic ventricles are shown (fig. 3.5 b).

In non-perfused embryos, endothelial β 1 integrin was less activated (-54% to control, fig. 3.5 c) and less VEGFR3 tyrosine phosphorylation was observed (normalized to total VEGFR3 and total protein) (ELISA, -75% to control, fig. 3.5 d). Protein analyses showed that HGF levels were down regulated (-30% to control) in heart blocked embryos (fig. 3.5 e), but the level of control protein was not changed significantly (fig. 3.5).

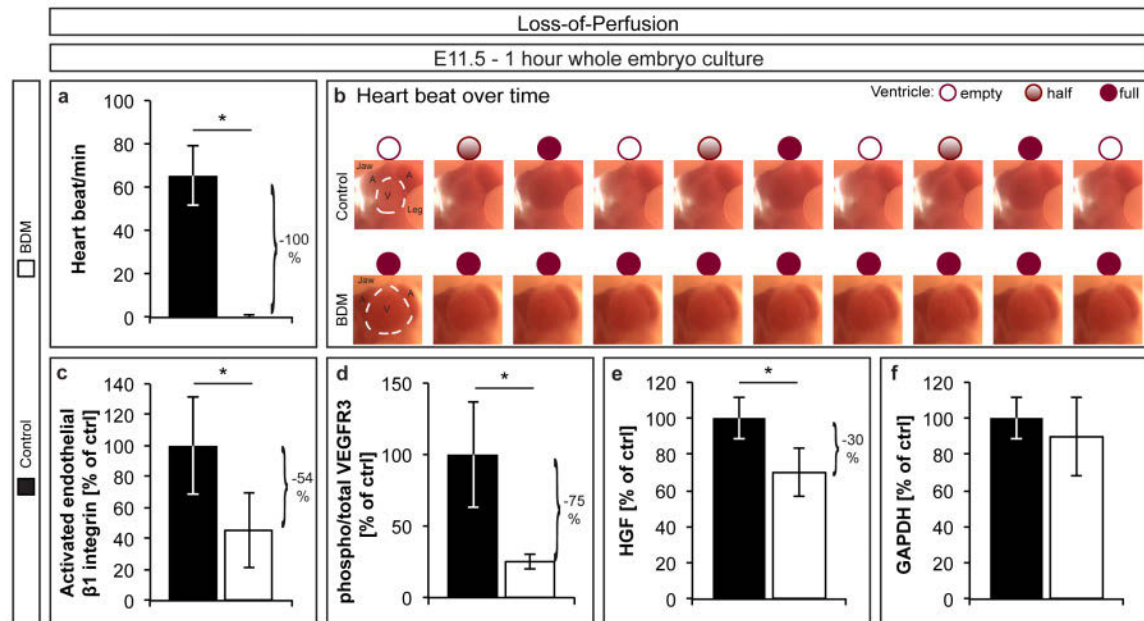


Figure 3.5: Loss-of-perfusion. (a-f) Pharmacologic loss-of-perfusion experiments in *ex vivo* cultivated E11.5 mouse embryos. The heart rate was entirely stopped using 2,3-Butanedion monoxime (BDM). (a) Embryonic heart rate (heartbeats per minute) one hour after treatment ($n \geq 10$). (b) Time-lapse images of the beating heart with schematic illustrations of empty, half-filled and filled ventricles on top. Both treatment and control images were taken at the same, evenly-spaced time points over approximately 5 seconds. (c) Quantification of fluorescence area of staining for activated $\beta 1$ integrin on LYVE-1⁺ hepatic endothelial cells ($n \geq 3$). (d) Hepatic VEGFR3 tyrosine phosphorylation normalized to total VEGFR3 (both determined by ELISA) and total protein ($n \geq 5$), (e) hepatic HGF protein concentration normalized to total protein ($n = 3$). (f) The protein concentration of hepatic GAPDH taken as a control protein normalized to total protein in the growing liver ($n = 4$). Reported values are the mean \pm standard deviation. Statistical significance was determined using Student's t-tests ($*P < 0.05$).

3.2.2 Gain-of-perfusion experiments

In gain-of-perfusion experiments, epinephrine bitartrate (epinephrine) was added to the culture medium to increase heart rate and the perfusion of E11.5 embryos. After *ex vivo* cultivation, the heart rate of epinephrine treated embryos was increased compared to control embryos (+29% to control, fig. 3.6 a). A time-lapse video analysis of the embryonic heartbeat after WEC was performed to visualize heartbeats of control and epinephrine treated embryos. Representative images of empty, half full or filled embryonic ventricles are shown (fig. 3.6 b).

The higher perfusion rate, caused by a faster beating heart, increases $\beta 1$ integrin activation on the liver endothelial cells (+37% to control, fig. 3.6 c). VEGFR3 tyrosine phosphorylation (+145% to control) as well as HGF levels were higher in embryos with increased heart rate (+30%, fig. 3.6 d and e). GAPDH as control protein was not changed (fig. 3.6 f).

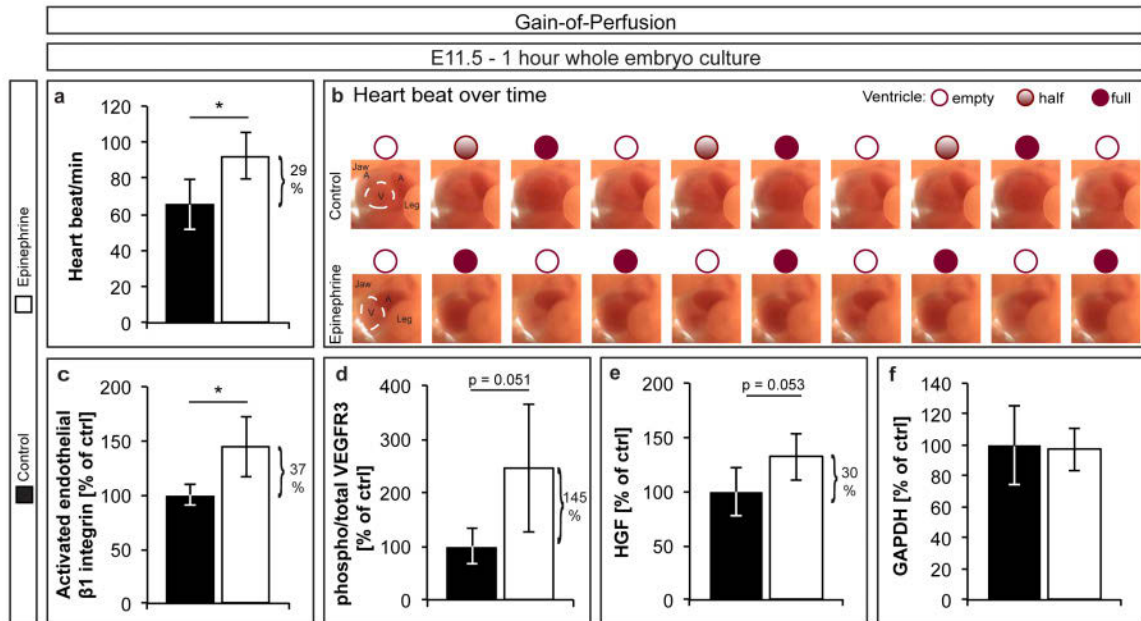


Figure 3.6: Gain-of-perfusion. (a-f) Pharmacologic gain-of-perfusion experiments in *ex vivo* cultivated E11.5 wt mouse embryos. The heart rate was increased with epinephrine. (a) Embryonic heart rate (heartbeats per minute) one hour after treatment (n = 13). (b) Time-lapse images of the beating heart with schematic illustrations of empty, half-filled and filled ventricles on top. Both treatment and control images were taken at the same, evenly-spaced time points over approximately 5 seconds. (c) Quantification of fluorescence area of staining for activated $\beta 1$ integrin on LYVE-1⁺ hepatic endothelial cells (n \geq 3). (d) Hepatic VEGFR3 tyrosine phosphorylation normalized to total VEGFR3 (both determined by ELISA) and total protein (n \geq 3) (e) hepatic HGF protein concentration normalized to total protein (n \geq 4). (f) The protein concentration of hepatic GAPDH taken as a control protein normalized to total protein in the growing liver (n = 4). Reported values are the mean \pm standard deviation. Statistical significance was determined using Student's t-tests (**P* < 0.05).

We could show that endothelial $\beta 1$ integrin activation as well as VEGFR3 tyrosine phosphorylation and HGF levels in the developing embryo liver are dependent on vascular perfusion of the organ, or rather the heartbeat.

3.3 Deletion of endothelial $\beta 1$ integrin

As $\beta 1$ integrin is well-known in mechanotransduction on EC and lymphatic ECs (Planas-Paz et al., 2012; Ross et al., 2013), it was chosen to be investigated in this work. To genetically prove if endothelial $\beta 1$ integrin is activated in a perfusion dependent manner and is followed by VEGFR3 tyrosine phosphorylation, endothelial specific KO of $\beta 1$ integrin were analyzed. Flk-1 Cre- $\beta 1$ integrin floxed embryos were directly isolated or *ex vivo* cultivated for either immunohistochemical or protein analyses. Heterozygous embryos were chosen as controls. The Flk-1 Cre was chosen as promoter as the deletion of $\beta 1$ integrin is effective from E11.5 onwards and the survival of the embryos is ensured over the initial liver developmental processes. It was shown before that those Flk-1 Cre- $\beta 1$ integrin homozygous embryos are embryonic lethal by E14.5 (Planas-Paz et al., 2012).

3.3.1 Endothelial $\beta 1$ integrin deletion on LSECs

Cryosections of the liver region from Flk-1 Cre- $\beta 1$ integrin floxed embryos were stained immunohistochemically and analyzed to visualize the success of the $\beta 1$ integrin deletion on liver endothelial cells. It could be shown that $\beta 1$ integrin is reduced by 51% on endothelial cells (fig. 3.7). Because of resolution limitations the knockout efficiency is indeed significantly reduced, but not precisely detectable with this method. A single cell sorting from liver single cell lysates was attempted, but sorted cells were not free from hepatocytes (data not shown).

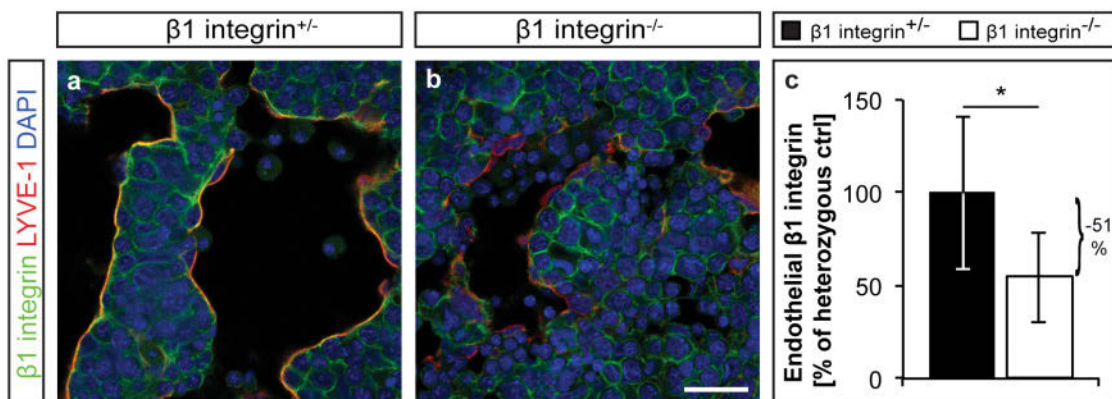


Figure 3.7: Endothelial $\beta 1$ integrin deletion on LSECs. (a,b) Transversal cross-sections through E13.5 mouse livers with endothelial cell-specific (a) heterozygous ($\beta 1$ integrin^{+/-}, control) and (b) homozygous ($\beta 1$ integrin^{-/-}) deletion of $\beta 1$ integrin. Sections were stained for LYVE-1 (red), $\beta 1$ integrin (green), and cell nuclei (DAPI, blue) to visualize the deletion in LSECs. (c) Quantification of endothelial $\beta 1$ integrin on liver sections of $\beta 1$ integrin^{+/-} and $\beta 1$ integrin^{-/-} mouse embryos ($n \geq 4$). Scale bar indicates 25 μm . Reported values are the mean \pm standard deviation. Statistical significance was determined using Student's t-test (* $P < 0.05$).

3.3.2 Endothelial $\beta 1$ integrin is required for growth of the developing liver

Liver growth of endothelial specific knockouts of $\beta 1$ integrin embryos was analyzed. Even with a macroscopic analysis, livers of homozygous KO embryos seem to be smaller (fig. 3.8 a-a'' and b-b'') compared to heterozygous KO embryos. For an exact quantification of the liver volume, embryo cross-sections of the liver region were stained immunohistochemically with DAPI for cell nuclei and a morphometric analysis was performed. E13.5 endothelial $\beta 1$ integrin KOs show a significant smaller liver compared to heterozygous controls (-30% liver volume, fig. 3.8). The effect was observed already at E12.5, but was not significant (data not shown).

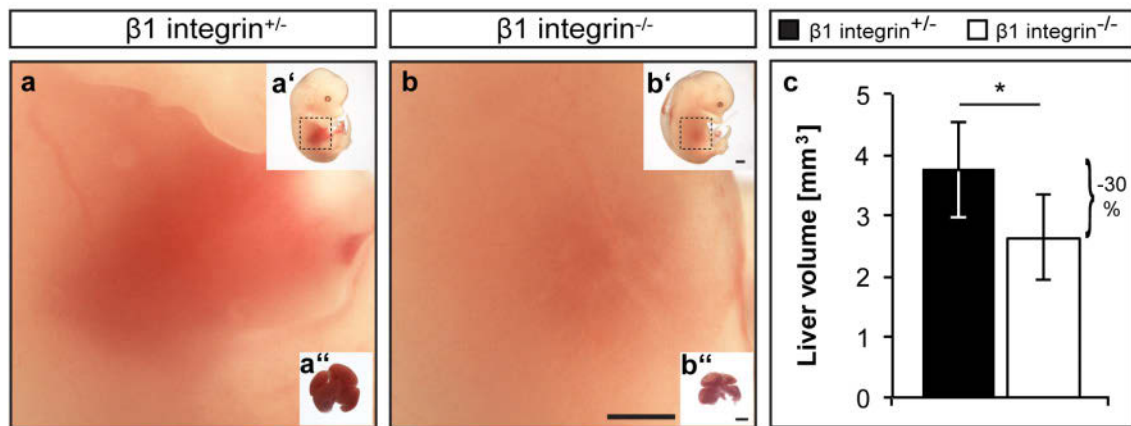


Figure 3.8: Endothelial $\beta 1$ integrin is required for growth of the developing liver. (a,b) Representative bright field images of (a, a', a'') $\beta 1$ integrin^{+/+} and (b, b', b'') $\beta 1$ integrin^{-/-} (a', b') E13.5 mouse embryos, (a, b) their abdomen (as outlined on the embryo), and (a'', b'') E14.5 livers. (c) Volume of livers isolated from E13.5 $\beta 1$ integrin^{+/+} and $\beta 1$ integrin^{-/-} embryos (n = 6). Scale bars indicate (a,b) 500 μ m, (a',b') 1 mm, (a'',b'') 1 mm. All values are the mean \pm standard deviation. Statistical significance was determined using Student's t-tests (*P < 0.05).

3.3.3 Endothelial $\beta 1$ integrin is required for organ survival and proliferation in the developing liver

To determine why the livers of endothelial specific $\beta 1$ integrin KO embryos are significantly smaller, cell proliferation and cell death were analyzed by immunofluorescent staining on liver cross-sections. The total cell proliferation was reduced in homozygous KO embryos analyzed by p-H3 staining on cryosections (fig. 3.9). The separate count of ECs and parenchymal cells showed that both cell populations had significantly less proliferation (data not shown).

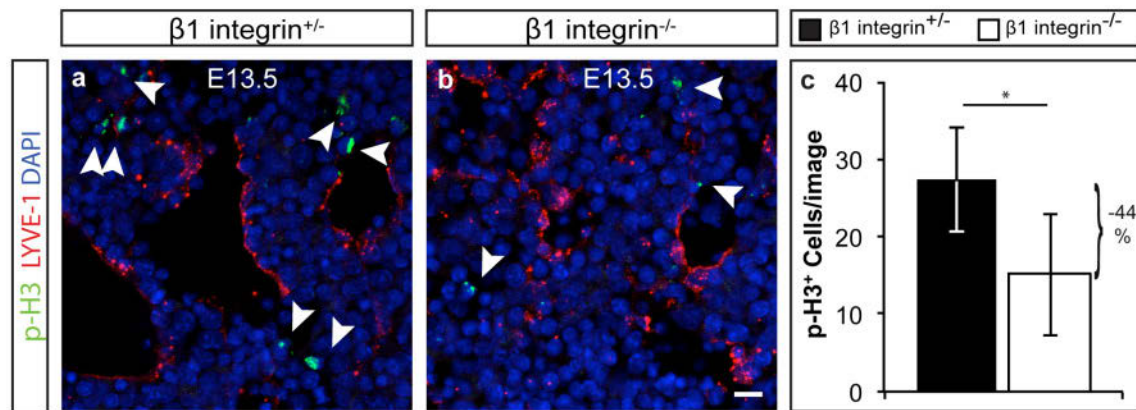


Figure 3.9: Endothelial $\beta 1$ integrin is required for cell proliferation in the developing liver. (a,b) Representative transversal sections through E13.5 livers of (a) $\beta 1$ integrin^{+/+} (control) and (b) $\beta 1$ integrin^{-/-} embryos stained for p-H3 (green, arrows pointing to proliferating cells), LYVE-1 (red) and cell nuclei (DAPI, blue). (c) Quantification of p-H3 positive cells per image of sections through E13.5 $\beta 1$ integrin^{+/+} and $\beta 1$ integrin^{-/-} livers (n = 6). Scale bar indicates 10 μ m. All values are means \pm standard deviation. Statistical significance was determined using Student's t-tests ($*P < 0.05$).

Apoptosis was analyzed by active caspase-3 staining on cross-sections. Apoptotic regions were identified in the liver periphery of homozygous endothelial specific $\beta 1$ integrin KO embryos, but never in the heterozygous controls. Interestingly those regions were also the first perfused, representing a growth zone for the early liver (E11.5), shown in 3.1. Active caspase-3 staining was significantly increased in homozygous endothelial specific $\beta 1$ integrin KO embryos (+106%, fig. 3.10). All cell types in those regions were affected, including ECs as well as parenchymal cells. This effect was also found significantly in E12.0, E12.5 and E13.0 endothelial $\beta 1$ integrin KO embryos (data not shown). Thus, endothelial $\beta 1$ integrin KO embryos phenocopy mouse embryos with a global HGF deficiency, which also show caspase-3 in the liver periphery and have smaller livers overall (Schmidt et al., 1995).

We could show that proliferation defects as well as apoptosis both play a role in liver volume reduction of endothelial $\beta 1$ integrin KO embryos. Showing that those embryos have both a liver growth and survival phenotype.

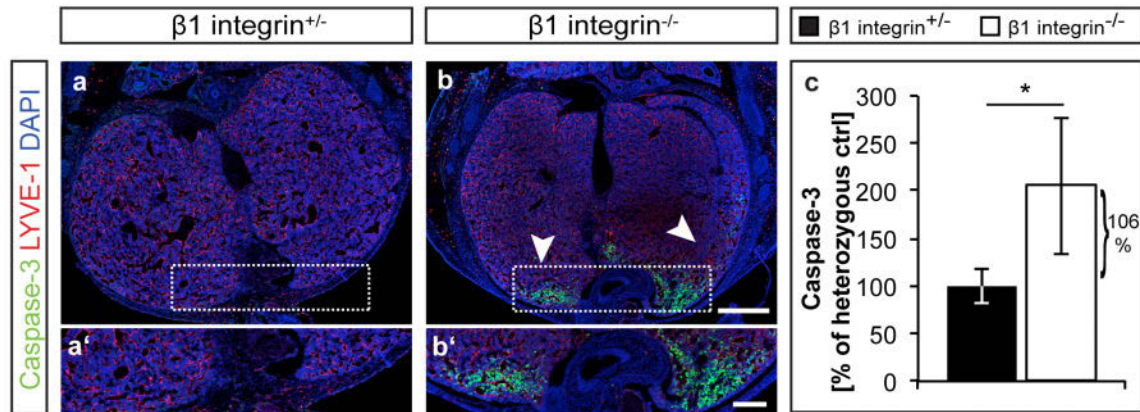


Figure 3.10: Endothelial $\beta 1$ integrin is required for the survival of the developing liver. (a,b) Representative transversal sections through E13.5 livers of (a) $\beta 1$ integrin^{+/+} and (b) $\beta 1$ integrin^{-/-} embryos stained for LYVE-1 (red), cleaved caspase-3 (green), and cell nuclei (DAPI, blue). (a',b') Magnifications of peripheral embryonic liver regions indicated in (a,b). (c) Quantification of active caspase-3⁺ area in E13.5 $\beta 1$ integrin^{+/+} versus $\beta 1$ integrin^{-/-} liver sections ($n \geq 5$). Scale bars indicate (a,b) 500 μm , and (a',b') 200 μm . All values are mean \pm standard deviation. Statistical significance was determined using Student's t-tests (* $P < 0.05$).

It was shown, that an endothelial deletion of $\beta 1$ integrin leads to decreased proliferation and increased cell death not just in ECs, but also in parenchymal cells as well as hepatocyte precursors (AFP and TUNEL staining, data not shown).

To exclude the possibility that cells at the liver periphery are dying because of a perfusion failure, vascular painting was performed in the endothelial $\beta 1$ integrin KO embryos. E13.5 hetero- and homozygous KOs were injected with RCA and *ex vivo* cultured for 3 hours, to paint all perfused vessels. Cross-sections of those liver regions showed that homozygous endothelial $\beta 1$ integrin KOs have a perfused liver, also in the active caspase-3 positive dying periphery, as seen in their heterozygous controls (fig. 3.11).

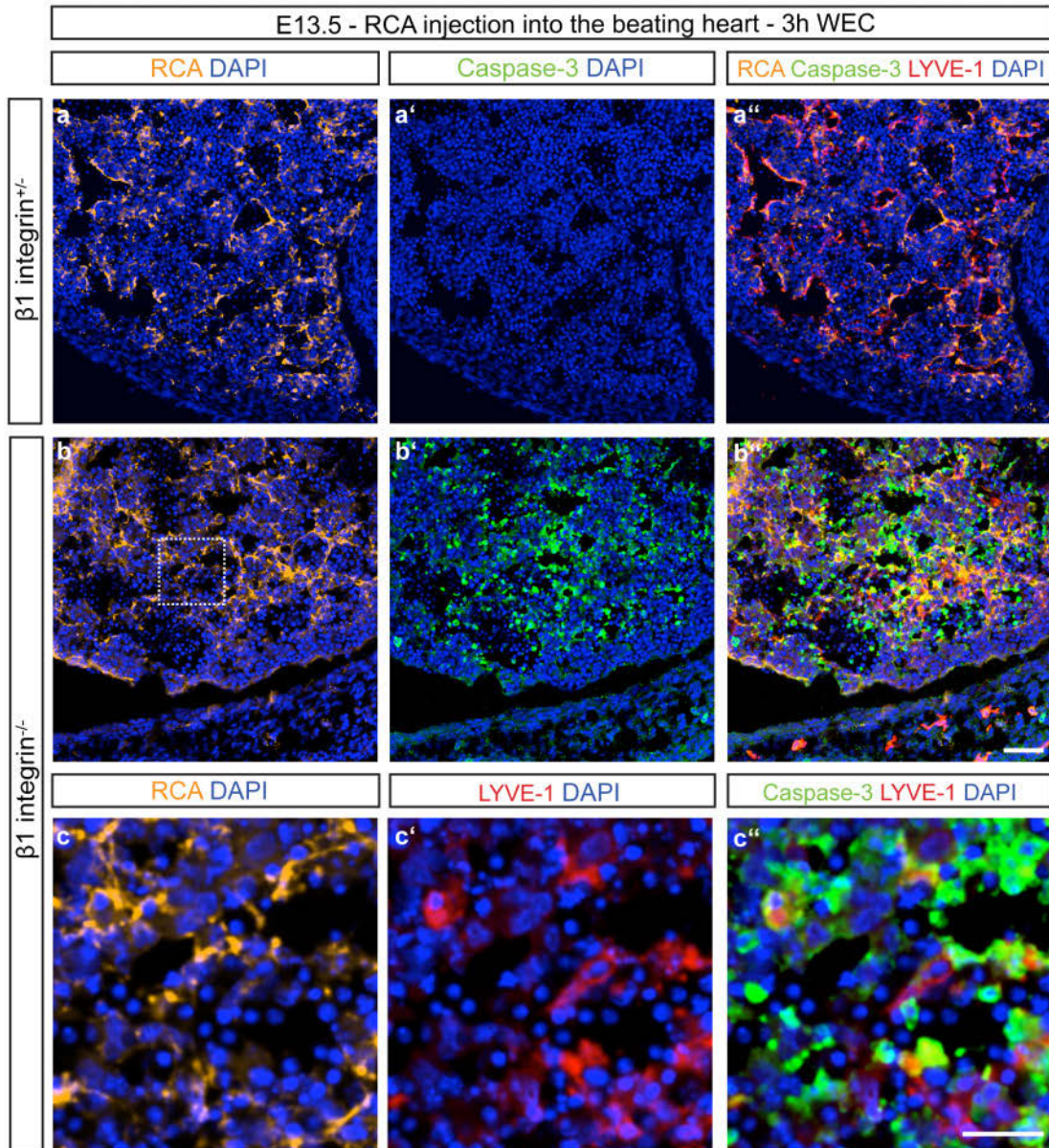


Figure 3.11: Cell death occurs in well-perfused liver regions of endothelial $\beta 1$ integrin-deficient mouse embryos. Representative transversal sections through E13.5 livers from (a-a'') $\beta 1$ integrin^{+/-} (control) and (b-c'') $\beta 1$ integrin^{-/-} embryos. To visualize perfused hepatic vessels, (a,b,c) RCA (orange) was injected into the beating heart and allowed to circulate for 3 hours in WEC. Sections were also stained for (a',b') Caspase-3 (active, green), (c') LYVE-1 (red) and cell nuclei (DAPI, blue). (a''-c'') Merged images. Scale bars (a-b'') 50 μ m and in (c-c'') 25 μ m.

Hypoxia in peripheral liver regions was excluded by Hif1- α staining. No difference in Hif1- α area was observed comparing $\beta 1$ integrin homozygous to heterozygous embryos (data not shown). We ruled out the possibility of hematopoietic stem cell abnormalities as the cause of the reduced liver size, because the number of CD34 positive cells was the same between $\beta 1$ integrin homozygous to heterozygous embryos (data not shown).

3.3.4 Endothelial $\beta 1$ integrin regulates VEGFR3 signaling and HGF levels

As $\beta 1$ integrin was previously described to interact with VEGFR3 (Planas-Paz et al., 2012; Zhang et al., 2005), VEGFR3 activation was analyzed in liver lysates of endothelial specific $\beta 1$ integrin KO. In liver lysates of E12.5 endothelial $\beta 1$ integrin KO, decreased VEGFR3 tyrosine phosphorylation normalized to total VEGFR3 (ELISA) was reduced (-53% to heterozygous control, fig. 3.12 a).

Hepatocyte growth factor (HGF) was analyzed, as it is a reported angiocrine signal (Ding et al., 2010) and an important growth factor for liver development (Schmidt et al., 1995). We have also shown that endothelial $\beta 1$ integrin KO embryos phenocopy the HGF KO embryos (Schmidt et al., 1995), as they both harbor a smaller liver and caspase-3 in the liver periphery (see fig. 3.8 and 3.10). The HGF level was found to be dependent on perfusion as shown above in loss- and gain-of-perfusion experiments (fig. 3.5 and 3.6). HGF levels were significantly decreased in liver lysates of $\beta 1$ integrin homozygous KO embryos (-69% compared to control, fig. 3.12 b). Levels of control protein GAPDH were not affected (fig. 3.12 c).

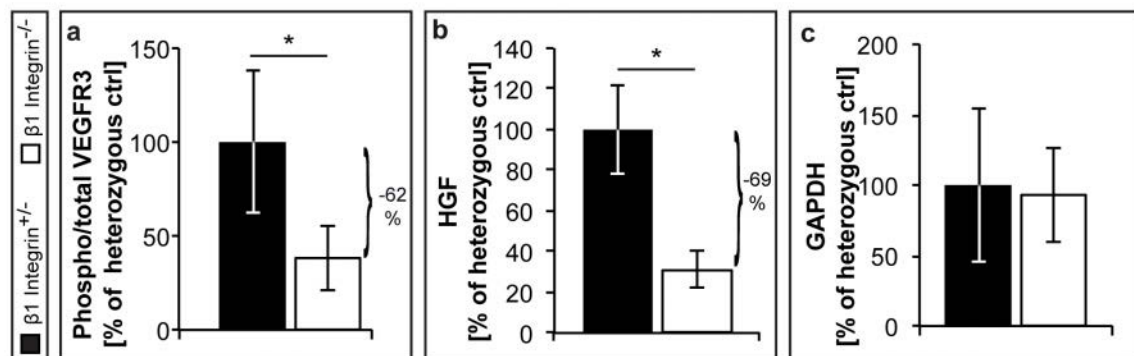


Figure 3.12: Endothelial $\beta 1$ integrin is required for VEGFR3 activation and angiocrine HGF production. (a) VEGFR3 tyrosine phosphorylation normalized to total VEGFR3 ($n = 4$), (b) HGF expression ($n \geq 4$), and (c) GAPDH expression ($n \geq 3$) in E12.5 liver lysates, all normalized to total protein (BCA) in $\beta 1$ integrin^{+/-} and $\beta 1$ integrin^{-/-} mouse embryos. Reported values are the mean \pm standard deviation. Statistical significance was determined using Student's t-tests (* $P < 0.05$).

We assume that endothelial $\beta 1$ integrin regulates angiocrine signals, which are needed for a proper liver growth and survival. Those findings lead to the conclusion that $\beta 1$ integrin is required for VEGFR3 tyrosine phosphorylation and HGF levels in the developing liver.

3.3.5 Endothelial $\beta 1$ integrin is required for perfusion-dependent VEGFR3 tyrosine phosphorylation

To support the hypothesis that $\beta 1$ integrin on ECs is mechanically activated by the perfusion of the liver vessels, gain-of-perfusion experiments were performed in endothelial $\beta 1$ integrin KO embryos. Hetero- and homozygous E11.5 KO embryos were *ex vivo* cultured with the addition of epinephrine to the culture medium for 1 hour. We could demonstrate that embryos with homozygous deletion of $\beta 1$ integrin were not able to respond to increased heart rate (fig. 3.13) and had no increase in VEGFR3 tyrosine phosphorylation in response to the faster beating heart, unlike their heterozygous controls.

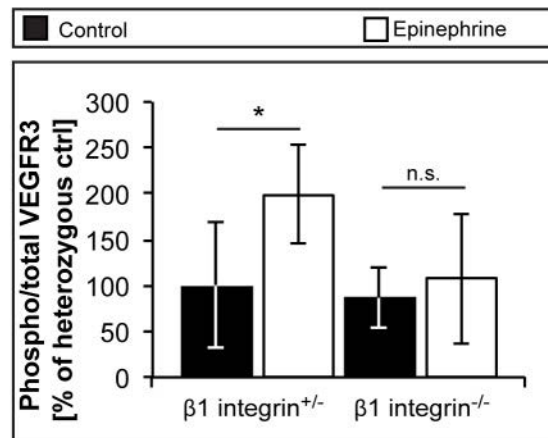


Figure 3.13: $\beta 1$ integrin is required for perfusion-dependent VEGFR3 tyrosine phosphorylation. Quantification of VEGFR3 tyrosine phosphorylation, normalized to total VEGFR3 protein, in liver lysates from E11.5 $\beta 1$ integrin^{+/-} and $\beta 1$ integrin^{-/-} mouse embryos one hour after stimulation with either PBS (control) or epinephrine (to increase the heart rate) in WEC; $n \geq 3$. Reported values are the mean \pm standard deviation. Statistical significance was determined using Student's t-tests ($*P < 0.05$).

The findings of this experiment show that $\beta 1$ integrin is essential to sense blood flow and thus activating VEGFR3, by its tyrosine phosphorylation.

3.4 Deletion of VEGFR3 – Requirement of VEGFR3 for HGF production, liver growth and survival

As discussed above, VEGFR3 was shown to be involved in mechanotransduction (Planas-Paz et al., 2012). We were also able to show, that increased heart rate leads to more VEGFR3 tyrosine phosphorylation in the liver and that VEGFR3 activation is decreased in the $\beta 1$ integrin KO embryonic liver. To further confirm our results that VEGFR3 is directly involved in liver growth and survival, VEGFR3 KOs were analyzed.

VEGFR3 conditional KO embryos were induced by gavage of tamoxifen at E10.5 and E11.5 in Rosa CreERT2-VEGFR3^{flox/flox} mothers (VEGFR3 flox mice (Zarkada et al., 2015)). The deletion is lethal at E14.5. We received those embryos in collaboration from Kari Alitalo's Lab, such that matings, genotyping and analyses of KO efficiency were done there (data not shown here). They offered prefixed embryos for cross-sections and immunofluorescence analyses and deep frozen livers for protein analysis for our lab. Living embryos were not available, so *ex vivo* cultivation could not be performed. Rosa Cre was chosen for optimal KO efficiency in the liver vessels, still receiving endothelial specific KO embryos as VEGFR3 is exclusively expressed on vessels (data not shown, performed by S. Fang from K. Alitalos Lab).

As with $\beta 1$ integrin KO embryos, VEGFR3 KO embryos were cross-sectioned and stained for morphometric analyses. VEGFR3 homozygous KO embryos showed significantly smaller livers compared to wild type littermates (-38%, fig. 3.14 a-c). Furthermore, they also had active caspase-3 positive areas in their liver periphery, indicating that the peripheral liver growth zones, which are the first perfused regions in the wild types (see 3.1), undergo apoptosis when VEGFR3 is missing (fig. 3.14 d-f). To confirm that $\beta 1$ integrin is upstream of VEGFR3, as we hypothesize from our previous results (shown in 3.3), we analyzed the activation of endothelial $\beta 1$ integrin in those VEGFR3 KO embryos and found no change in endothelial $\beta 1$ integrin activation on peripheral liver vessels (fig. 3.14 g). Protein analysis showed that VEGFR3 KOs have also decreased HGF levels compared to controls (fig. 3.14 h).

In addition, VEGF-C global KOs (from K. Alitalos Lab from former collaborations) were analyzed for liver size and apoptosis, which were also found to phenocopy the $\beta 1$ integrin KOs (data not shown).

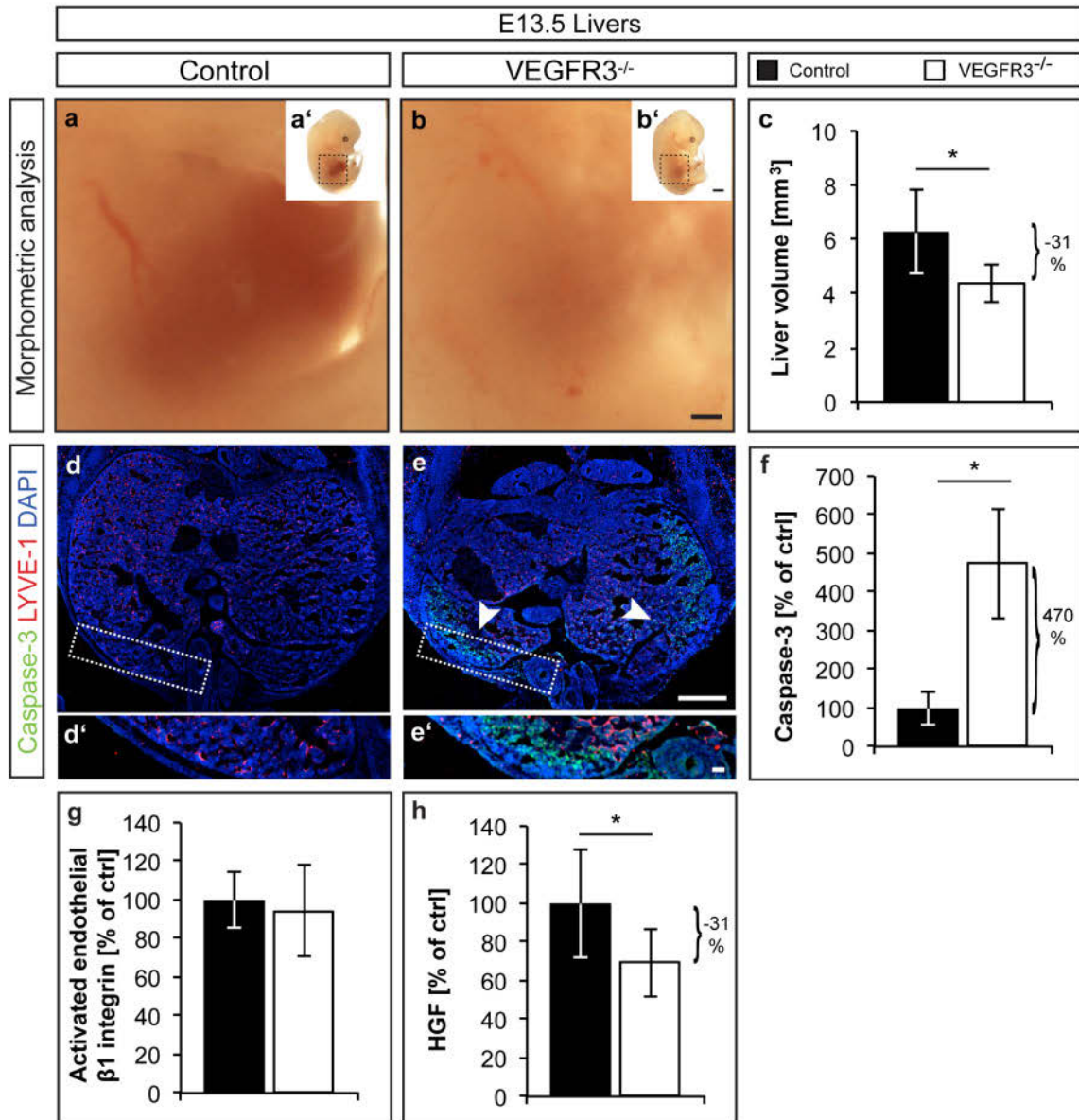


Figure 3.14: VEGFR3 is required for liver growth and survival and HGF production. Representative bright field images of (a,b) the abdominal region of (a') an E13.5 tamoxifen-injected control littermate and (b') an E13.5 VEGFR3^{-/-} mouse embryo. (c) Liver volume of E13.5 control versus VEGFR3^{-/-} embryos as determined via morphometric analysis (n ≥ 4). (d,e) Representative transversal sections through E13.5 livers of control and VEGFR3^{-/-} embryos stained for cell nuclei (DAPI, blue), LYVE-1 (red) and caspase-3 (green). (d',e') Magnifications of peripheral embryonic liver regions as indicated in d and e. (f) Quantification of cleaved caspase-3 positive area in sections from E13.5 control and VEGFR3^{-/-} livers (n ≥ 4). (g) Activated β1 integrin activation on endothelial cells (n ≥ 4). (h) Analysis of HGF protein concentrations in lysates from VEGFR3^{-/-} versus control mouse embryonic livers (n ≥ 7). Scale bars indicate in (a,b) 500 μm, (a',b') 1 mm, (d,e) 500 μm, and (d',e') 50 μm. All values are means ± standard deviation. Statistical significance was determined using Student's t-tests (*P < 0.05).

Taken together, these data show that as well as total genetic deletion of VEGFR3, the deletion of its ligand VEGF-C (data not shown) or its proposed mechano-receptor β 1 integrin resulted in the same phenocopy of global HGF KO embryos. In all genetic deletions, the embryonic liver was dying in its peripheral and first perfused growth zones (as shown here for wt), which results in a significantly decreased liver size.

We assume that mechanoinduction of β 1 integrin via blood perfusion activates VEGFR3 tyrosine phosphorylation in parallel to VEGFR3 ligand induction for proper angiocrine signal production shown for HGF for a proper liver growth and survival.

3.5 Ex vivo liver perfusion

Shown before by pharmacological loss- and gain-of-perfusion experiments in the embryo blood perfusion activates $\beta 1$ integrin and increases VEGFR3 tyrosine phosphorylation contributing to angiocrine signaling, shown for HGF (fig. 3.5 and 3.6). To demonstrate that perfusion of the liver induces mechanotransduction and angiocrine signaling via activation of $\beta 1$ integrin and VEGFR3 tyrosine phosphorylation, adult mouse livers were *ex vivo* perfused with a defined buffer to exclude the possibility that blood components, such as bile acids, affect angiocrine signaling. The portal vein was cannulated and the buffer, a pre-warmed and oxygenated KRH buffer, was infused into the mouse liver at different perfusion rates (schematic drawing fig. 3.15). Whereas 4 ml/min was chosen as the normal flow rate, with 2 ml/min as decreased or 6 and 8 ml/min as increased perfusion rates (calculation by T. Buschmann and N. Eichhorst based on values from rats (Sies, 1978)). *Ex vivo* liver perfusions were performed by N. Eichhorst.

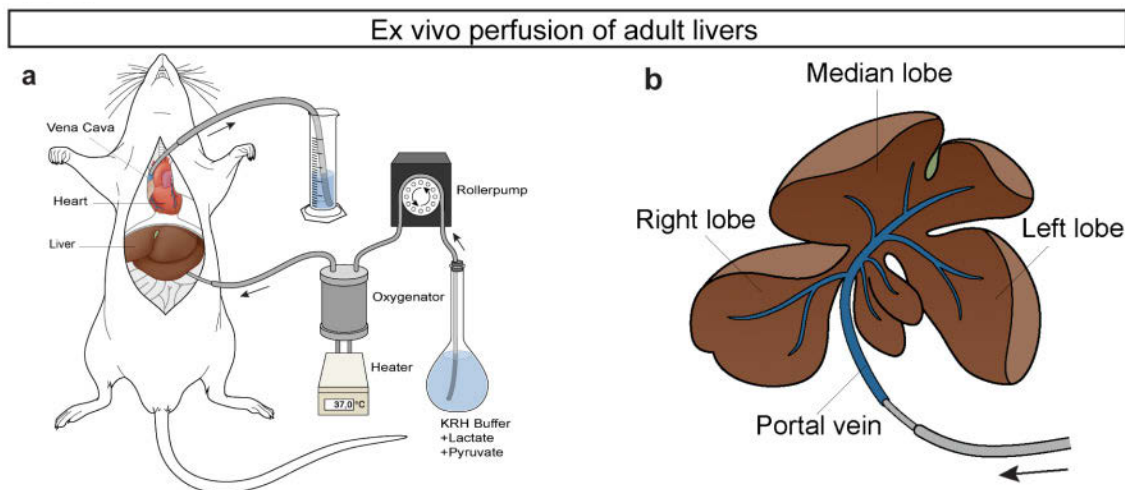


Figure 3.15: Ex vivo liver perfusion. (a) Schematic drawing of an *ex vivo* liver perfusion experiment. The adult liver is perfused at different rates with an oxygenated and heated Krebs-Henseleit buffer. (b) Illustration of an *ex vivo* perfused mouse liver. Illustrations from Y. Koh, drafted by J. Axnick.

On liver cross-sections it could be observed that an increased perfusion rate of 8 ml/min compared to 4 ml/min resulted in dilated liver vessels (fig. 3.16 a and b). Similar results were found by T. Buschmann after partial hepatectomy in mice (Buschmann et al., in prep.). The activation of $\beta 1$ integrin on highly perfused vessels was also increased (fig. 3.16 c).

In liver lysates, it could be shown that VEGFR3 tyrosine phosphorylation correlates with the perfusion rate. A low perfusion rate leads to less VEGFR3 tyrosine phosphorylation than a higher perfusion rate (fig. 3.16 d). As HGF in adult mice is also

stored in the basement membrane and it is possibly first released from this storage, decreased HGF levels were found to correlate with increasing liver perfusion, pointing to the fact, that HGF is released from the BM and is wash out by perfusion (data not shown). Therefore, phospho-c-Met analysis was performed, to see if released HGF activated its receptor c-Met. With a 2 ml/min perfusion rate, almost no tyrosine phosphorylation of c-Met was detectable, but in normal and also in high perfusion set up the c-Met tyrosine phosphorylation was correlating with the perfusion rate (fig. 3.16 e).

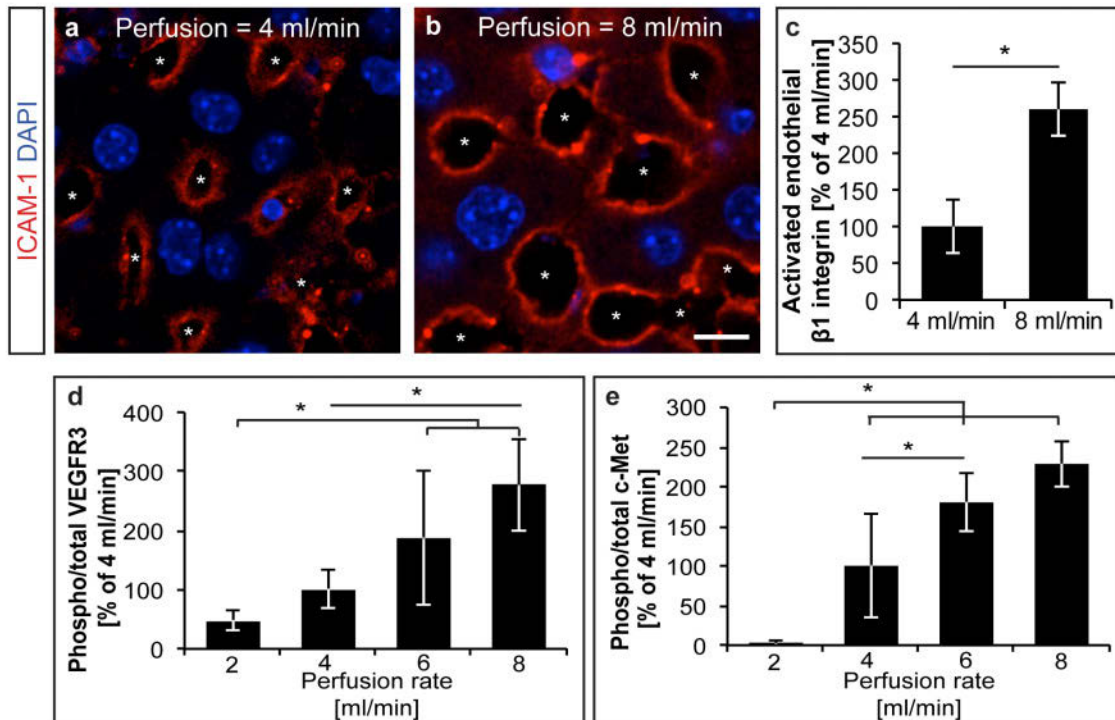


Figure 3.16: Ex vivo liver perfusion activates $\beta 1$ integrin, VEGFR3, and angiocrine signaling. (a,b) Representative sections from livers after 1 hour ex vivo perfusion at either (a) 4 ml/min or (b) 8 ml/min flow rates. Liver sections were stained for the adult hepatic endothelial cell marker ICAM-1 (red) and cell nuclei (DAPI, blue). Hepatic vascular lumens are indicated by asterisks. (c) Fluorescent area of activated $\beta 1$ integrin normalized to ICAM-1 staining in sections of livers perfused ex vivo ($n \geq 5$). Amount of (d) tyrosine phosphorylated VEGFR3 normalized to total VEGFR3 ($n \geq 4$) and (e) phosphorylated tyrosine c-Met normalized to total c-Met ($n \geq 3$), both determined by ELISA and normalized to total protein) in lysates of adult livers perfused ex vivo at 2, 4, 6 and 8 ml/min. Scale bar (a,b) 10 μm . Reported values are means \pm standard deviation. Statistical significance was determined using (c) Student's t-test or (d,e) one-way ANOVA followed by Tukey's multiple comparisons post-hoc test. (* P values: * < 0.05).

With this experiment we could show that VEGFR3 activation as well as HGF signaling, shown here by c-Met tyrosine phosphorylation, correlate with the perfusion of adult mouse livers and is independent of blood components. Furthermore, a higher perfusion was shown to dilate the sinusoidal vessels and activates more endothelial $\beta 1$ integrin.

3.6 *In vitro* studies – Human hepatocytes

Hepatocytes have *in vivo* high proliferative properties, e.g. after partial hepatectomy the liver is able to regenerate (Michalopoulos, 2011). In contrast, they are said to be difficult to culture and are non-proliferative *in vitro* (LeCouter et al., 2003). Therefore, it is likely that an important stimulus for hepatocyte growth and survival is missing from *in vitro* culture. To confirm our results in human cells, cell culture experiments were performed with primary human liver sinusoidal microvascular endothelial cells (LSECs) and primary human hepatocytes. LSECs were stretched to mechanically stress them and afterwards the conditioned medium was transferred to the hepatocytes (fig. 3.17 a-a'' and b-b''). The VEGFR3 tyrosine phosphorylation on LSECs was analyzed after the stretching. Proliferation and survival of hepatocytes was examined. Those experiments were performed mainly by Linda Lorenz, who was supervised in line with this thesis.

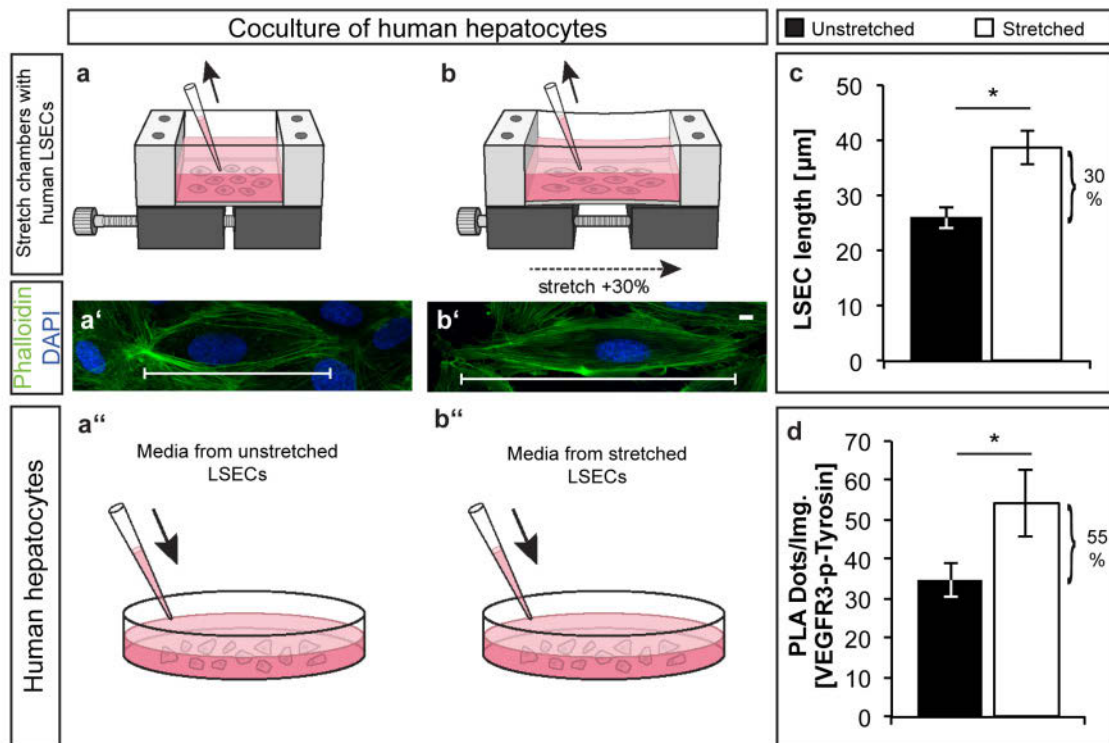


Figure 3.17: Mechanical stimulation of LSECs increases VEGFR3 tyrosine phosphorylation. (a,b) Illustrations of (a) mechanically unstretched and (b) mechanically stretched human LSECs on stretch chambers. Schematized pipette tips indicate how media is taken for application in hepatocyte cell culture shown below. (a',b') Representative image of mechanically unstretched and stretched human LSECs stained for cell nuclei (DAPI) and cytoskeleton (Phalloidin), and illustrations of human hepatocytes supplemented with media from (a'') mechanically unstretched and (b'') mechanically stretched LSECs. (c) Quantification of human LSEC lengths without and after mechanical stretching (n = 3). (d) Quantification of PLA on LSECs without and after mechanical stretching (n = 4). Scale bars indicate in (a',b') 5 µm. Reported values are the mean ± standard deviation. Statistical significance was determined using Student's t-test. (*P values: * < 0.05). Illustrations by Y. Koh, drawn and pre-illustrated from J. Axnick.

After mechanical stretching the LSECs showed a 30% elongation (fig. 3.17 a', b' and c) as well as an increase in VEGFR3 tyrosine phosphorylation (fig. 3.17 d).

The proliferation of human hepatocytes in conditioned medium from stretched versus unstretched LSECs was further investigated. In different donors (selected data shown here) an increase of proliferating hepatocytes (HNF4- α positive cells) could always be observed (fig. 3.18).

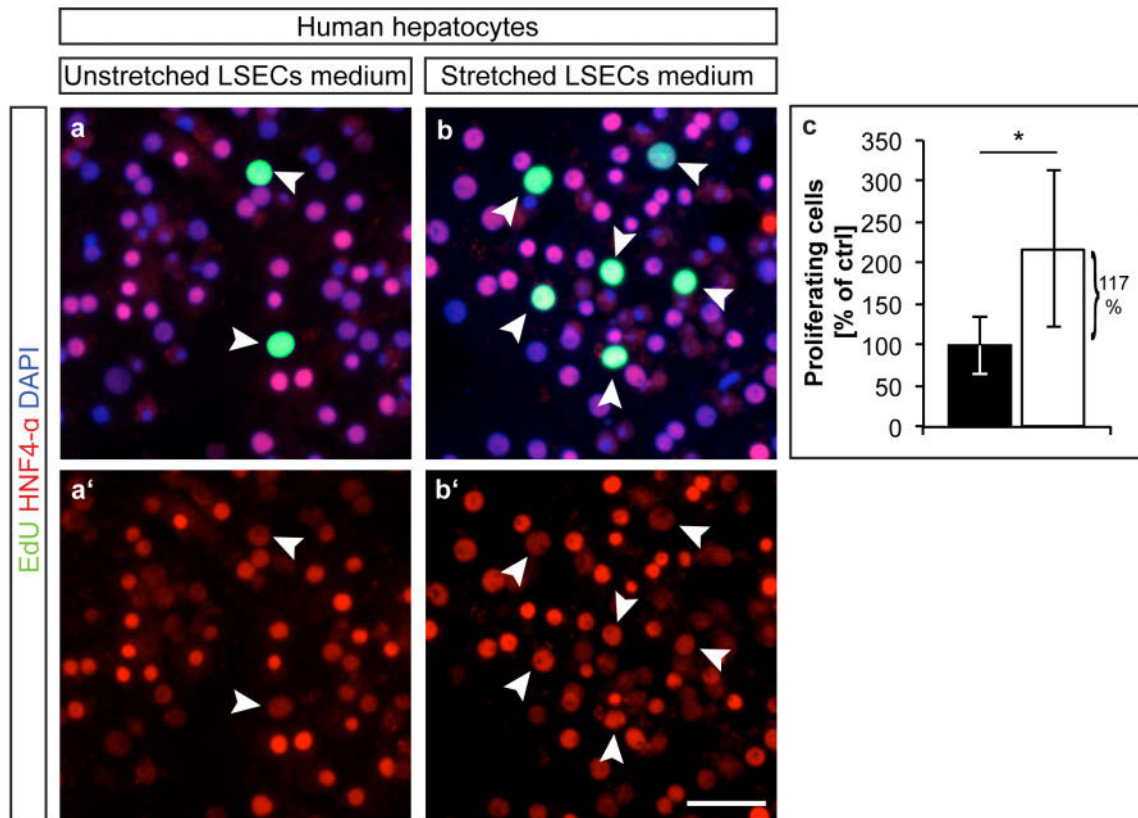


Figure 3.18: Proliferation of primary human hepatocytes upon treatment with mechanoinduced angiocrine signals. (a,b) Primary human hepatocytes (donor: female, 12 years old, BMI 20.2) treated for 6 hours with media from (a, a') unstretched human LSECs and (b, b') stretched human LSECs in the presence of EdU. The human hepatocytes are stained for HNF4- α (red), EdU (green) and cell nuclei (DAPI, blue). (c) Quantification of proliferation of human hepatocytes (donor: male, 27 years, BMI 20.5) after cultivation in conditioned media for 6 h ($n \geq 6$). Scale bar: 50 μm . All values are the mean \pm standard deviation. Statistical significance was determined using Student's t-test (* P values: * < 0.05).

We showed that coculture with conditioned medium from mechanical induced human LSECs could enhance the proliferation of human hepatocytes *in vitro*. Furthermore, VEGFR3 tyrosine phosphorylation was increased after mechanical stretching of LSECs, indicating that also VEGFR3 dependent signaling plays a role for enhanced hepatocyte proliferation.

3.7 *In vivo* loss-of-perfusion experiments by myocardial infarction

In humans, congenital heart diseases as well as cardiac failures can be associated with hepatic complications (Asrani et al., 2012; Naschitz et al., 2000; Samsky et al., 2013). Although heart-liver-interactions are often described, they have not been well-studied (Naschitz et al., 2000). To manipulate blood perfusion in the adult mouse system and to set up a model system for human cardiogenic hepatic diseases, left-ventricular myocardial infarctions (MI) in adult mice were induced. Therefore, surgeries with permanent ligation of the left anterior descending coronary artery (LAD) were chosen to create severe cardiac complications and to impair the cardiac function in adult mice extensively. Surgeries were performed by Carina Klüppel and Stefanie Becher. Afterwards, the livers of MI mice were analyzed and liver function tests were performed to detect liver failures after MI.

3.7.1 MI success

A successful myocardial infarction (MI) surgery was monitored by an ECG (data not shown) and the discoloring of the mouse hearts 1 hour after the permanent ligation of the LAD (fig. 3.19 e, greyish heart).

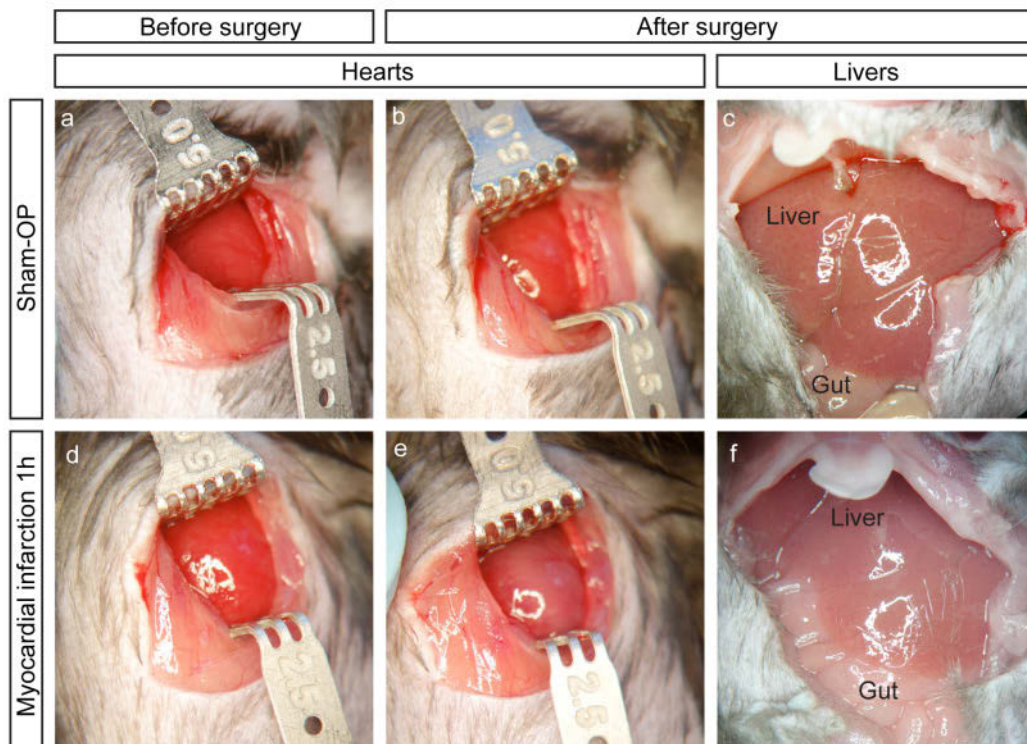


Figure 3.19: Discoloring of mouse hearts and livers after MI. (a,b) Hearts of sham operated (Sham-OP) mice and (d-e) hearts of mice with left myocardial infarction before (a,d) and right after ligation of the LAD (b,e). (c,f) Livers in the body cavity of mice with Sham-OP (c) or MI (f) right after ligation of the LAD.

After sacrificing sham and MI mice, the infarction size of the left ventricle per area at risk was examined with a TTC staining for further confirmation of a successful surgery (done by C. Klüppel, fig. 3.20). Ischemic areas in the heart appear white, whereas functional regions appear red or blue. The infarction size per area at risk (78%) was significantly increased after MI surgery with permanent ligation of the LAD in mice after 1 day, indicating a successful surgery and a severe cardiogenic failure (fig. 3.20 c).

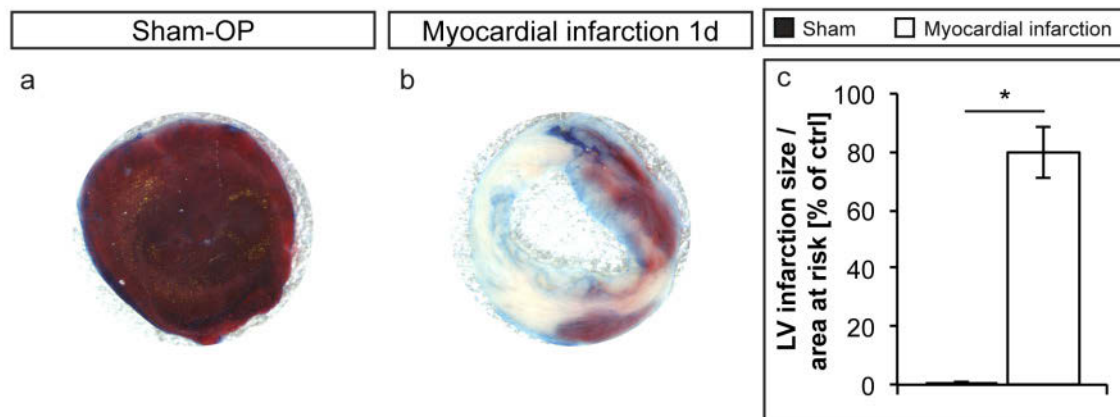


Figure 3.20: Infarction size of the left ventricle per area at risk after MI surgery. (a,b) Cross-sections (1 mm) of the middle part of mouse hearts of sham operated (Sham-OP) mice (a) and mice with left myocardial infarction (b) after TTC staining. (c) Quantification of the infarction size of the left ventricle per area at risk (n = 4). All values are the mean \pm standard deviation. Statistical significance was determined using Student's t-test. (*P value: * < 0.05).

3.7.2 Analysis of the liver damage after myocardial infarction

The livers of MI mice were observed by eye to have a pale color compared to sham animals, which could possibly result from less perfusion (fig. 3.19 f). Immunofluorescent staining of liver cross-sections of sham and MI mice showed that the livers of ischemia mice had foci with collapsed vessels as well as foci with dilated vessels (fig. 3.21 b' and b''). Those findings are similar to observations in human patients with ACLI or ischemic hepatitis, respectively, who show elevated hepatic venous pressure combined with impaired perfusion, resulting in a variable degree of architectural collapse around the central veins, depending on the duration of cardiac ischemia (Samsky et al., 2013). Those collapsed regions are proposed to result from the decreased cardiac function through permanent MI. Whereas the regions with dilated vessels may compensate the collapsed regions after recovery of the infarction, due to the fact that mice are quite healthy and motile after this severe surgery.

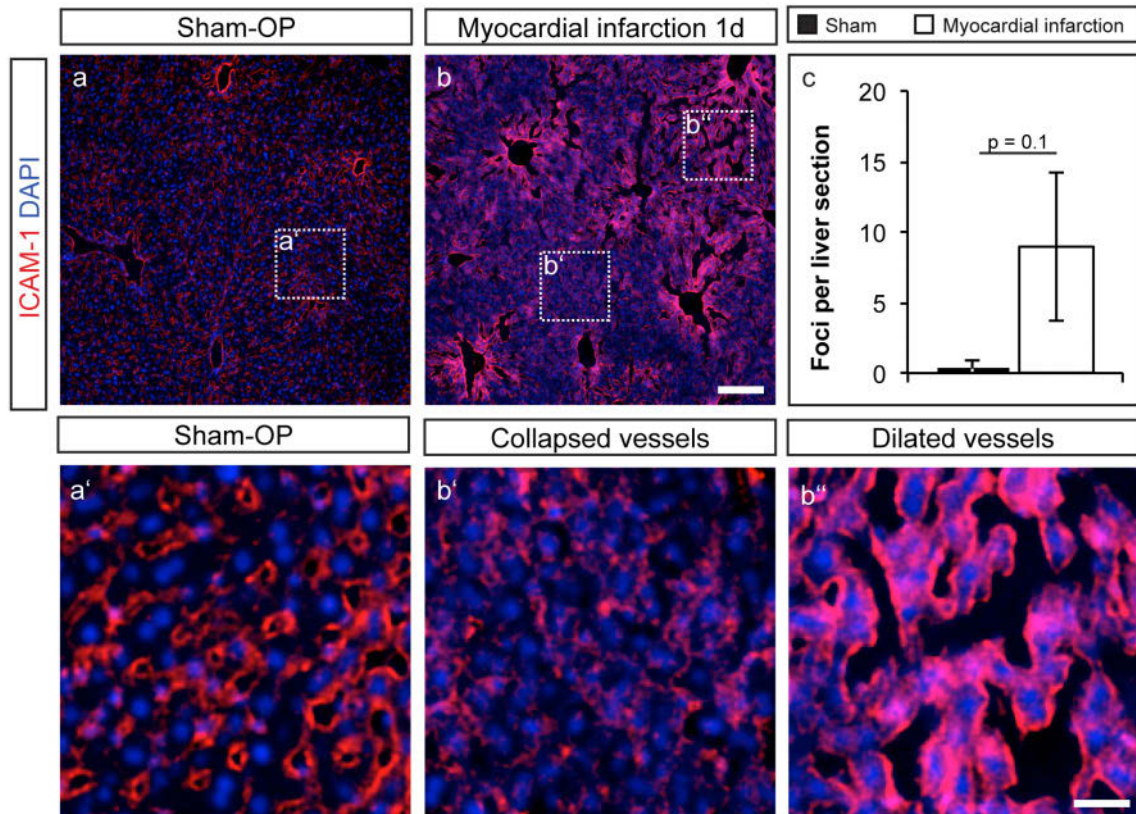


Figure 3.21: Foci of collapsed and dilated vessels after MI surgery. (a,b) Representative cross-sections of livers after 1d permanent MI. (a'-b'') Magnifications of boxes indicated in (a,b). (c) Quantification of number of foci with collapsed vessels on liver sections (n = 3). Scale bars (a,b) 100 μ m, (a'-b'') 25 μ m. All values are the mean \pm standard deviation. Statistical significance was determined using Student's t-test. (*P value: * < 0.05).

Furthermore, in regions with collapsed liver vessels an increased staining of active caspase-3 was found (fig. 3.22). Since only a few foci were affected, we did not attempt to quantify the staining.

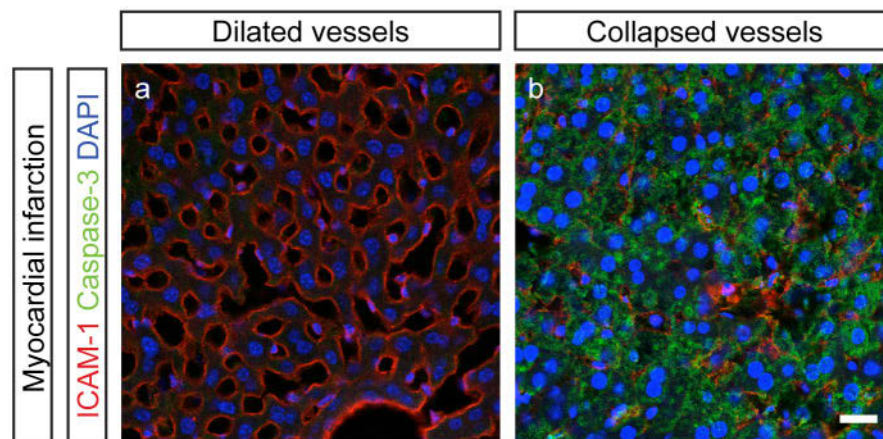


Figure 3.22: Apoptosis in collapsed liver regions after MI. (a) Liver region with dilated vessels and (b) with collapsed vessels 1 day after permanent MI. Scale bar (a,b) 50 μ m.

3.7.3 Liver function tests

In humans, liver function tests give information about hepatic ischemia or ACLI after cardiogenic complications (Samsky et al., 2013). High elevations of LDH, AST as well as ALT are reported after cardiac injury and are associated with liver damages (Naschitz et al., 2000). Therefore, liver function tests were also performed for no-reflow MI animals. High increase of AST and LDH levels could be observed in all animals after permanent MI surgery (fig. 3.23 a, b and d). However, ALT elevation was observed in only 1/3 of mice (fig. 3.23 c). AST levels were examined at different time points (1 hour, 1 day and 2 days). A sharp increase of AST levels 1 day after permanent MI was observed, whereas 2 days later, the levels returned to baseline (fig. 3.23 b).

ALT, AST and LDH are common liver function values, whereas one has to consider that high AST and LDH levels can also result from the cardiac defects if the isotype is not specified. But in literature values over 1000 U/L for AST (in human cases) are reported to be specific for ischemic hepatic liver damages (Hickman and Potter, 1990).

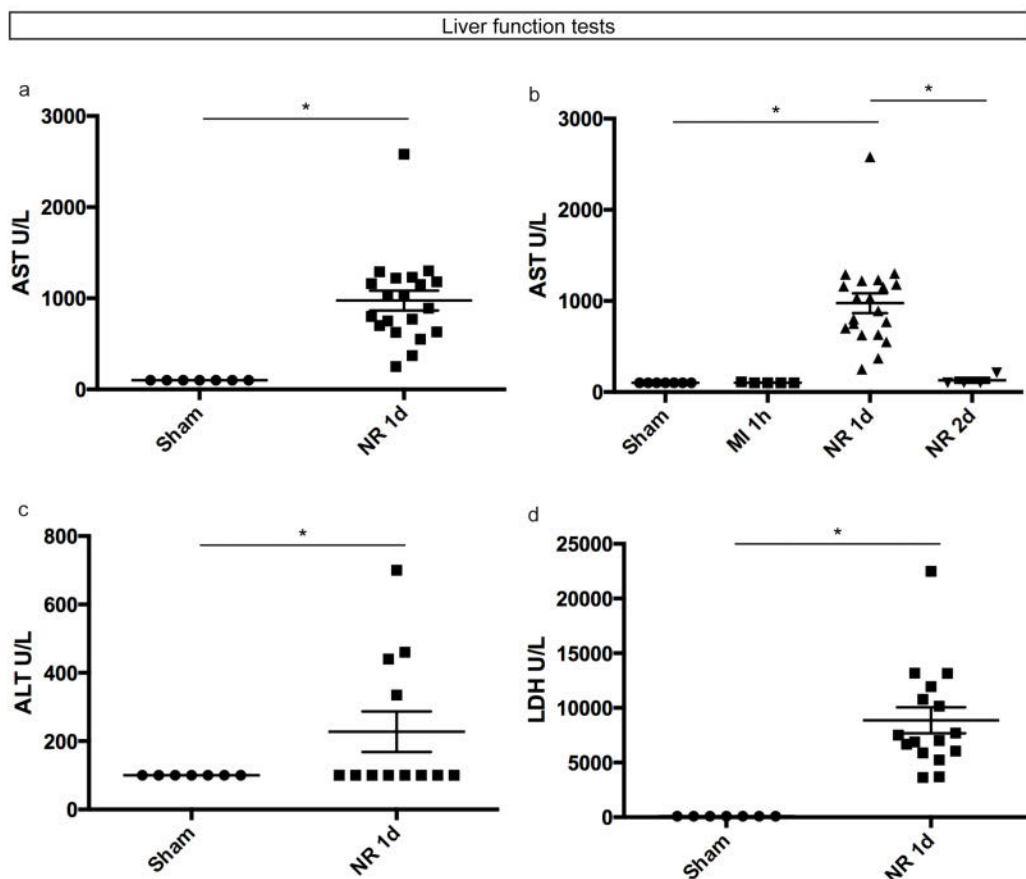


Figure 3.23: Liver function tests. Dot blot of liver function tests from plasma of Sham and permanent MI mice 1d after surgery. (a) AST levels 1 d after surgery and (b) AST levels after 1 hour, 1 day and 2 days after LAD ligation. (c) ALT level 1 d after surgery. (d) LDH level 1 d after surgery. All lines are means \pm standard deviation. Statistical significance was determined using Student's t-test. (* P value: * $<$ 0.05).

We were able to show that our MI model leads to an increase of liver function test markers, pointing to a liver damage in those mice. The most liver specific marker ALT was just increased in 1/3 of all mice, pointing to the fact that mice are able to recover fast after severe cardiac complications and to the fact of variability.

3.7.4 Mechanotransduction of the liver after MI

After visual observation of the permanent MI livers and liver function tests, mechanistic analyses were performed with this low-perfusion model to confirm if our previous findings can be applied to this model. Therefore, endothelial β 1 integrin and VEGFR3 activation were analyzed as well as HGF amount and tyrosine phosphorylation of c-Met in mice after permanent MI surgery. β 1 integrin was found to be less activated in endothelial cells (fig. 3.24 a) of MI mice 1 day after surgery, as well as VEGFR3 tyrosine is also less phosphorylated (fig. 3.24 b). A tendency of decreased HGF expression after MI could be observed, but significantly less c-Met tyrosine phosphorylation was found (fig. 3.24 c and d). GAPDH serves as control and was not changed (fig. 3.24 e).

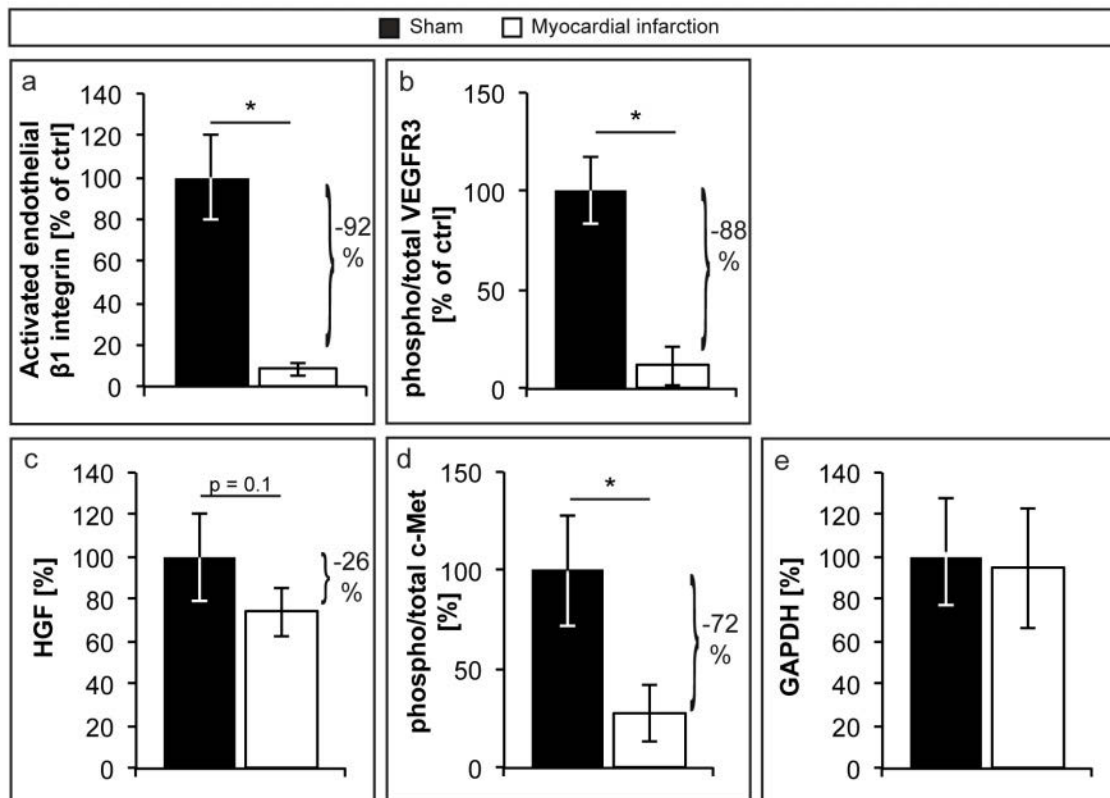


Figure 3.24: Decreased endothelial $\beta 1$ integrin activation, VEGFR3 tyrosine phosphorylation and c-Met tyrosine phosphorylation after MI surgery. (a) Quantification of fluorescence area of staining for activated $\beta 1$ integrin on ICAM-1⁺ hepatic endothelial cells 1 hour after MI (n = 3). (b) Hepatic VEGFR3 tyrosine phosphorylation normalized to total VEGFR3 (both determined by ELISA) and total protein 1 day after permanent MI (n \geq 3). (c) Hepatic HGF protein concentration normalized to total protein 1 day after permanent MI (n \geq 4). (d) Hepatic c-Met tyrosine phosphorylation normalized to total c-Met (both determined by ELISA) and total protein 1 day after permanent MI (n \geq 4). (e) The protein concentration of hepatic GAPDH taken as a control protein normalized to total protein 1 day after permanent MI (n \geq 4). All values are the mean \pm standard deviation. Statistical significance was determined using Student's t-tests (* $P < 0.05$).

Those results pointing to the fact that impaired liver function (high liver function test values) correlate with endothelial $\beta 1$ integrin activation and VEGFR3 tyrosine phosphorylation. Furthermore, decreased c-Met tyrosine phosphorylation indicates an involvement of HGF signaling in liver damage after left ventricular myocardial infarction.

With the MI infarction model, we could reproduce our flow-dependent findings made with mouse embryos in WEC and with *ex vivo* perfusion with adult mice. The activation of endothelial $\beta 1$ integrin and VEGFR3 tyrosine phosphorylation as well as flow-dependent HGF production and signaling were found to be decreased after left-ventricular MI.

4. Discussion

Angiocrine signals were recently identified as key regulators of important developmental, regenerative and maintaining processes. The focus of this thesis was the identification and further investigation of mechanoinduced angiocrine signals. We identified $\beta 1$ integrin and VEGFR3 as key regulators of flow-mediated mechanotransduction followed by angiocrine signaling. Those findings were investigated by studying liver development and flow alterations in the adult liver. Using the mouse embryo model, investigations of the onset of vascular perfusion could be easily performed, and genetic deletions of $\beta 1$ integrin and VEGFR3 were also analyzed. *Ex vivo* perfusion of the adult mouse liver was used to confirm these findings and exclude the influence of blood components. Finally, the myocardial infarction model showed the relevance of these findings for human diseases.

4.1 Mechanism

In this thesis it was shown that endothelial mechanotransduction induces angiocrine signaling to promote tissue growth and survival. Evidence was found that $\beta 1$ integrin is required for transducing changes in blood perfusion into changes in angiocrine signaling, such as HGF production and signaling. Furthermore, it was shown that during embryonic development, VEGFR3 is required for HGF production and that it is located downstream of $\beta 1$ integrin. As $\beta 1$ integrin and VEGFR3 also have pro-angiogenic properties it is likely that they promote angiogenesis in addition to their angiocrine signal functions.

Taken together, these findings indicate a critical contribution of mechanotransduced angiocrine signaling is required for organ maintenance to prevail over organ failure. It is likely that this mechanoinduced angiocrine signaling also plays a role during different physiological and pathophysiological processes.

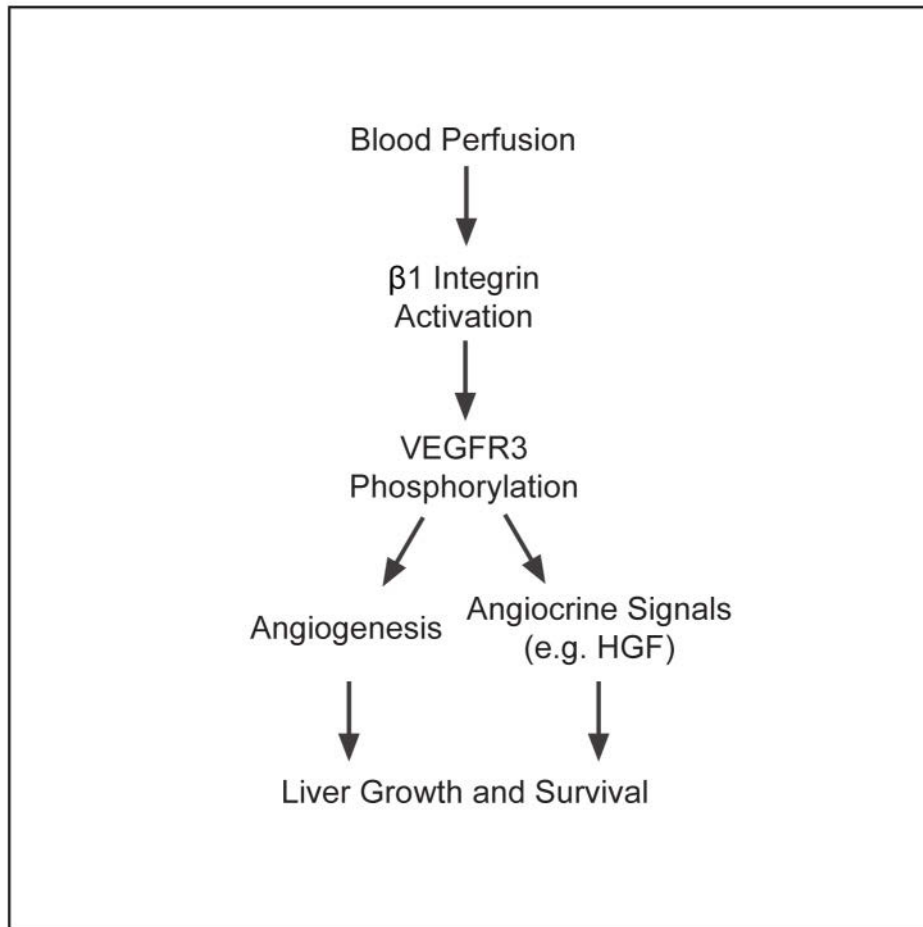


Figure 4.1: Model. All findings support the following mechanism: Blood perfusion in the liver periphery activates endothelial $\beta 1$ Integrin, which is required for VEGFR3 tyrosine phosphorylation. Both are known to be required for angiogenesis. But angiocrine HGF levels are also regulated by this mechanism. HGF is required for proper liver growth and survival.

4.2 Critical Discussion

4.2.1 Mechanotransduction via $\beta 1$ integrin and VEGFR3

Integrins are heterodimeric transmembrane receptors. Here we focused on $\beta 1$ integrin as it has large impact on organ physiology, which was proven by several deletions of this receptor (Avraamides et al., 2008; Ingber, 1991; Planas-Paz et al., 2012; Ross et al., 2013). Just one compartment of the integrin heterodimer, *i.e.* the $\beta 1$ subunit, was investigated in this thesis. Whether the α integrin subunit is also involved in angiocrine signaling and HGF production requires further investigation. The $\alpha 5$ integrin would be a likely candidate, as $\alpha 5$ integrin KO mice also show vascular defects, and functional blocking of $\alpha 5\beta 1$ integrins impairs VEGFR3 tyrosine phosphorylation (Zhang et al., 2005). The $\alpha 5\beta 1$ integrin is a fibronectin receptor. Fibronectin is known to increase

VEGFR3 tyrosine phosphorylations (Zhang et al., 2005), also suggesting an involvement of $\beta 1$ integrin and possibly $\alpha 5$ integrin.

The composition of the basement membrane and its involvement into $\beta 1$ integrin-dependent angiocrine signaling should be analyzed, as integrins are connected to the ECM. Interestingly, the adult liver has a specialized BM, as it is discontinuous. But during embryonic liver development and liver regeneration this basement membrane is known to be continuous, as it is also seen under pathological conditions. Angiocrine signaling was also shown to be involved in liver fibrosis (Ding et al., 2014). An increase in extracellular matrix formation is typical for liver fibrosis (Bataller and Brenner, 2005), indicating that $\beta 1$ integrin signaling may also be altered during liver fibrosis due to these changes of the extracellular matrix.

Moreover, the role of the ligand-dependent activation of VEGFR3 should be further investigated. Later stage conditional VEGF-C KO mice at around E14.5 show defects in hematopoietic stem cell growth in the embryonic liver (Fang et al., 2016), but earlier stage global VEGF-C KO mice at around E13.5 are also pointing to the same phenotype described here in this thesis (data not shown). In this thesis, no changes in the count of hematopoietic cells in $\beta 1$ integrin KO embryos were observed (data not shown), pointing to a different role of VEGF-C over the time of liver development. Furthermore, heterodimers of VEGFR3 and VEGFR2 could be analyzed, as those heterodimers were described previously and interactions of both receptors were found to be critical (Coon et al., 2015; Nilsson et al., 2010; Zarkada et al., 2015).

Furthermore, the intracellular signaling pathway should be studied. Src family kinases are known to be located downstream of $\beta 1$ integrin signaling (Reinehr et al., 2013), but also the integrin-linked kinase (ILK) is known to be crucial for integrin signaling. Conditional ILK deletion in hepatocytes is leading to apoptosis and hepatitis (Gkretsi et al., 2007). VEGFR3 tyrosine phosphorylation leads to the activation of signal transduction pathways such as the mitogen-activated protein kinase (MAPK) cascade or phosphatidylinositol 3 kinase (PI3K) and Akt signaling pathways with a wide range of cellular responses (Reinehr et al., 2013; Zhang et al., 2005).

$\beta 1$ integrin and VEGFR3 were previously described in literature as harboring mechanotransductive properties (Friedland et al., 2009; Galvagni et al., 2010; Planas-Paz et al., 2012; Ross et al., 2013; Zhang et al., 2005). However, we identified that angiocrine signaling via blood flow-mediated $\beta 1$ integrin activation and VEGFR3 tyrosine phosphorylation is crucial for liver development, liver damage in adult MI mice and probably also for *in vitro* proliferation of human hepatocytes.

4.2.2 Perfusion induced angiocrine signaling

We identified for the first time that blood perfusion can regulate organ growth and survival via angiocrine signaling. As we have shown, hypo-perfusion and therefore decreased mechanotransduction must be distinguished from hypoxia as well as defined from angiogenic phenotypes, when fewer blood vessels are formed to supply the tissues, which also leads to hypoxia. With the adult system of *ex vivo* perfusion a constant oxygenation was assured to exclude that apoptosis in the liver arises from hypoxia. However, further experiments with different oxygen levels in *ex vivo* perfusion are required to better distinguish between the role of blood perfusion and oxygenation.

We also provided evidence that $\beta 1$ integrin and VEGFR3 are responsible for proper angiocrine signal production, shown here for HGF. Both endothelial $\beta 1$ integrin and VEGFR3 KOs show reduced HGF levels and are phenocopies of HGF KOs, described previously (Schmidt et al., 1995). These findings point to the fact that endothelial-derived HGF is the main source for embryonic liver development, although other sources have been described (Nakamura et al., 2011). But overall, the contribution of other angiocrine signals should be investigated further.

The relative mild effects after MI can be explained by the fact that mice behave different compared to humans after myocardial infarction. They recover very well, even with an infarction after permanent ligation of the LAD, whereas humans would suffer greatly or even die. It would be possible that the mouse livers can recover through regeneration after myocardial infarction. If the hearts recover and begin to pump more blood through the mouse body again, the healthy regions of the liver will need to compensate for the higher flow rate of the recovering heart by vessel dilation. In further studies it needs to be checked if those regions will regenerate, as in *ex vivo* perfusions vessel dilation was observed with high flow rates, which also showed increase in angiocrine signaling (similar results found by T. Buschmann, in prep.). Furthermore, it still needs to be clarified whether passive congestion of the liver or hypoxia can be really excluded or if hypotension is the main factor for liver damage.

4.3 Outlook

It is likely that the mechanoinduced angiocrine signaling via endothelial $\beta 1$ integrin and VEGFR3 activation also participates in different physiological and pathophysiological processes. In this thesis the embryonic development was used, as well as MI and cell culture of human primary liver cells, as a model to study organ growth and damage. Organ development is often considered to be similar to organ regeneration (Hata et al., 2007). For liver regeneration, angiocrine involvement was previously investigated by several groups (Ding et al., 2010; Hu et al., 2014). However, most of these studies are concentrated on the pro-angiogenic phase 1-4 days after partial hepatectomy, also called the inductive phase. Our mechanism provided here appears to be involved in liver regeneration, suggesting that it is an earlier trigger for the onset of liver regeneration (Buschmann et al., in prep.). Upon partial hepatectomy, the same amount of blood has to pass through a smaller liver mass (Michalopoulos, 2010). Potentially, this simple mathematical conclusion results in increased perfusion as well as enhanced mechanotransduction directly promoting or even initiating liver regeneration. Therefore, it is worthwhile to investigate the role of mechanotransduction for liver regeneration (Buschmann et al., in prep.). The role of the mechanism investigated in this thesis should be also analyzed in the context of liver regeneration. It should be investigated whether endothelial $\beta 1$ integrin and VEGFR3 are involved in the same manner as described here and if HGF is directly produced from ECs in this very initial phase of liver regeneration. In adults, HGF is stored in the basement membrane and is cleaved by metalloproteases. It is also likely that this stored HGF is used for the initial trigger of liver regeneration regulated by angiocrine signaling. This differs from embryonic development, where HGF is produced from ECs to further contribute to liver regeneration, as shown for the inductive phase before, and to refill the storages. In this context it would be highly beneficial to analyze the contribution of other angiocrine signals.

The participation of the space of Disse is worth to be further investigated as well. It is a unique niche in the body, which can be identified by electron microscopy between the sinusoids and the hepatocytes instead of a dense basement membrane. This space of Disse is thought to be a stem cell niche for liver regeneration, as it harbors stellate cells and those cells are controversially discussed to have stem cell properties (Kordes and Häussinger, 2013). But as flow changes are often reported in liver pathology or seem obvious after partial hepatectomy right before liver regeneration takes places, a buffer or a recognition role for blood flow alterations in the space of Disse should be reconsidered.

Moreover, a model for cardiogenic-induced organ complications after congenital heart diseases as well as after MI was provided in this thesis. Congenital cardiogenic diseases as well as myocardial complications were known to be associated with liver dysfunctions (Asrani et al., 2012; Naschitz et al., 2000; Samsky et al., 2013). These dysfunctions seem to be perfusion dependent, as left-ventricular cardiac failure often leads to liver dysfunction up to liver necrosis and is differentiated to hypoxic damage (Clarke, 1950; Killip and Payne, 1960; Seth and Nath, 2009; Weinberg and Bolande, 1970). We were able to show that after left-ventricular MI in mice, liver dysfunction occurs, as liver function tests showed increased liver damage markers and sinusoidal structure was altered post-MI. Embryonic heart beat alterations also led to changes in angiocrine signaling, pointing to an involvement of our mechanism in congenital heart diseases followed by liver complications. Therefore, it would be worthwhile to work with human liver samples from patients after MI or from children suffering from congenital heart diseases who also have liver dysfunction, to determine if this mechanism can be directly transferred to human pathophysiology.

New targets for the development of new treatments of organ diseases influenced by macro- and microvascular pathologies are greatly needed, and these will require a better understanding of the molecular causes of these diseases.

References

- Abdel-Misih, S.R., and Bloomston, M. (2010). Liver anatomy. *Surg Clin North Am* 90, 643-653.
- Allen, L.A., Felker, G.M., Pocock, S., McMurray, J.J., Pfeffer, M.A., Swedberg, K., Wang, D., Yusuf, S., Michelson, E.L., Granger, C.B., *et al.* (2009). Liver function abnormalities and outcome in patients with chronic heart failure: data from the Candesartan in Heart Failure: Assessment of Reduction in Mortality and Morbidity (CHARM) program. *Eur J Heart Fail* 11, 170-177.
- Anthony, P.P., Ishak, K.G., Nayak, N.C., Poulsen, H.E., Scheuer, P.J., and Sobin, L.H. (1978). The morphology of cirrhosis. Recommendations on definition, nomenclature, and classification by a working group sponsored by the World Health Organization. *J Clin Pathol* 31, 395-414.
- Asrani, S.K., Asrani, N.S., Freese, D.K., Phillips, S.D., Warnes, C.A., Heimbach, J., and Kamath, P.S. (2012). Congenital heart disease and the liver. *Hepatology* 56, 1160-1169.
- Avraamides, C.J., Garmy-Susini, B., and Varnier, J.A. (2008). Integrins in angiogenesis and lymphangiogenesis. *Nat Rev Cancer* 8, 604-617.
- Baeyens, N., Bandyopadhyay, C., Coon, B.G., Yun, S., and Schwartz, M.A. (2016). Endothelial fluid shear stress sensing in vascular health and disease. *J Clin Invest* 126, 821-828.
- Baeyens, N., Nicoli, S., Coon, B.G., Ross, T.D., Van den Dries, K., Han, J., Lauridsen, H.M., Mejean, C.O., Eichmann, A., Thomas, J.L., *et al.* (2015). Vascular remodeling is governed by a VEGFR3-dependent fluid shear stress set point. *Elife* 4.
- Bataller, R., and Brenner, D.A. (2005). Liver fibrosis. *J Clin Invest* 115, 209-218.
- Biasi, F., Chiarpotto, E., Lanfranco, G., Capra, A., Zummo, U., Chiappino, I., Scavazza, A., Albano, E., and Poli, G. (1994). Oxidative stress in the development of human ischemic hepatitis during circulatory shock. *Free Radic Biol Med* 17, 225-233.
- Borowiak, M., Garratt, A.N., Wustefeld, T., Strehle, M., Trautwein, C., and Birchmeier, C. (2004). Met provides essential signals for liver regeneration. *Proc Natl Acad Sci U S A* 101, 10608-10613.
- Brand, T. (2003). Heart development: molecular insights into cardiac specification and early morphogenesis. *Dev Biol* 258, 1-19.
- Buschmann, T., Eglinger, J., and Lammert, E. (2012). Angiogenesis and Liver Regeneration. In *Liver Regeneration*, D. Haussinger, ed. (Berlin/Boston: Walter de Gruyter GmbH & Co. KG), pp. 145-158.
- Bynum, T.E., Boitnott, J.K., and Maddrey, W.C. (1979). Ischemic hepatitis. *Dig Dis Sci* 24, 129-135.
- Calmont, A., Wandzioch, E., Tremblay, K.D., Minowada, G., Kaestner, K.H., Martin, G.R., and Zaret, K.S. (2006). An FGF response pathway that mediates hepatic gene induction in embryonic endoderm cells. *Dev Cell* 11, 339-348.

- Carlson, T.R., Hu, H., Braren, R., Kim, Y.H., and Wang, R.A. (2008). Cell-autonomous requirement for beta1 integrin in endothelial cell adhesion, migration and survival during angiogenesis in mice. *Development* 135, 2193-2202.
- Clarke, W.T. (1950). Centrilobular hepatic necrosis following cardiac infarction. *Am J Pathol* 26, 249-255.
- Cohen, S.B., Ginde, S., Bartz, P.J., and Earing, M.G. (2013). Extracardiac Complications in Adults with Congenital Heart Disease. *Congenit Heart Dis* 8, 370-380.
- Collardeau-Frachon, S., and Scoazec, J.Y. (2008). Vascular development and differentiation during human liver organogenesis. *Anat Rec (Hoboken)* 291, 614-627.
- Coon, B.G., Baeyens, N., Han, J., Budatha, M., Ross, T.D., Fang, J.S., Yun, S., Thomas, J.L., and Schwartz, M.A. (2015). Intramembrane binding of VE-cadherin to VEGFR2 and VEGFR3 assembles the endothelial mechanosensory complex. *J Cell Biol* 208, 975-986.
- Dai, C., Brissova, M., Reinert, R.B., Nyman, L., Liu, E.H., Thompson, C., Shostak, A., Shiota, M., Takahashi, T., and Powers, A.C. (2013). Pancreatic islet vasculature adapts to insulin resistance through dilation and not angiogenesis. *Diabetes* 62, 4144-4153.
- Ding, B.S., Cao, Z., Lis, R., Nolan, D.J., Guo, P., Simons, M., Penfold, M.E., Shido, K., Rabbany, S.Y., and Rafii, S. (2014). Divergent angiocrine signals from vascular niche balance liver regeneration and fibrosis. *Nature* 505, 97-102.
- Ding, B.S., Nolan, D.J., Butler, J.M., James, D., Babazadeh, A.O., Rosenwaks, Z., Mittal, V., Kobayashi, H., Shido, K., Lyden, D., *et al.* (2010). Inductive angiocrine signals from sinusoidal endothelium are required for liver regeneration. *Nature* 468, 310-315.
- Drake, C.J., and Fleming, P.A. (2000). Vasculogenesis in the day 6.5 to 9.5 mouse embryo. *Blood* 95, 1671-1679.
- Dumont, D.J., Jussila, L., Taipale, J., Lymboussaki, A., Mustonen, T., Pajusola, K., Breitman, M., and Alitalo, K. (1998). Cardiovascular failure in mouse embryos deficient in VEGF receptor-3. *Science* 282, 946-949.
- Elvevold, K., Smedsrod, B., and Martinez, I. (2008). The liver sinusoidal endothelial cell: a cell type of controversial and confusing identity. *Am J Physiol Gastrointest Liver Physiol* 294, G391-400.
- Enzan, H., Himeno, H., Hiroi, M., Kiyoku, H., Saibara, T., and Onishi, S. (1997). Development of hepatic sinusoidal structure with special reference to the Ito cells. *Microsc Res Tech* 39, 336-349.
- Fang, S., Nurmi, H., Heinolainen, K., Chen, S., Salminen, E., Saharinen, P., Mikkola, H.K., and Alitalo, K. (2016). Critical requirement of VEGF-C in transition to fetal erythropoiesis. *Blood* 128, 710-720.
- Fassler, R., and Meyer, M. (1995). Consequences of lack of beta 1 integrin gene expression in mice. *Genes Dev* 9, 1896-1908.
- Fernandez, M., Semela, D., Bruix, J., Colle, I., Pinzani, M., and Bosch, J. (2009). Angiogenesis in liver disease. *J Hepatol* 50, 604-620.
- Ferrara, N., Gerber, H.P., and LeCouter, J. (2003). The biology of VEGF and its receptors. *Nat Med* 9, 669-676.

Friedland, J.C., Lee, M.H., and Boettiger, D. (2009). Mechanically activated integrin switch controls alpha5beta1 function. *Science* 323, 642-644.

Galvagni, F., Pennacchini, S., Salameh, A., Rocchigiani, M., Neri, F., Orlandini, M., Petraglia, F., Gotta, S., Sardone, G.L., Matteucci, G., *et al.* (2010). Endothelial cell adhesion to the extracellular matrix induces c-Src-dependent VEGFR-3 phosphorylation without the activation of the receptor intrinsic kinase activity. *Circ Res* 106, 1839-1848.

Gkretsi, V., Mars, W.M., Bowen, W.C., Barua, L., Yang, Y., Guo, L., St-Arnaud, R., Dedhar, S., Wu, C., and Michalopoulos, G.K. (2007). Loss of integrin linked kinase from mouse hepatocytes in vitro and in vivo results in apoptosis and hepatitis. *Hepatology* 45, 1025-1034.

Gouysse, G., Couvelard, A., Frachon, S., Bouvier, R., Nejjari, M., Dauge, M.C., Feldmann, G., Henin, D., and Scoazec, J.Y. (2002). Relationship between vascular development and vascular differentiation during liver organogenesis in humans. *J Hepatol* 37, 730-740.

Griscom, N.T., Colodny, A.H., Rosenberg, H.K., Fliegel, C.P., and Hardy, B.E. (1977). Diagnostic Aspects of Neonatal Ascites - Report of 27 Cases. *Am J Roentgenol* 128, 961-969.

Haiko, P., Makinen, T., Keskitalo, S., Taipale, J., Karkkainen, M.J., Baldwin, M.E., Stacker, S.A., Achen, M.G., and Alitalo, K. (2008). Deletion of vascular endothelial growth factor C (VEGF-C) and VEGF-D is not equivalent to VEGF receptor 3 deletion in mouse embryos. *Mol Cell Biol* 28, 4843-4850.

Hata, S., Namae, M., and Nishina, H. (2007). Liver development and regeneration: from laboratory study to clinical therapy. *Dev Growth Differ* 49, 163-170.

Häussinger, D. (1983). Hepatocyte heterogeneity in glutamine and ammonia metabolism and the role of an intercellular glutamine cycle during ureogenesis in perfused rat liver. *Eur J Biochem* 133, 269-275.

Häussinger, D. (2014). Liver - Overview. In *Metabolism of Human Diseases*, E. Lammert, and M. Zeeb, eds. (Wien Heidelberg New York Dordrecht London: Springer), pp. 173-180.

Hickman, P.E., and Potter, J.M. (1990). Mortality associated with ischaemic hepatitis. *Aust N Z J Med* 20, 32-34.

Hu, J., Srivastava, K., Wieland, M., Runge, A., Mogler, C., Besemfelder, E., Terhardt, D., Vogel, M.J., Cao, L., Korn, C., *et al.* (2014). Endothelial cell-derived angiopoietin-2 controls liver regeneration as a spatiotemporal rheostat. *Science* 343, 416-419.

Huh, D., Hamilton, G.A., and Ingber, D.E. (2011). From 3D cell culture to organs-on-chips. *Trends Cell Biol* 21, 745-754.

Hynes, R.O. (2007). Cell-matrix adhesion in vascular development. *J Thromb Haemost* 5 *Suppl 1*, 32-40.

Iboleon-Dy, M.A. (2009). The Liver in Shock. In *Liver: A Complete Book on Hepato-Pancreato-Biliary Diseases*, M.a. Mahtab, and S. Rahman, eds. (Noida: Elsevier), pp. 403-405.

Ingber, D. (1991). Integrins as mechanochemical transducers. *Curr Opin Cell Biol* 3, 841-848.

- Ingber, D.E. (2008). Tensegrity and mechanotransduction. *J Bodyw Mov Ther* 12, 198-200.
- Ishibashi, H., Nakamura, M., Komori, A., Migita, K., and Shimoda, S. (2009). Liver architecture, cell function, and disease. *Semin Immunopathol* 31, 399-409.
- Kaipainen, A., Korhonen, J., Mustonen, T., van Hinsbergh, V.W., Fang, G.H., Dumont, D., Breitman, M., and Alitalo, K. (1995). Expression of the *fms*-like tyrosine kinase 4 gene becomes restricted to lymphatic endothelium during development. *Proc Natl Acad Sci U S A* 92, 3566-3570.
- Karkkainen, M.J., Haiko, P., Sainio, K., Partanen, J., Taipale, J., Petrova, T.V., Jeltsch, M., Jackson, D.G., Talikka, M., Rauvala, H., *et al.* (2004). Vascular endothelial growth factor C is required for sprouting of the first lymphatic vessels from embryonic veins. *Nat Immunol* 5, 74-80.
- Killip, T., 3rd, and Payne, M.A. (1960). High serum transaminase activity in heart disease. Circulatory failure and hepatic necrosis. *Circulation* 21, 646-660.
- Kinoshita, T., Sekiguchi, T., Xu, M.J., Ito, Y., Kamiya, A., Tsuji, K., Nakahata, T., and Miyajima, A. (1999). Hepatic differentiation induced by oncostatin M attenuates fetal liver hematopoiesis. *Proc Natl Acad Sci U S A* 96, 7265-7270.
- Kordes, C., and Häussinger, D. (2013). Hepatic stem cell niches. *J Clin Invest* 123, 1874-1880.
- Kubo, S.H., Walter, B.A., John, D.H., Clark, M., and Cody, R.J. (1987). Liver function abnormalities in chronic heart failure. Influence of systemic hemodynamics. *Arch Intern Med* 147, 1227-1230.
- Lammert, E., Cleaver, O., and Melton, D. (2001). Induction of pancreatic differentiation by signals from blood vessels. *Science* 294, 564-567.
- LeCouter, J., Moritz, D.R., Li, B., Phillips, G.L., Liang, X.H., Gerber, H.P., Hillan, K.J., and Ferrara, N. (2003). Angiogenesis-independent endothelial protection of liver: role of VEGFR-1. *Science* 299, 890-893.
- Lei, L., Liu, D., Huang, Y., Jovin, I., Shai, S.Y., Kyriakides, T., Ross, R.S., and Giordano, F.J. (2008). Endothelial expression of beta1 integrin is required for embryonic vascular patterning and postnatal vascular remodeling. *Mol Cell Biol* 28, 794-802.
- Lemaigre, F., and Zaret, K.S. (2004). Liver development update: new embryo models, cell lineage control, and morphogenesis. *Curr Opin Genet Dev* 14, 582-590.
- Licht, A.H., Raab, S., Hofmann, U., and Breier, G. (2004). Endothelium-specific Cre recombinase activity in *flk-1-Cre* transgenic mice. *Dev Dyn* 229, 312-318.
- Lohela, M., Bry, M., Tammela, T., and Alitalo, K. (2009). VEGFs and receptors involved in angiogenesis versus lymphangiogenesis. *Curr Opin Cell Biol* 21, 154-165.
- Mammoto, A., Connor, K.M., Mammoto, T., Yung, C.W., Huh, D., Aderman, C.M., Mostoslavsky, G., Smith, L.E., and Ingber, D.E. (2009). A mechanosensitive transcriptional mechanism that controls angiogenesis. *Nature* 457, 1103-1108.
- Mammoto, T., and Ingber, D.E. (2010). Mechanical control of tissue and organ development. *Development* 137, 1407-1420.

- Masai, T., Sawa, Y., Ohtake, S., Nishida, T., Nishimura, M., Fukushima, N., Yamaguchi, T., and Matsuda, H. (2002). Hepatic dysfunction after left ventricular mechanical assist in patients with end-stage heart failure: role of inflammatory response and hepatic microcirculation. *Ann Thorac Surg* 73, 549-555.
- Matsumoto, K., Yoshitomi, H., Rossant, J., and Zaret, K.S. (2001). Liver organogenesis promoted by endothelial cells prior to vascular function. *Science* 294, 559-563.
- Michalopoulos, G.K. (2007). Liver regeneration. *J Cell Physiol* 213, 286-300.
- Michalopoulos, G.K. (2010). Liver regeneration after partial hepatectomy: critical analysis of mechanistic dilemmas. *Am J Pathol* 176, 2-13.
- Michalopoulos, G.K. (2011). Liver regeneration: alternative epithelial pathways. *Int J Biochem Cell Biol* 43, 173-179.
- Murray, J.F., Dawson, A.M., and Sherlock, S. (1958). Circulatory changes in chronic liver disease. *Am J Med* 24, 358-367.
- Nakamura, T., Sakai, K., Nakamura, T., and Matsumoto, K. (2011). Hepatocyte growth factor twenty years on: Much more than a growth factor. *J Gastroenterol Hepatol* 26, 188-202.
- Naschitz, J.E., Slobodin, G., Lewis, R.J., Zuckerman, E., and Yeshurun, D. (2000). Heart diseases affecting the liver and liver diseases affecting the heart. *Am Heart J* 140, 111-120.
- National Vital Statistics System, N.C.f.H.S., CDC (2010). 10 Leading Causes of Death by Age Group, United States –2010, U.S.D.o.H.H. Services, ed. (Atlanta: Produced by: Office of Statistics and Programming, National Center for Injury Prevention and Control, CDC using WISQARS™).
- Nilsson, I., Bahram, F., Li, X., Gualandi, L., Koch, S., Jarvius, M., Soderberg, O., Anisimov, A., Kholova, I., Pytowski, B., *et al.* (2010). VEGF receptor 2/3 heterodimers detected in situ by proximity ligation on angiogenic sprouts. *EMBO J* 29, 1377-1388.
- Palmes, D., and Spiegel, H.U. (2004). Animal models of liver regeneration. *Biomaterials* 25, 1601-1611.
- Partanen, T.A., Arola, J., Saaristo, A., Jussila, L., Ora, A., Miettinen, M., Stacker, S.A., Achen, M.G., and Alitalo, K. (2000). VEGF-C and VEGF-D expression in neuroendocrine cells and their receptor, VEGFR-3, in fenestrated blood vessels in human tissues. *FASEB J* 14, 2087-2096.
- Planas-Paz, L., Strilic, B., Goedecke, A., Breier, G., Fassler, R., and Lammert, E. (2012). Mechanoinduction of lymph vessel expansion. *EMBO J* 31, 788-804.
- Potocnik, A.J., Brakebusch, C., and Fassler, R. (2000). Fetal and adult hematopoietic stem cells require beta1 integrin function for colonizing fetal liver, spleen, and bone marrow. *Immunity* 12, 653-663.
- Rafii, S., Butler, J.M., and Ding, B.S. (2016). Angiocrine functions of organ-specific endothelial cells. *Nature* 529, 316-325.
- Reinehr, R., Sommerfeld, A., and Häussinger, D. (2013). The Src family kinases: distinct functions of c-Src, Yes, and Fyn in the liver. *Biomol Concepts* 4, 129-142.

- Rogers, A.B., and Dintzis, R.Z. (2012). The Liver and the Gallbladder. In *Comparative Anatomy and Histology*, P.M. Treuting, S. Dintzis, D. Liggitt, and C.W. Frevert, eds.
- Ross, T.D., Coon, B.G., Yun, S., Baeyens, N., Tanaka, K., Ouyang, M., and Schwartz, M.A. (2013). Integrins in mechanotransduction. *Curr Opin Cell Biol* 25, 613-618.
- Samsky, M.D., Patel, C.B., DeWald, T.A., Smith, A.D., Felker, G.M., Rogers, J.G., and Hernandez, A.F. (2013). Cardiohepatic interactions in heart failure: an overview and clinical implications. *J Am Coll Cardiol* 61, 2397-2405.
- Schmidt, C., Blatt, F., Goedecke, S., Brinkmann, V., Zschesche, W., Sharpe, M., Gherardi, E., and Birchmeier, C. (1995). Scatter Factor/Hepatocyte Growth-Factor Is Essential for Liver Development. *Nature* 373, 699-702.
- Schünke, M., Schulte, E., and Schumacher, U. (2015). Organe des Verdauungssystems und ihre Leitungsbahnen. In *Prometheus - LernAtlas der Anatomie*, M. Schünke, E. Schulte, and U. Schumacher, eds.
- Seeto, R.K., Fenn, B., and Rockey, D.C. (2000). Ischemic hepatitis: clinical presentation and pathogenesis. *Am J Med* 109, 109-113.
- Serini, G., Napione, L., Arese, M., and Bussolino, F. (2008). Besides adhesion: new perspectives of integrin functions in angiogenesis. *Cardiovasc Res* 78, 213-222.
- Seth, A., and Nath, R.K. (2009). Liver in Congestive Cardiac Failure. In *Liver: A Complete Book on Hepato-Pancreato-Biliary Diseases*, M.a. Mahtab, and S. Rahman, eds. (Noida: Elsevier), pp. 399-402.
- Sherlock, S. (1950). THE LIVER IN HEART FAILURE
RELATION OF ANATOMICAL, FUNCTIONAL, AND CIRCULATORY CHANGES.
- Shin, D., and Monga, S.P. (2013). Cellular and molecular basis of liver development. *Compr Physiol* 3, 799-815.
- Si-Tayeb, K., Lemaigre, F.P., and Duncan, S.A. (2010). Organogenesis and development of the liver. *Dev Cell* 18, 175-189.
- Sies, H. (1978). The use of perfusion of liver and other organs for the study of microsomal electron-transport and cytochrome P-450 systems. *Methods Enzymol* 52, 48-59.
- Sorensen, K.K., Simon-Santamaria, J., McCuskey, R.S., and Smedsrod, B. (2015). Liver Sinusoidal Endothelial Cells. *Compr Physiol* 5, 1751-1774.
- Stupack, D.G. (2005). Integrins as a distinct subtype of dependence receptors. *Cell Death Differ* 12, 1021-1030.
- Sugiyama, Y., Takabe, Y., Nakakura, T., Tanaka, S., Koike, T., and Shiojiri, N. (2010). Sinusoid development and morphogenesis may be stimulated by VEGF-Flk-1 signaling during fetal mouse liver development. *Dev Dyn* 239, 386-397.
- Suksaweang, S., Lin, C.M., Jiang, T.X., Hughes, M.W., Widelitz, R.B., and Chuong, C.M. (2004). Morphogenesis of chicken liver: identification of localized growth zones and the role of beta-catenin/Wnt in size regulation. *Dev Biol* 266, 109-122.
- Tallquist, M.D., Soriano, P., and Klinghoffer, R.A. (1999). Growth factor signaling pathways in vascular development. *Oncogene* 18, 7917-7932.

Tammela, T., Zarkada, G., Wallgard, E., Murtomaki, A., Suchting, S., Wirzenius, M., Waltari, M., Hellstrom, M., Schomber, T., Peltonen, R., *et al.* (2008). Blocking VEGFR-3 suppresses angiogenic sprouting and vascular network formation. *Nature* 454, 656-660.

Tortora, G.J., and Derrickson, B.H. (2006). *Anatomie und Physiologie*, 1st ed edn (Weinheim: WILEY-VCH Verlag GmbH & Co. KGaA).

Uehara, Y., Minowa, O., Mori, C., Shiota, K., Kuno, J., Noda, T., and Kitamura, N. (1995). Placental defect and embryonic lethality in mice lacking hepatocyte growth factor/scatter factor. *Nature* 373, 702-705.

Ventura, A., Kirsch, D.G., McLaughlin, M.E., Tuveson, D.A., Grimm, J., Lintault, L., Newman, J., Reczek, E.E., Weissleder, R., and Jacks, T. (2007). Restoration of p53 function leads to tumour regression in vivo. *Nature* 445, 661-665.

Wang, C., Baker, B.M., Chen, C.S., and Schwartz, M.A. (2013). Endothelial cell sensing of flow direction. *Arterioscler Thromb Vasc Biol* 33, 2130-2136.

Wang, L., Wang, X., Xie, G., Wang, L., Hill, C.K., and DeLeve, L.D. (2012). Liver sinusoidal endothelial cell progenitor cells promote liver regeneration in rats. *J Clin Invest* 122, 1567-1573.

Weinberg, A.G., and Bolande, R.P. (1970). The liver in congenital heart disease. Effects of infantile coarctation of the aorta and the hypoplastic left heart syndrome in infancy. *Am J Dis Child* 119, 390-394.

Wisse, E., De Zanger, R.B., Jacobs, R., and McCuskey, R.S. (1983). Scanning electron microscope observations on the structure of portal veins, sinusoids and central veins in rat liver. *Scan Electron Microsc*, 1441-1452.

Wu, F.M., Ukomadu, C., Odze, R.D., Valente, A.M., Mayer, J.E., Jr., and Earing, M.G. (2011). Liver disease in the patient with Fontan circulation. *Congenit Heart Dis* 6, 190-201.

Yang, J.T., Rayburn, H., and Hynes, R.O. (1993). Embryonic mesodermal defects in alpha 5 integrin-deficient mice. *Development* 119, 1093-1105.

Zaret, K.S. (2000). Liver specification and early morphogenesis. *Mech Dev* 92, 83-88.

Zaret, K.S., and Grompe, M. (2008). Generation and regeneration of cells of the liver and pancreas. *Science* 322, 1490-1494.

Zarkada, G., Heinolainen, K., Makinen, T., Kubota, Y., and Alitalo, K. (2015). VEGFR3 does not sustain retinal angiogenesis without VEGFR2. *Proc Natl Acad Sci U S A* 112, 761-766.

Zeeb, M., Axnick, J., Planas-Paz, L., Hartmann, T., Strilic, B., and Lammert, E. (2012). Pharmacological manipulation of blood and lymphatic vascularization in ex vivo-cultured mouse embryos. *Nat Protoc* 7, 1970-1982.

Zhang, H., Pu, W., Tian, X., Huang, X., He, L., Liu, Q., Li, Y., Zhang, L., He, L., Liu, K., *et al.* (2016). Genetic lineage tracing identifies endocardial origin of liver vasculature. *Nat Genet* 48, 537-543.

Zhang, X., Groopman, J.E., and Wang, J.F. (2005). Extracellular matrix regulates endothelial functions through interaction of VEGFR-3 and integrin alpha5beta1. *J Cell Physiol* 202, 205-214.

Zorn, A.M. (2008). Liver development. In StemBook (Cambridge (MA)).

Zovein, A.C., Luque, A., Turlo, K.A., Hofmann, J.J., Yee, K.M., Becker, M.S., Fassler, R., Mellman, I., Lane, T.F., and Iruela-Arispe, M.L. (2010). Beta1 integrin establishes endothelial cell polarity and arteriolar lumen formation via a Par3-dependent mechanism. *Dev Cell* 18, 39-51.

List of Publications

Recent publications:

Parts of this thesis are planned to be used for publication in the following paper:

- 2016 Axnick, J., Buschmann, T., Klüppel, C., Lorenz, L., Fang, S., Nurmi, H., Eichhorst, N., Alitalo, K., Häusinger, D., Lammert, E.: **β 1 integrin-dependent mechanotransduction induces angiocrine signaling required to promote liver growth and survival.**
Original research article, under revision (2016)
Contributions in detail are listed in 2.10.

The following paper was finalized due to revision within the time of the thesis:

- 2012 Zeeb, M.*, Axnick, J.*, Planas-Paz, L., Hartmann, T., Strilić, B., Lammert, E.: **Pharmacological manipulation of blood and lymphatic vascularization in ex vivo-cultured mouse embryos.**
Nat Protoc. 2012 Nov;7(11):1970-82.
*(equally contributing 1st position)
Methods paper, impact factor 9.6 (2015)

Other publications:

- 2012 Axnick, J., Lammert, E.: **Vascular lumen formation.**
Curr Opin Hematol. 2012 May;19(3):192-8.
Review article, Impact Factor 3.3 (2015)
- 2011 Lammert, E., Axnick, J.: **Vascular lumen formation.**
In *Angiogenesis: Biology and Pathology*. Cold Spring Harb Perspect Med. 2011. Ed. by Klagsbrun M, D'Amore P.
Review article, Impact Factor 10.5 (2015)
- 2010 Strilić, B., Eglinger, J., Krieg, M., Zeeb, M., Axnick, J., Babál, P., Müller, D.J., Lammert, E.: **Electrostatic cell-surface repulsion initiates lumen formation in developing blood vessels.**
Curr Biol. 2010 Nov 23;20(22):2003-9.
Original research article, impact factor 9.0 (2015).

Abbreviations

SI units and symbols were used in this thesis.

ACLI	Acute cardiogenic liver injury
ALT	alanine transaminase
ASH	Alcoholic steatohepatitis
AST	aspartate transaminase
AF	Alexa fluor
BDM	2,3-butanedione monoxime
BM	Basement membrane
BMI	Body mass index
BMP2	bone morphogenic protein-2
CD	Cluster of differentiation
CXCR4/7	Stromal-derived factor-1 receptors
DAPI	4',6-diamidino-2-phenylindole
DMEM	Dulbecco's modified Eagle's medium
E	Embryonic day
ECs	Endothelial Cells
ECM	Extra cellular matrix
ECG	Electrocardiogram
EDTA	Ethylenediaminetetraacetic acid
EdU	5-ethynyl-2'-deoxyuridine
ELISA	Enzyme-linked immunosorbent assay
FBS	Fetal bovine serum
FGF	Fibroblast growth factors
FITC	Fluorescein isothiocyanate
Fik-1	Fetal liver kinase/ VEGFR2
GAPDH	Glyceraldehyde 3-phosphate dehydrogenase
HGF	Hepatocyte growth factor
Hif1- α	Hypoxia-inducible factor 1- α
ICAM-1	Intercellular Adhesion Molecule 1
IHC	Immunohistochemistry
ILK	Integrin-linked kinase
KO	Knockout
KRH	Krebs-Ringer-Hepes buffer

LAD	Left anterior descending artery
LDH	Lactate dehydrogenase
LSECs	Liver sinusoidal endothelial cells
LYVE-1	Lymphatic vessel endothelial hyaluronan receptor
MAPK	Mitogen-activated protein kinase
MI	Myocardial infarction
NASH	Non-alcoholic steatohepatitis
P	Passage
PBS	Phosphate buffered saline
PCR	Polymerase chain reaktion
PECAM-1	Platelet endothelial cell adhesion molecule-1
PFA	Paraformaldehyde
p-H3	phospho-Histone H3
PI3K	Phosphatidylinositol 3 kinase
PLA	Proximity ligation assay
RCA	Ricinus communis agglutinin
RT	Room temperature
SD	Standard deviation
STM	Septum transversum mesenchyme
TGF- β 1	transforming growth factor- β 1
TTC	Triphenyl tetrazolium chloride
VE	Vascular endothelial-Cadherins
VEGFR1/2/3	Vascular endothelial growth factor receptor-1/2/3
VEGF-A/C/D	Vascular endothelial growth factor-A/C/D
WEC	Whole embryo culture
Wnt2	Wnt family member 2
WT	Wild-type

List of Figures

Figure 1.1: Mouse and human livers.	2
Figure 1.2: Blood flow through the liver.	4
Figure 1.3: Portal liver lobule.	5
Figure 1.4: Integrins.	9
Figure 1.5: VEGFR3.	11
Figure 3.1: Liver growth during murine embryonic development.	29
Figure 3.2: Hepatic vascular perfusion.	30
Figure 3.3: Hepatic cell proliferation in perfused liver periphery versus non-perfused liver center at E11.5.	31
Figure 3.4: Specialized liver vessels and peripheral β 1 integrin activation and VEGFR3 tyrosine phosphorylation on LSECs.	32
Figure 3.5: Loss-of-perfusion.	34
Figure 3.6: Gain-of-perfusion.	35
Figure 3.7: Endothelial β 1 integrin deletion on LSECs.	36
Figure 3.8: Endothelial β 1 integrin is required for growth of the developing liver. ...	37
Figure 3.9: Endothelial β 1 integrin is required for cell proliferation in the developing liver.	38
Figure 3.10: Endothelial β 1 integrin is required for the survival of the developing liver.	39
Figure 3.11: Cell death occurs in well-perfused liver regions of endothelial β 1 integrin-deficient mouse embryos.	40
Figure 3.12: Endothelial β 1 integrin is required for VEGFR3 activation and angiocrine HGF production.	41
Figure 3.13: β 1 integrin is required for perfusion-dependent VEGFR3 tyrosine phosphorylation.	42
Figure 3.14: VEGFR3 is required for liver growth and survival and HGF production.	44
Figure 3.15: <i>Ex vivo</i> liver perfusion.	46
Figure 3.16: <i>Ex vivo</i> liver perfusion activates β 1 integrin, VEGFR3, and angiocrine signaling.	47
Figure 3.17: Mechanical stimulation of LSECs increases VEGFR3 tyrosine phosphorylation. (a,b)	48

Figure 3.18: Proliferation of primary human hepatocytes upon treatment with mechanoinduced angiocrine signals.....	49
Figure 3.19: Discoloring of mouse hearts and livers after MI.....	50
Figure 3.20: Infarction size of the left ventricle per area at risk after MI surgery.	51
Figure 3.21: Foci of collapsed and dilated vessels after MI surgery.....	52
Figure 3.22: Apoptosis in collapsed liver regions after MI.....	52
Figure 3.23: Liver function tests.....	53
Figure 3.24: Decreased endothelial β1 integrin activation, VEGFR3 tyrosine phosphorylation and c-Met tyrosine phosphorylation after MI surgery.....	55
Figure 4.1: Model.....	57

Acknowledgements

I would like to thank...

...Prof. Dr. Eckhard Lammert (Ecki) for his supervision, coaching and mentoring and for giving me the opportunity to write my thesis. It was a pleasure to work in his lab and to learn from him.

...Prof. Dr. Ulrich Rütger for mentoring and very constructive follow-up meetings.

...Prof. Dr. Dieter Häussinger for the opportunity to work within the SFB 974 and for collaboration.

...Prof. Dr. Kari Alitalo, S. Fang and H. Nurmi for collaboration and scientific exchange.

...Nicole Eichhorst (Prof. Dr. D. Häussinger) for *ex vivo* liver perfusions.

...Stefanie Becher (Prof. Dr. M. Kelm) for MI surgeries, technical support and great input.

...My graduate schools iGK SFB 974 and iGrad for coordinated graduate programs.

...Tobias Buschmann for our teamwork in the “liver team”.

...Carina Klüppel for MI surgeries, being a great student and now a great colleague.

...Linda Lorenz for being a great master student and super team player in the “liver team”.

...Alena Welters for extensive medical, scientific and private discussions.

...Silke Otter, best bench-mate, for always motivating me and always having an open ear.

...Sofia Urner for always having a great heart and an open ear.

...Daniel Eberhard for his critical and constructive support.

...Molly Kelly-Goss and Mary Gearing for “private lessons” and English discussions.

...and all the other present and former members of the institute of metabolic physiology for the support, great discussions and a great working atmosphere: S. Jakob, B. Bartosinska, A. Branopolski, Dr. L. Planas-Paz, Dr. M. Zeeb, Dr. J. Eglinger, E. Hedderich, A. Wies, F. Demir and all the others.

...meinem lieben Ehemann, Thorsten Scholten, für seine bedingungslose Unterstützung all die Jahre, egal wie verrückt meine Ideen und Pläne auch waren und für seine Liebe.

...meinen lieben Eltern, die immer an mich geglaubt haben, egal welche Noten oder Abschlüsse ich hatte.

...meiner Familie (besonders Thomas, Beate, Zoe und Tessa) für all die schönen Momente.

Declaration

Eidesstattliche Erklärung

An Eidesstatt erkläre ich, dass

- ich die vorgelegte Dissertation selbstständig und ohne unzulässige fremde Hilfe unter der Beachtung der "Grundsätze zur Sicherheit guter wissenschaftlicher Praxis an der Heinrich-Heine-Universität Düsseldorf" angefertigt habe und dass ich diese in der jetzigen oder einer ähnlichen Form noch keiner anderen Fakultät eingereicht habe;
- die Dissertation noch nicht veröffentlicht wurde (Veröffentlichungen nach § 6 (3) der Promotionsordnung bleiben hiervon ausgenommen).

Jennifer Axnick

Düsseldorf, September 2016